EXPERIMENTAL INVESTIGATION FOR DEVELOPMENT OF COMPACTED GRAPHITE IRON (CGI) AND ITS CHARACTERIZATION

A Thesis submitted to Gujarat Technological University

for the Degree of

Doctor of Philosophy

in

Mechanical Engineering

By

MAMTA AMBALAL PATEL

Enrollment No. 159997119019

under supervision of

Dr. KOMAL G DAVE

GUJARAT TECHNOLOGICAL UNIVERSITY

AHMEDABAD

April - 2025

EXPERIMENTAL INVESTIGATION FOR DEVELOPMENT OF COMPACTED GRAPHITE IRON (CGI) AND ITS CHARACTERIZATION

A Thesis submitted to Gujarat Technological University

for the Degree of

Doctor of Philosophy

in

Mechanical Engineering

By

MAMTA AMBALAL PATEL

Enrollment No. 159997119019

under supervision of

Dr. KOMAL G DAVE

GUJARAT TECHNOLOGICAL UNIVERSITY

AHMEDABAD

April - 2025

© Mamta Ambalal Patel

DECLARATION

I declare that the thesis entitled **"EXPERIMENTAL INVESTIGATION FOR DEVELOPMENT OF COMPACTED GRAPHITE IRON (CGI) AND ITS CHARACTERIZATION"** submitted by me for the degree of Doctor of Philosophy is the record of research work carried out by me during the period from **2015** to **2025** under the supervision of **Dr. KOMAL G DAVE** and this has not formed the basis for the award of any degree, diploma, associateship, fellowship, titles in this orany other University or other institution of higher learning.

I further declare that the material obtained from other sources has been duly acknowledged in the thesis. I shall be solely responsible for any plagiarism or other irregularities if noticed in the thesis.

Signature of the Research Scholar: Date: 28/4/25

Name of Research Scholar: **MAMTA AMBALAL PATEL**

Place: **VADODARA, Gujarat, India**

CERTIFICATE

I certify that the work incorporated in the thesis **"EXPERIMENTAL INVESTIGATION FOR DEVELOPMENT OF COMPACTED GRAPHITE IRON (CGI) AND ITS CHARACTERIZATION"** submitted by Mrs. **MAMTA AMBALAL PATEL** was carried out by the candidate under my supervision. To the best of my knowledge: (i) the candidate has not submitted the same research work to any other institution for any degree/diploma, associateship, fellowship, or other similar titles (ii) the thesis submitted is a record of original research work done by the Research Scholar during the period of study under my supervision, and (iii) the thesis represents independent research work on the part of the Research Scholar.

Signature of Supervisor: Kg dave

Date: 28/4/25

Name of Supervisor: **Dr. KOMAL G DAVE**

Place: **VADODARA, Gujarat, India**

Course-work Completion Certificate

This is to certify that Mrs. **MAMTA AMBALAL PATEL** enrolment no. **159997119019** is enrolled for PhD program in the branch **MECHANICAL ENGINEERING** of Gujarat Technological University, Ahmedabad.

(Please tick the relevant option(s))

☐ She has been exempted from the course-work (successfully completed during Ph.D Course)

☐ She has been exempted from the Research Methodology Course only (successfully completed during Ph.D Course)

☑ She has successfully completed the PhD course work for the partial requirement for the award of a PhD Degree. Her performance in the course work is as follows-

Grade Obtained in Research Methodology [PH001]	Grade Obtained in Self-Study Course (Core Subject) [PH002]
BC	**BB**

Kgdave

Supervisor's Sign

Dr. KOMAL G DAVE

Originality Report Certificate

It is certified that PhD Thesis titled **"EXPERIMENTAL INVESTIGATION FOR DEVELOPMENT OF COMPACTED GRAPHITE IRON (CGI) AND ITS CHARACTERIZATION"** by **Mrs. MAMTA AMBALAL PATEL** has been examined by us. We undertake the following:

a. A thesis has significant new work/knowledge as compared to already been published or is under consideration to be published elsewhere. No sentence, equation, diagram, table, paragraph, or section has been copied verbatim from previous work unless itis placed under quotation marks and duly referenced.

b. The work presented is original and own work of the author (i.e. there is no plagiarism). No ideas, processes, results, or words of others have been presented as the Author's work.

c. There is no fabrication of data or results which have been compiled/analyzed.

d. There is no falsification by manipulating research materials, equipment, or processes,or changing or omitting data or results such that the research is not accurately represented in the research record.

e. The thesis has been checked using **www.drillbitplagiarism.com (copy of originality report attached)** and found within limits as per GTU Plagiarism Policy and instructions issued from time to time (i.e. permitted similarity index <=10%).

Signature of the Research Scholar: Date: 28/4/25

Name of Research Scholar: **Mrs. MAMTA AMBALAL PATEL**

Signature of Supervisor: Date: 28/4/25

Name of Supervisor: **Dr. KOMAL G DAVE**

Place: **AHMEDABAD, Gujarat, India**

DrillBit

The Report is Generated by DrillBit Plagiarism Detection Software

Submission Information

Author Name	Mamta Patel
Title	Thesis_Mamta_R6_Comment Complianced
Paper/Submission ID	3513698
Submitted by	mercymamta@yahoo.com
Submission Date	2025-04-16 22:12:23
Total Pages, Total Words	159, 25513
Document type	Thesis

Result Information

Similarity **5 %**

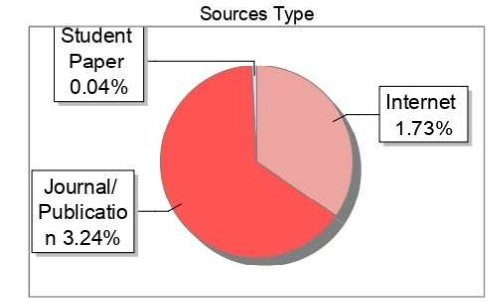

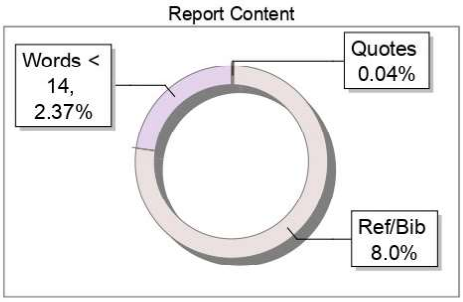

Exclude Information

Quotes	Not Excluded
References/Bibliography	Excluded
Source: Excluded < 14 Words	Not Excluded
Excluded Source	**0 %**
Excluded Phrases	Not Excluded

Database Selection

Language	English
Student Papers	Yes
Journals & publishers	Yes
Internet or Web	Yes
Institution Repository	Yes

A Unique QR Code use to View/Download/Share Pdf File

Ph.D. Thesis Non-Exclusive License to
GUJARAT TECHNOLOGICAL UNIVERSITY

In consideration of being a Research Scholar at Gujarat Technological University, and in the interests of the facilitation of research at the University and elsewhere, I, **Mrs. MAMTA AMBALAL PATEL** having **Enrollment No. 159997119019** hereby grant a non- exclusive, royalty-free, and perpetual license to the University on the following terms:

a. The University is permitted to archive, reproduce, and distribute my thesis, in whole or in part, and/or my abstract, in whole or in part (referred to collectively as the "Work") anywhere in the world, for non-commercial purposes, in all forms of media;

b. The University is permitted to authorize, sub-lease, sub-contract, or procure any of the acts mentioned in paragraph (a);

c. The University is authorized to submit the Work at any National / International Library, under the authority of their "Thesis Non-Exclusive License";

d. The Universal Copyright Notice (©) shall appear on all copies made under the authority of this license;

e. I undertake to submit my thesis, through my university, to any Library and Archives. Any abstract submitted with the thesis will be considered to form part of the thesis.

f. I represent that my thesis is my original work, does not infringe any rights of others, including privacy rights, and that I have the right to make the grant conferred by this non-exclusive license.

g. If third-party copyrighted material was included in my thesis for which, under the terms of the Copyright Act, written permission from the copyright owners is required, I have obtained such permission from the copyright owners to do the acts mentioned in paragraph (a) above for the full term of copyright protection.

h. I understand that the responsibility for the matter as mentioned in paragraph (g) rests with the authors / me solely. In no case shall GTU have any liability for any acts/omissions/errors/copyright infringement from the publication of the said thesis or otherwise.

i. I retain copyright ownership and moral rights in my thesis and may deal with the copyright in my thesis, in any way consistent with rights granted by me to my university

in this non-exclusive license.

j. GTU logo shall not be used /printed in the book (in any manner whatsoever) being published or any promotional or marketing materials or any such similar documents.

k. The following statement shall be included appropriately and displayed prominently in the book or any material being published anywhere: "The content of the published work is part of the thesis submitted in partial fulfillment for the award of the degree of Ph.D. in **MECHANICAL ENGINEERING** of the Gujarat Technological University".

l. I further promise to inform any person to whom I may hereafter assign or license my copyright in my thesis of the rights granted by me to my university in this nonexclusive license. I shall keep GTU indemnified from any claims from the Publisher(s) orany third parties at all times resulting or arising from the publishing or use or intendeduse of the book / such similar document or its contents.

m. I am aware of and agree to accept the conditions and regulations of Ph.D. including all policy matters related to authorship and plagiarism.

Date: 28/4/25

Place: **VADODARA, Gujarat, India**

Signature of the Research Scholar

Recommendation of the Supervisor: .....Approved.....

Signature of Supervisor

Thesis Approval Form

The viva voce of the PhD Thesis submitted by **Mrs. MAMTA AMBALAL PATEL** (Enrollment No. **159997119019**) entitled **"EXPERIMENTAL INVESTIGATION FOR DEVELOPMENT OF COMPACTED GRAPHITE IRON (CGI) AND ITS CHARACTERIZATION"** was conducted on ..... at Gujarat Technological University.

(Please tick any one of the following options)

☑ The performance of the candidate was satisfactory. We recommend that he/she be awarded the PhD degree.

☐ Any further modifications in research work recommended by the panel after 3 months from the date of the first viva-voce upon request of the Supervisor or request of Independent Research Scholar after which viva-voce can be re-conducted by the same panel again.

(briefly specify the modifications suggested by the panel)

☐ The performance of the candidate was unsatisfactory. We recommend that he/she should not be awarded the PhD degree.

(The panel must give justifications for rejecting the research work)

Kgdave

Dr. Komal G. Dave

Name and Signature of Supervisor with Seal

Dr. D. Shivalingappa

1) (External Examiner 1) Name and Signature

Dr. Vivek Patel

2) (External Examiner 2) Name and Signature

Abstract

Compacted Graphite Iron (CGI) belongs to the cast iron material family which is not appropriately rated but it is a potential engineering material that exhibits a unique microstructure combining properties of both gray iron and ductile iron. It is characterized by the presence of compacted graphite nodules dispersed within a matrix of ferrite and pearlite. The graphite particles look shorter, thicker, and stubby with rounded edges with densely interconnected with one another. This distinctive microstructure enables it to offer intermediate mechanical, physical, and manufacturing properties as compared to gray cast iron and ductile iron, making it suitable for a wide range of demanding applications in various industries.

The key challenges associated with the production of CGI, which involves careful control of the solidification conditions and alloy composition have been covered in this work. The compacted graphite iron microstructure formation remains stable over a range of approximately 0.008% magnesium (Mg), and the loss of as little as 0.001% magnesium leads to the graphite formation change in flake or nodular particles to vermicular forms which poses 25-40% change in mechanical properties. As a result, quality CGI production is quite challenging to secure desired chemistry using traditional foundries because it requires specialized knowledge and state-of-the-art infrastructure that can instantaneously measure and control the molten metal chemicals. However, within known limitations, the author attempted to establish CGI production processes using traditional foundries.

The mechanical properties of CGI have been tailored by adjusting the manufacturing parameters, allowing designers and engineers to optimize the material for specific applications especially where a combination of static and thermal loads act simultaneously. It is also worth noting the associated several limitations, such as poor machinability and the need for specialized foundries for mass-scale quality production. The author has successfully produced developed CGI by exploring traditional foundry processes by making multiple trials by varying the chemical composition and production processes. Later, this research is extended to assess the commercial viability of developed CGI material and outline the potential design optimization opportunities toward cost-effective centrifugal pump volute designing as an alternative to equivalent grades of GCI and DI materials.

In conclusion, compacted graphite iron represents promising mechanical and thermal properties which make this material quite a potential alternative to overcome many of the industrial product designing needs against GCI and DI. Moreover, CGI shows its prominence for cost-effective product designing even for static loading applications as studied with reference to outcome gained by commercial viability assessment while centrifugal pump designing. However, it is also necessary to admit the CGI production challenges associated with traditional foundry processes but with ongoing research and development efforts, CGI is expected to continue expanding its market presence and contributing to advancements in engineering and manufacturing industries.

The present thesis has been written into a total of six chapters and each chapter includes the information as mentioned below.

CHAPTER 1 introduces CGI, its microstructure, material properties, application, and associated production challenges

CHAPTER 2 presents the crux of a comprehensive literature review made to study the CGI microstructure sensitivity to the prevalent chemical composition and production processes. Along with this, recent developments in this domain are also outlined. Apart from this, it also contains the objective and scope of the present study.

CHAPTER 3 covers a detailed narration of experimental iterations that have been conducted in a direction to unveil the intrinsic behavior of CGI microstructure formation and establish a reliable production process. It also includes the information regarding the CGI quality assurance.

CHAPTER 4 explains the chemical, microstructure, and mechanical testing results obtained through the exploration of various potential CGI production methods, including pilot production to see process variance to boost user confidence. Along with the snapshot of results, a technical feasibility discussion has been outlined in the direction of freezing the reliable CGI production method.

CHAPTER 5 narrates the technical and commercial viability assessment made while designing the industrial pump volute using all the potential materials including GCI, CGI, and DI. Outcomes using these materials have been compared and its underlying cost implications have been analyzed by means of should cost analysis technique.

CHAPTER 6 outlines the critical conclusion drawn with reference to the learning achieved and the contribution made at the end of the present research investigation. The shortcomings and possibilities to extend the scope for future work have been narrated.

Keywords: Compacted Graphite Iron (CGI), Vermicular microstructure, Cast iron, Chemical composition, Material testing.

Acknowledgment

I am deeply grateful to all those who have supported me throughout the journey of research and to complete Ph.D. study.

Firstly, I express my sincere gratitude to my supervisor, **Dr. KOMAL G. DAVE, Professor, Mechanical Engineering Department, LDCE, Ahmedabad** for their valuable guidance, support, and encouragement, and for showing immense faith in me throughout the research work. Her expertise, motivation, and constructive feedback were instrumental in shaping my research and enabling me to complete my thesis successfully.

I would like to extend my heartfelt thanks to my Doctoral Progress Committee members: **Dr. G. H. UPADHYAY, Principal, MGITER, Navsari,** and **Dr. BHARATI REHANI, Consultant, TCR Advanced Engineering Pvt. Ltd., Vadodara** whose insightful comments and suggestions helped me to refine research and improve the quality of results.

I am also grateful to **Mr. ANKUSH KACHOLE,** technical head of Himgiri Castings Pvt. Ltd, Halol, and **Mr. BHARAT VYAS,** owner of Nodule Cast, Vadodara for their unwavering technical guidance and experimental facilitation in their industry.

I would like to acknowledge my family members, especially my husband **Dr. PRUTHVISH PATEL**, source of inspiration to work hard. They have been my pillar of strength and support throughout my academic journey. Their love, encouragement, and staunch support gave me the motivation to pursue my Ph.D. and complete it successfully.

I also express my sincere thanks to all the Ph.D. section staff, Vice-Chancellor of Gujarat Technological University (GTU), and others who have supported me, directly or indirectly, in my academic pursuits.

Finally, I thank Almighty God for giving me the wisdom, health, and strength to undertake and complete this research task.t, this accomplishment would not have been possible.

- **MAMTA AMBALAL PATEL**
  Enrollment No. 159997119019

Table of Contents

DECLARATION I
CERTIFICATE II
Course-work Completion Certificate III
Originality Report Certificate IV
Ph.D. Thesis Non-Exclusive License to VI
Thesis Approval Form VIII
Abstract IX
Acknowledgment XII
Table of Contents XIII
List of Abbreviation XVI
List of Symbols XVII
List of Figures XVIII
List of Tables XXI
List of Appendices XXIII

CHAPTER 1 INTRODUCTION **1**

1.1 Introduction 1
1.2 Compacted graphite iron 1
1.2.1 Morphology of CGI 3
1.2.2 Production process 4
1.2.3 Material properties 5
1.2.4 Applications 7
1.3 Sand casting of cast iron 8
1.4 Mechanical testing 10
1.4.1 Tensile properties 10
1.4.1.1 Tensile strength (UTS - Ultimate Tensile Strength) 10
1.4.1.2 Yield strength 10
1.4.1.3 Elongation at break 10
1.4.1.4 Modulus of elasticity (Young's modulus) 10
1.4.1.5 Poisson's ratio 11
1.4.2 Hardness 11
1.5 Metallurgy testing 11
1.5.1 Optical microscope 11

1.5.2 Scanning electron microscope 12
1.5.3 Spectrometer 12
1.6 Finite Element Analysis aided Numerical Simulation 13

CHAPTER 2 LITERATURE REVIEW 15
2.1 Compacted graphite iron 16
2.2 Microstructure 17
2.3 Chemical composition 19
2.4 Mechanical strengths 24
2.5 Physical properties 30
2.6 Production process 34
2.7 Production process control 36
2.8 Product simulation 38
2.9 Literature summary 39
2.10 Research gap 40
2.11 Objectives of present work 41
2.12 Scope of present research work 41

CHAPTER 3 COMPACTED GRAPHITE IRON PRODUCTION USING TRADITIONAL FOUNDRY PRACTICES 43
3.1 Production process 43
3.2 Experimental procedure 44
3.2.1 Material selection 44
3.2.2 Experimental setup 46
3.3 Metal treatment approaches 50
3.3.1 Experimental iterations 50
3.3.2 Method-1: Mg addition by sandwich treatment 51
3.3.3 Method-2: Mg + Sulfur addition 53
3.3.4 Method-3: Mg addition + CaSi inoculant treatment 56
3.4 Experimentation validation 57
3.5 Metallurgical characterization 59
3.5.1 Chemical assessment 59
3.5.2 Microstructure assessment 60
3.5.3 Scanning electron microscope (SEM) 61

3.6 Mechanical characterization 61
3.6.1 Tensile strength testing 62
3.6.2 Hardness testing 63
3.6.3 Density of material 64

CHAPTER 4 RESULT AND DISCUSSION 67
4.1 CGI production process 67
4.1.1 Production method-1: Mg addition by sandwich treatment 67
4.1.2 Production method-2: Mg + Sulfur addition 69
4.1.3 Production method-3: Mg addition + CaSi inoculant treatment 70
4.2 Results of validation experiments 74

CHAPTER 5 TECHNICAL VIABILITY ASSESSMENT OF DEVELOPED COMPACTED GRAPHITE IRON 79
5.1 Materials selection 79
5.2 Product designing 81
5.2.1 FEA simulation approach 83
5.2.2 Design assessment by FEA simulation 87
5.3 Design optimization 97
5.4 Should cost analysis 101
5.5 Result discussion 103

CHAPTER 6 CONCLUSION, CONTRIBUTION, INDUSTRIAL APPLICATION AND FUTURE SCOPE 105
6.1 Conclusion 105
6.1.1 CGI mass production feasibility using traditional foundry processes 105
6.1.2 CGI commercial viability for cost-effective product designing 106
6.2 Contribution 107
6.3 Industrial application 108
6.4 Future scope 109

LIST OF REFERENCES 111

LIST OF PUBLICATIONS 119

ANNEXURE 1 121

List of Abbreviation

GCI	Gray cast iron
CGI	Compacted graphite iron
DI	Ductile iron
CRCA	Cold rolled closed annealed
CRC	Cold rolled coil
FR	Foundry return
FEA	Finite element analysis
FE	Finite element
CAD	Computer-aided design
3D	3-dimensional
MISO	Multilinear isotropic hardening model
ASTM	American society of testing and materials
BS	British standards

List of Symbols

Mg	Magnesium
CGI	Compacted graphite iron
DI	Ductile iron
FeS	Ferrous Sulfur
FeSiMg	Ferrous Silicon Magnesium
CaSi	Calcium Silicon
MgS	Magnesium Sulfur
C	Carbon
Si	Silicon
Mn	Manganese
P	Phosphorous
S	Sulfur
Mg	Magnesium
Cu	Copper
Sn	Tin
Cr	Chromium
Ni	Nickle
Fe	Ferrous
Al	Aluminum
Ca	Calcium
Ba	Barium
D_o	Outer diameter of pipe, mm
σ	Yield/Ultimate strength, MPa
D_i	Inner diameter of pipe, mm
A	Pipe cross-section area = $\frac{\pi}{4}$ $(D_o^2 - D_i^2)$, mm^2
σ_t	Yield/Ultimate tensile strength, MPa
σ_c	Yield/Ultimate compressive strength, MPa
ϵ	Strain
E	Young's modulus, GPa
K	Plasticity co-efficient
n	Strain hardening co-efficient

List of Figures

Figure 1.1 3D microstructure of compacted graphite iron. MEV 395X (ASM,1996) 2

Figure 2.1 Three-dimension graphite shapes using deep-etched scanning electron micrographs 17

Figure 2.2 Roundness shape factor definition 18

Figure 2.3 Various planes of polish which can cause improperly interpret the nodular graphite (Chuang et al., 2015) 18

Figure 2.4 The stable CGI plateau exists over a range of approximately 0.008% magnesium and is separated from gray iron by an abrupt transition 19

Figure 2.5 Optimised initial sulfur level range as a function of other elements used for graphite compaction. The table highlights the sulfur range, for compacted iron formation with different spheroidizers in an iron composition of 3.5% C, 2.1% Si, 0.75%, Mn, and 0.0.1 to 0.08% 21

Figure 2.6 The effect of nickel, copper, and tin on composition matrix ranging from CGI to GCI for 25 mm (1in.) wall thickness 21

Figure 2.7 The optimum range for carbon and silicon contents for CG iron 22

Figure 2.8 The microstructure chessboard per inoculation variation and modification 23

Figure 2.9 85–100% pearlitic cast irons ultimate tensile and yield strengths. Nodularity content <0% denotes the presence of 100% flake graphite in proportion to -5% 26

Figure 2.10 Charpy absorbed energy obtained for different metrics 28

Figure 2.11 Ferritic, pearlitic, and higher-nodularity CG fatigue curves with reference of Table 2.5 data 30

Figure 2.12 85-100% pearlite cast irons elastic modulus with reference to nodularity and temperature 30

Figure 2.13 Pearlitic and Ferritic compacted graphite iron castings Stress-strain, Image recreated from Nechtelberger et al., (1982) 31

Figure 2.14 0-20% nodularity CGI Brinell hardness with reference to pearlite 32

Figure 2.15 Volume shrinkage and Dimensional change comparison for irons poured in green sand molds. Image recreated from Sergeant & Evans, (1978) 33

Figure 2.16 Graphite shape influence on cast iron chilling tendency. Type A uniformly

distributed and randomly oriented graphite flakes. Type D, Inter-dendritic segregated and randomly oriented graphite flakes. Image recreated from Stefanescu et al., (1983) 35

Figure 2.17 The effect of holding time on nodularity (Hernando, 2017) 36

Figure 2.18 Typical CGI production process flow 37

Figure 2.19 The immersion-type sampler 39

Figure 2.20 SinterCast probe and Mg reaction 39

Figure 3.1 Experiment preparation: (a) Ferrous Sulphide (FeS), (b) Pig Iron, (c) FeSiMg, (d) CRC Chips, (e) FR, and (f) CRCA 46

Figure 3.2 Melting of the molten metals (a) Melting in induction furnace, (b) Partitioned ladle, and (c) Graphite stirrer 47

Figure 3.3 Melting of the molten metals (a) Heating of molten metal (b) Realtime temperature measurement and (c) Prepare crucible for heating 48

Figure 3.4 Melting of the molten metals (a) Button sample size, (b) Sand mold preparation, and (c) Poured specimens 48

Figure 3.5 Metal treatment process flows 52

Figure 3.6 CGI production (a) Ladle for Sandwich treatment through MgFeSi, (b) Base metal treatment, (c) Casting pouring, (d) Poured specimen, and (e) Specimen policing for chemical and microstructure testing 54

Figure 3.7 Poured molten metal in button sample 58

Figure 3.8 Metal treatment process followed while pilot trials, per Method-3 58

Figure 3.9 Optical emission spectrometer 60

Figure 3.10 Metallurgical microscope 61

Figure 3.11 Scanning Electron Microscope 62

Figure 3.12 (a) ASTM-E8 standard specimen dimensions (units in mm), and (b) Universal tensile machine 64

Figure 3.13 Brinell Hardness tester 64

Figure 3.14 Density measurement 65

Figure 4.1 Microstructure of casted samples with 2% Nital 69

Figure 4.2 Microstructure using 2% Nital 70

Figure 4.3 Microstructure of samples with 2% Nital 71

Figure 4.4 Volume fraction of all Samples 72

Figure 4.5 Deep-etched scanning electron micrographs show shorter, thicker, and rounded edges at 300X 73

Figure 4.6 Microstructure at 100x magnification 74

Figure 4.7 As polished volume fraction using a metallurgical microscope 75

Figure 4.8 Broken specimens after the test 76

Figure 5.1 Multilinear stress-strain properties of GCI, CGI, and DI per Table 5.2 82

Figure 5.2 Definition of loads, (a) Hydrotest, (b) Tension, (c) Compressive, and (d) Bending 85

Figure 5.3 FEA results, (a) Hydrotest, (b) Tension, (c) Compressive, and (d) Bending, for CGI 86

Figure 5.4 6x4x8 inch volute geometry 89

Figure 5.5 Mesh convergence study performed on CGI baseline volute geometry 90

Figure 5.6 Hexahedron meshing of volute assembly 91

Figure 5.7 Hydrotest pressure loading, and constraint definition 92

Figure 5.8 Yield and Ultimate total strain results of baseline volute geometry using (a) GCI, (b) CGI, (c) DI 96

Figure 5.9 FEA simulation design exploration using ANSYS while design optimization 98

Figure 5.10 CGI volute results against rated baseline pressures while designing them over (a) GCI, and (b) DI 100

List of Tables

Table 1.1 Categorization of cast irons based on commercial designation, microstructural characteristics, and physical properties after fracture 2

Table 1.2 Compacted graphite irons material grades per ASTM 842, and BS EN 16079:2011 6

Table 1.3 Comparison of CGI & SGI tensile and compressive properties 6

Table 1.4 Mechanical properties of developed CGI 7

Table 2.1 Comparative mechanical properties of Cast Irons ASTM A48, ASTM A842, and ASTM A536 25

Table 2.2 CGI properties accordance with ISO 16112 27

Table 2.3 CGI properties accordance with ASTM A 842 27

Table 2.4 Compressive properties of various CGI configurations (Shao et al., 1998) 28

Table 2.5 CGI fatigue properties from rotating-bending tests 29

Table 3.1 Chemical composition of base iron material for method-1 53

Table 3.2 Chemical composition of base iron for Method-2 56

Table 3.3 Experimental parameters 56

Table 3.5 Chemical composition of base metal for pilot trials 59

Table 4.1 Chemical composition and microstructure remark 68

Table 4.2 Chemical composition post-metal treatment 69

Table 4.3 Assessment of chemical and graphite composition at varying holding times of casted samples 73

Table 4.4 Chemical composition of pre-inoculant treated metal 76

Table 4.5 Chemical composition of final treated metal 76

Table 4.6 Mechanical and metallurgical properties of samples of Table 4.5 77

Table 5.1 Compacted graphite iron material grades per ASTM 842 and BS EN 16079:2011 80

Table 5.2 GCI, CGI, and DI materials properties 80

Table 5.3 Permissible loads estimation using GCI v/s CGI v/s DI 87

Table 5.4 Permissible loads estimation error%, FEA v/s Analytical from Table 5.3 data 88

Table 5.6 Design margin using CGI over GCI and DI for simplified pipe geometry 98

List of Appendices

ANNEXURE 1 Quality Assessment Reports

CHAPTER 1

INTRODUCTION

1.1 Introduction

Cast irons are alloys with a base of iron and carbon that undergo eutectic solidification, and these are categorized accordance with ferrous alloys, as similar to steel materials. It contains various compositions, including silicon (Si), manganese (Mn), phosphorus (P), sulfur (S), and trace elements such as titanium (Ti), antimony (Sb), and tin (Sn) along with various alloying elements. The variation in cast iron properties is governed by variations in the balance of carbon and silicon, combined with various metallic or non-metallic elements, apart from modifications of production procedures adopted for melting, casting, and heat treatment. The cast iron categorization is shown in Table 1.1 (Mohammed, 2011).

White iron and gray iron are so named due to the distinct appearances of their fracture surfaces. The fracture surfaces are visible in the form of white crystalline and gray with very fine facets in white and gray cast iron respectively. Mottled iron falls between the characteristics of gray iron and white iron, as its fracture exhibits a combination of gray and white zones. In contrast, ductile iron earns its name because it displays measurable ductility in its as-cast state, its property is not similar to the white or gray iron in a typical tensile test. Malleable iron begins as white iron undergoes a process called "malleableization," which involves heat treatment to enhance ductility. Compacted graphite (CG) cast iron is characterized by graphite that is interconnected within eutectic cells similar to flake graphite in gray iron. However, the graphite in CG iron is coarser and more rounded as shown in Figure 1.1

1.2 Compacted graphite iron

Compacted graphite iron (CGI), also known as vermicular graphite iron, has indeed emerged as a significant material within the cast iron family due to its unique properties. Historically, the production of CGI was not intentional and often arose as a byproduct of attempts to

produce spheroidal graphite ductile iron with insufficient levels of magnesium (Mg) or cerium (Ce) in the melts. It wasn't until around 1965 that the distinct properties of CGI iron were recognized and appreciated (Composition & sMorphology, 1965). Researchers and manufacturers began to understand that such unintended microstructure, featuring compacted or vermicular graphite, offered valuable properties that set it apart from traditional gray cast iron (GCI) and ductile iron (DI). The distinct manufacturing technologies necessary to consistently produce CGI were subsequently developed and refined. The accidental discovery of CG iron's distinct properties led to intentional research and development efforts, establishing CGI iron as a sought-after material for various applications, especially in sectors like automotive and industrial machinery where its specific combination of properties provides substantial benefits. Today, CGI is deliberately produced to achieve its advantageous properties, making it a crucial and distinct member of the cast iron family.

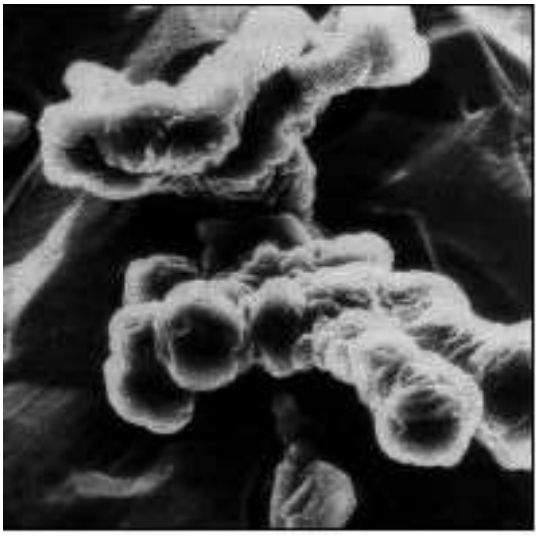

Figure 1.1 3D microstructure of compacted graphite iron. MEV 395X (ASM,1996)

Table 1.1 Categorization of cast irons based on commercial designation, microstructural characteristics, and physical properties after fracture

Commercial Designation	Carbon-rich phase	Matrix	Fracture	Final structure after
Gray iron	Lamellar graphite	Pearlite	Gray	Solidification
Ductile iron	Spheroidal graphite	Ferrite, Pearlite, Austenite	Silver-gray	Solidification or heat treatment

Compacted graphite iron	Vermicular graphite	Ferrite, Pearlite	Gray	Solidification
White iron	Fe3C	Pearlite, Martensite	White	Solidification and heat treatment
Mottled iron	Lamellar graphite + Fe3C	Pearlite	Mottled	Solidification
Malleable iron	Temper graphite	Ferrite, Pearlite	Silver-gray	Heat treatment

1.2.1 Morphology of CGI

The class of cast iron family is characterized by their graphite shape morphology. The graphite particle within compacted graphite iron (CGI) looks separate, worm-shaped, or vermicular particles. These particles exhibit an elongated, random orientation like gray iron; however, they differ by being shortened and thicker than the graphite flakes that have been observed in gray iron, and they possess rounded edges. Where the longer flakes of graphite particles are prone to crack under tensile loading. However, the spheroidal graphite particles in DI show higher bonding and fracture resistance. The mechanical characteristics of CGI are therefore intermediate when compared to those of GCI and DI. While viewed in two dimensions, these compacted graphite particles resemble vermicular structures.

The SEM (Scanning Electron Microscope) image of Figure 1.1, reveals a deeper reality, and it shows interconnections between these 'worms' and their neighboring structures within the eutectic cell. This intricate graphite morphology resembles a coral-like formation with rounded edges, and uneven surfaces and it promotes robust adhesion between the graphite and the iron matrix. The morphology of compacted graphite iron (CGI) refers to its microstructure the arrangement and shape of the graphite particles within the iron matrix. The distinctive feature of CGI is the presence of compacted or vermicular graphite, which sets it apart from other types of cast iron. This microstructure offers a unique combination of properties, including improved mechanical strength, thermal conductivity, and thermal expansion characteristics. Here's a detailed explanation of the morphology of CGI:

Compacted graphite nodules

The key feature of CGI is the presence of compacted graphite nodules. These nodules are irregularly shaped, shorter, and thicker compared to the flakes found in gray iron. It is intermediate in shape between the thin flakes in gray iron and the spherical nodules in ductile iron.

Vermicular structure

The compacted graphite in CGI forms a vermicular or worm-like structure within the iron matrix. This structure consists of interconnected, irregularly shaped graphite nodules that resemble worms or vermicular when viewed under a microscope.

Interconnected graphite network

The graphite particles in CGI are interconnected, forming a three-dimensional network within the iron matrix. This interconnected structure provides improved mechanical properties, including higher strength and better resistance to crack propagation.

Graphite-matrix interface

The interface between the compacted graphite nodules and the iron matrix is an important aspect of CGI's morphology. The strong bond at this interface contributes to the enhanced mechanical properties of CGI.

Uniform distribution

The compacted graphite nodules are typically evenly distributed throughout the iron matrix, ensuring consistent mechanical properties across the material. A matrix of ferrite and graphite forms while the austenite decomposes during the eutectoid transformation (Ko & Konig, 2010). This process requires carbon reallocation, and this can be accomplished by carbon diffusion to graphite from austenite. This graphite morphology is critical for ferrite growth to determine the number of prism planes in the structure. Microstructure formation is sensitive to various melt treatment elements, alloys, and process parameters. Accordance to the ISO 16112 standard (Anon 2016), CGI graphite particles are predominant in the vermicular form (equivalently type IV per ASTM A247 or form III per ISO 945-1). The spheroidal graphite content is referred in 0.043% of nodularity detected by image analysis per the criteria mentioned in the SinterCast nodularity rating chart (Anon 1997) which depends on the roundness shape factor to quantify each particle between compacted or nodular.

1.2.2 Production process

Compacted graphite iron also known as vermicular cast iron (VCI), is a highly versatile and innovative engineering material that has gained significant consideration and popularity in recent years. This material was accidently created in 1948; due to inadequate Mg, Ce, and

La (Alonso et al., 2016) treatment in the molten metal, intended to produce ductile iron (DI). It is a unique form of cast iron that exhibits a distinctive microstructure, combining the characteristics of both gray iron and ductile iron.

Compacted graphite iron microstructure is formed by the addition of magnesium in the desulfurized base iron, similar to DI. CGI formation remains stable within a plateau of 0.008% Mg, which is quite narrow than Mg range available in commercial ductile iron. This limitation poses a great challenge for quality CGI production. If Mg content falls to a lower range, it leads to flake-type graphite formation in the casting, causing an immediate drop of 20-30% in strength and stiffness. While contrarily with higher Mg, nodularity promotes which affects the thermal conductivity, machinability, and casting shrinkage.

Moreover, active Mg fades at a rate of 0.001% every five minutes after the base metal treatment, where active oxygen and/or sulfur content consume the active Mg, which disturbs the stable CGI plateau. Similarly, it is also sensitive to the addition of inoculant because an increment of 0.08% of inoculation shifts the CGI plateau towards higher nodularity to gain as much as >30% nodular graphite and conversely, forms flakes at depleting inoculation.

The changes that led to graphite microstructure reflect the criticalness of simultaneous control of the inoculant and the requisite adjustment of chemical elements (magnesium, cerium, lanthanum, calcium, sulfur, and oxygen) to ensure reliable CGI production at the industry scale. Therefore, CGI production mandates need for continuous chemical monitoring and enables it to be adjusted on a real-time basis. As a result, the currently available CGI production process relies on a measure-and-control-based, two-step metal treatment approach.

1.2.3 Material properties

The mechanical and physical properties of cast materials are governed by metallurgical properties like chemical composition, graphite shape, proportion of nodules, and perlite/ferrite ratio. It is important to note that an increment in pearlite causes a rapid gain in hardness and increase in nodularity percentage, which enhances mechanical strength as well as stiffness, but it has a contrary influence on castability, machinability, and thermal conductivity. In addition, the machinability of CGI is impacted by interconnected graphite bond strength, chemical alloy of magnesium and sulfur (MgS). Therefore, when designing a product for a particular application, it’s important to select the appropriate CGI grade.

The CGI material grades are differentiated with reference to ASTM 842 ("Standard Specification for Compacted Graphite Iron Castings," 2018) and equivalent BS EN 16079:2011 (European Committee for Standardization, 2011), as listed in Table 1.2. Due to its higher perlite content, EN-GJV-500 has stronger strength than EN-GJV-300, but its machinability is compromised.

Table 1.2 Compacted graphite irons material grades per ASTM 842, and BS EN 16079:2011

ASTM 842 Material Grade	BS EN 16079 Material Grade	Matrix Structure	Tensile Strength (MPa)	Yield Strength (MPa)	Elongation (%)	Modulus of Elasticity (GPa)	Thermal Conductivity (W/m°K)
300	EN-GJV-300	Ferritic	300-375	210-260	2.0-5.0	130-145	47
350	EN-GJV-350	Ferritic-Pearlitic	350-425	245-295	1.5-4.0	135-150	43
400	EN-GJV-400	Pearlitic-Ferritic	400-475	280-330	1.0-3.5	140-150	39
450	EN-GJV-450	Predominantly Pearlitic	450-525	315-365	1.0-2.5	145-155	38
---	EN-GJV-500	Pearlitic	500-575	350-400	0.5-2.0	145-160	36

Inline to one of the objectives of the present investigation, the authors have attempted to produce CGI (M. Patel & Dave, 2023) using traditional foundry processes whose mechanical properties are outlined in Table 1.4, which is quite similar to ASTM A842 CGI-400.

Table 1.3 Comparison of CGI & SGI tensile and compressive properties

Property	CGI	SGI, Min-Max	
Tensile strength			
0.1% proof stress, MPa (ksi)	246(35.7)	224(32.5)	261(37.8)
0.2% proof stress, MPa (ksi)	242(35.1)	236(34.2)	273(39.6)
Compressive stress			
0.1% proof stress, MPa (ksi)	322(46.7)	247(35.8)	284(41.2)
0.2% proof stress, MPa (ksi)	350(50)	250(36.3)	284(41.6)

E. Nechtelberger, (1980) has studied the tensile-compressive strength behavior and outlined comparative data of CGI and SGI in Table 1.3, the variations in tensile and compressive

strengths are being observed in the cast iron material family, which is primarily caused by the stiffness posed by the geometrical shape of the graphite content. SGI consists more in the form of spheroidal graphite, so tensile and compressive strengths are almost similar, but CGI shows somewhat more dominant compressive strength than tensile strength.

Steve Dawson et al., (1999) and Cohen et al., (2000) have reported that the machining rate is adversely influenced due to the nature of microstructure content like graphite bonding, its shape, perlite content, etc. GCI shows excellent machinability due to graphite flakes, which increase crack propagation intensity for easy chip formation. But machinability worsens while graphite transforms from flakes to spheroidal and nodularity increases, so that CGI offers an intermediate machining rate compared to GCI and DI constituents.

Table 1.4 Mechanical properties of developed CGI

Material	Density (kg/m^3)	Poisson's ratio	Young's Modulus (GPa)	Yield Strength (MPa)	Strain at Yield	Ultimate Strength (MPa)	Strain at Break
CGI, Developed	7000	0.26	155	292	0.41%	471	2.9%

1.2.4 Applications

Compacted Graphite Iron (CGI) is a type of cast iron that has gained popularity in various applications due to its unique graphite structure - which is compacted and irregularly shaped - and offers a combination of mechanical and physical properties that lie between gray and ductile irons. It demonstrates a tensile strength that's approximately 70% higher, an elastic modulus that's around 35% higher, and nearly double the fatigue strength compared to gray cast irons. These unique attributes, including its strength, ductility, and thermal conductivity, along with recent developments in production control, make CGI an ideal material that has gained significant attention in recent times. This set of properties has led to its considerable use in the production of automotive engines, machine components, and various other applications. Such salient advantages are:

While comparing with GCI:

- Design and cost optimization through superior strength
- Ability to use fracture-splitting (Hahnel & Wisniewski, n.d.)
- Better strain energy absorption against impact

- Better life expectancy due to improved wear resistance
- Improved design reliability through consistent as-cast properties

While comparing with DI:

- Improved thermal conductivity and heat transfer rate
- Reduced manufacturing cost through better machinability
- Better castability so favors for complex geometry

This makes CGI well-suited for several applications in different industries as below:

Automotive Industry: CGI is extensively used in the automotive sector, particularly for manufacturing engine components such as cylinder blocks, cylinder heads, and exhaust manifolds. Its superior strength and reduced weight compared to traditional gray iron make it an excellent choice for enhancing fuel efficiency and reducing emissions.

Heavy Machinery: In industries like construction, mining, and agriculture, where heavy-duty components are required, CGI finds application in parts like engine blocks, cylinder liners, and gearbox housings. Its high strength-to-weight ratio and excellent wear resistance make it suitable for such demanding applications.

Industrial Pumps and Valves: CGI's thermal conductivity and corrosion resistance make it a preferred material for manufacturing industrial pumps and valves that handle high-temperature fluids or corrosive substances.

Compressor Components: In air compressors, CGI is often used for parts such as compressor housings, pistons, and cylinder liners due to its ability to withstand high pressures and temperature fluctuations.

Wind Turbine Hubs and Gearboxes: CGI's mechanical properties, including its damping capabilities, make it suitable for critical components in wind turbines such as hubs and gearboxes, helping enhance reliability and performance.

1.3 Sand casting of cast iron

Generally, the sand casting process involves the production of CGI objects by pouring molten material (usually metal) into a mold where it solidifies. There are several types of casting processes, and the choice depends on factors such as the material being cast, the intricacy of the design, and production requirements. A general overview of the sand-casting process is as follows:

Pattern making

The process begins with the creation of a pattern, which is a replica of the final object. The pattern is typically made of wood, metal, or plastic and has the same shape and dimensions as the desired casting.

Mold preparation

A mold is created by packing a material (usually sand or metal) around the pattern. This material is chosen based on the casting method. In some cases, a mold may consist of two or more parts that are assembled to create the complete mold cavity.

Mold assembly

The mold is assembled, and the pattern is placed inside. In some processes, a core may be used to create internal features of the casting.

Melting

The material to be cast, often metal, is melted in a furnace. The temperature is carefully controlled to achieve the desired molten state.

Pouring

The molten material is poured into the mold. The pouring process must be done carefully to ensure that the mold is filled and to avoid defects such as air bubbles.

Solidification

The molten material cools and solidifies inside the mold. This process can be influenced by factors such as cooling rate and alloy composition.

Finishing

The casting may undergo various finishing processes to achieve the final product. This can include machining, grinding, polishing, or other techniques to meet specific dimensional and surface finish requirements.

Inspection and Quality control

The finished casting is inspected for defects, and quality control measures are taken to ensure that it meets the required standards. Non-destructive testing methods may be employed.

1.4 Mechanical testing

The intermediate nature of CGI microstructure formation imparts certain mechanical properties that bridge the gaps for specific product applications. Some of the major mechanical properties are tested as follows.

1.4.1 Tensile properties

The tensile properties of compacted graphite iron are essential indicators for understanding its tensile behavior while product designing. It's important to note that the tensile properties are going to be varied due to multiple influential parameters like specific alloy composition, heat treatment, and manufacturing process. Tensile properties are outlined through multiple mechanical parameters.

1.4.1.1 Tensile strength (UTS - Ultimate Tensile Strength)

The UTS is the maximum stress that a material can withstand while being stretched or pulled before necking, which is when the specimen's cross-section starts to significantly contract. The tensile strength of CGI typically falls in the range of 500 to 700 megapascals (MPa).

1.4.1.2 Yield strength

CGI exhibits a yield point, which is the stress at which the material begins to deform plastically. The yield strength of CGI is generally in the range of 300 to 500 MPa.

1.4.1.3 Elongation at break

Elongation at break is a measure of the plastic deformation a material can undergo before failure. For CGI, the elongation at break is typically in the range of 2% to 10%. This property is important for applications where some degree of ductility is required.

1.4.1.4 Modulus of elasticity (Young's modulus)

Young's Modulus is a measure of a material's stiffness or rigidity. The modulus of elasticity for CGI is in the range of 150 to 170 gigapascals (GPa). It represents the slope of the initial linear portion of the stress-strain curve.

1.4.1.5 Poisson's ratio

Poisson's ratio is the ratio of the transverse strain to the axial strain. For CGI, Poisson's ratio is typically around 0.26 to 0.30.

1.4.2 Hardness

Hardness is a measure of a material's resistance to deformation, indentation, or scratching. For Compacted Graphite Iron (CGI), hardness is an important mechanical property that influences its performance in different applications. The hardness of CGI is commonly measured using the Brinell hardness test. The Brinell hardness test involves indenting a spherical indenter into the material and measuring the diameter of the impression. The Brinell hardness for Compacted Graphite Iron is usually in the range of 170 to 250 HB.

1.5 Metallurgy testing

The metallurgical characteristics of CGI are pivotal in influencing its mechanical and physical attributes. This research focuses on investigating the microstructure and volume fraction using an optical microscope. Additionally, the surface morphology of the specimen is examined at higher magnifications through a scanning electron microscope (SEM). Furthermore, chemical analyses are conducted using a spectrometer at the Aardhya laboratory located in GIDC, Vadodara.

1.5.1 Optical microscope

An optical microscope is a crucial tool in metal metallurgy testing, providing a non-destructive method for examining the microstructure of metallic materials. It consists of several key components, including an objective lens, an eyepiece, and an illumination source. The objective lens is responsible for magnifying the specimen, and the eyepiece further magnifies the image, allowing the observer to see fine details. The illumination source, often positioned beneath the specimen, ensures proper visibility by directing light onto the sample.

Metallurgical samples are typically prepared by cutting, mounting, grinding, and polishing to achieve a flat and smooth surface. This preparation is essential for accurate observations under the microscope. Once the sample is ready, it is placed on the microscope stage for examination. The optical microscope enables metallurgists to analyze features such as grain

size, grain boundaries, inclusions, and phases within the metal. By examining the microstructure, researchers can gain insights into the mechanical and thermal processing history of the material, helping them understand its properties and behavior under different conditions.

1.5.2 Scanning electron microscope

The Scanning Electron Microscope (SEM) not only excels at capturing highly detailed two-dimensional images but has also proven effective in enabling three-dimensional image analysis, thereby enhancing its versatility. Through the application of advanced techniques such as stereo-pair imaging or the use of a tilt series featuring images from diverse angles, the SEM facilitates the construction of three-dimensional models representing the sample surface. This capability to generate 3D images is particularly advantageous when studying intricate structures, including biological specimens, nanomaterials, and complex surface features. Researchers can gain a more thorough understanding of spatial relationships, surface topography, and depth information within the sample. The SEM's capacity to offer detailed three-dimensional insights plays a crucial role in advancing various scientific disciplines, empowering researchers to delve into and visualize the micro and nanoscale architecture of materials with unparalleled detail.

1.5.3 Spectrometer

A spectrometer serves as an indispensable tool in the realm of chemical analysis, offering a precise and systematic approach to understanding the composition of diverse substances. Operating on the fundamental principle of separating and measuring the wavelengths of electromagnetic radiation emitted or absorbed by a sample, the spectrometer provides detailed insights into its molecular and elemental makeup. Through techniques such as absorption, emission, or fluorescence spectroscopy, a spectrometer can identify specific chemical species and quantify their concentrations within a given sample. In the field of analytical chemistry, this instrument is utilized for a broad spectrum of applications, ranging from environmental monitoring and pharmaceutical analysis to material characterization. The data generated by a spectrometer not only facilitates qualitative identification but also enables quantitative analysis, contributing significantly to scientific research, quality control processes, and the advancement of various industries reliant on accurate chemical information.

1.6 Finite Element Analysis aided Numerical Simulation

Finite Element Analysis (FEA) is a powerful numerical technique employed in product engineering to simulate and analyze the behavior of conceptual products under various conditions. It plays a pivotal role in understanding how different materials and designs respond to external forces, enabling engineers to optimize structures for safety, efficiency, and performance. At its core, FEA breaks down complex structures into smaller, manageable elements, allowing for a detailed examination of their mechanical response. The entire structure is discretized into finite elements, each representing a small portion of the overall geometry. These elements are interconnected at nodes, forming a mesh that mirrors the actual structure. The analysis begins by applying boundary conditions and loading to the model. These could include forces, pressures, or constraints that mimic real-world scenarios. FEA then utilizes mathematical formulations, often based on principles of physics and mechanics, to compute the behavior of each element and the overall system.

This study is complimented by doing FEA simulation powered by ANSYS which is one of the most versatile FEA software suites that is used for engineering simulation. It can solve a wide range of mechanical problems, including static and dynamic problems, structural analysis, heat transfer, fluid problems, acoustic problems, and electromagnetic problems. Such software was founded in 1970 and incorporated in 1994. It is used in many industries, including Aerospace, Defense, Automotive, and Biomedical. Some benefits of using ANSYS include:

- Accurately performing advanced engineering simulations
- Optimizing features like geometrical design and boundary conditions
- Running multiple solver technologies in parallel to provide fast solutions
- Simulating the interaction between dynamic, static, and fluid elements

CHAPTER 2

LITERATURE REVIEW

Compacted Graphite Iron (CGI) emerges as a focal point, captivating researchers, and industries alike due to its unique properties and potential cost-effective applications. This literature review investigates the expansive realm of CGI, aiming to provide a comprehensive understanding of its characteristics and the methodologies employed for its cost-effective development.

The literature surveyed here encompasses a wide array of studies, experiments, and analyses conducted to unravel the intricacies of CGI and its cost-effective development. Researchers have explored various alloying elements, casting techniques, and heat treatment processes to optimize CGI's properties while keeping a vigilant eye on economic feasibility. By synthesizing this body of knowledge, this review aims to shed light on the current state of CGI research, identifying key trends, challenges, and promising avenues for future exploration. As industries worldwide strive for sustainability and economic viability, understanding the distinction between CGI's metallurgical properties and its cost-effective development becomes paramount. Through an in-depth exploration of the existing literature, this review seeks to contribute valuable insights to the ongoing discourse surrounding CGI, shaping the trajectory of its application in diverse industrial landscapes.

This literature review gives the information about effects of various input parameters on control casting technology for compacted graphite iron. The literature review has been classified based on the various methodologies used for CGI development by the adoption of thermal analysis and controlled process as described below.

1) Compacted graphite iron
2) Microstructure of CGI
3) Chemical composition
4) Mechanical Strengths
5) Physical properties

6) Production process
7) Production process control
8) Product simulation

2.1 Compacted graphite iron

The CGI was accidentally created in 1948; due to inadequate Mg, Ce, and La (Millis et al., 1949) treatment in the molten metal, intended to produce DI. Generally, CGI is identified by iron morphology where graphite particles are in the form of shorter, thicker, stubby with rounded edges of individual worm shapes which is known as compacted or vermicular graphite. CGI is a high-performance cast iron engineering material with a combination of excellent mechanical properties, such as high strength, good wear resistance, and thermal conductivity (Millis et al., 1949). CGI has gained widespread use in various applications, including heavy-duty engines, brake systems, and structural components (M. Patel & Dave, 2022).

Compacted graphite depends on the roundness of flakes. Stefanescu D.M. et.al., (2018) and Riposan Iulian, (2018) have concluded that raising the degree of compactness improves the ductility, corrosion resistance, and impact resistance but simultaneously declining properties such as machinability, thermal conductivity, and dampening capacity. Therefore, CGI exhibits intermediate mechanical properties of GCI and DI spheroidal cast iron. However, its thermal conductivity is better than DI, which makes it a distinct material for combined loading of heavy-duty and thermal applications. These mechanical properties are dominated by the CGI matrix - which can be controlled by many of the treatment variables such as charge material, graphite shape governing elements, chemical composition, cooling rate, pouring temperature, and holding temperature, etc.

The foremost CGI application is where thermal & mechanical boundary conditions prevail simultaneously. Such as cylinder blocks, heads, hydraulic housings, flywheels, bearing caps, and heavy castings components of passenger vehicles (Hughes & Powell, 1984),(Xu et al., 2018). It outclasses the GCI by 10-20% lighter weight along with superior strength & stiffness.

2.2 Microstructure

Cast irons are distinguished by their graphite shape (Dawson Steve & Schroeder, 2000). If graphite shapes in iron morphology consist in the form of longer flakes, worms, and spheres, it is classified as GCI, CGI, and DI respectively, as shown in Figure 2.1. Those are substantiated by nodularity content in the range of <5%, <20% & >25% respectively.

Graphite shapes and their matrix are more visible through 3D deep-etch scanning electron micrographs shown in Figure 2.1. Compacted graphite interlocks into the iron matrix, as a result, it furnishes strong bonding with iron whereas round edges resist the crack formation so overall It gives superior strength in CGI in comparison to GCI.

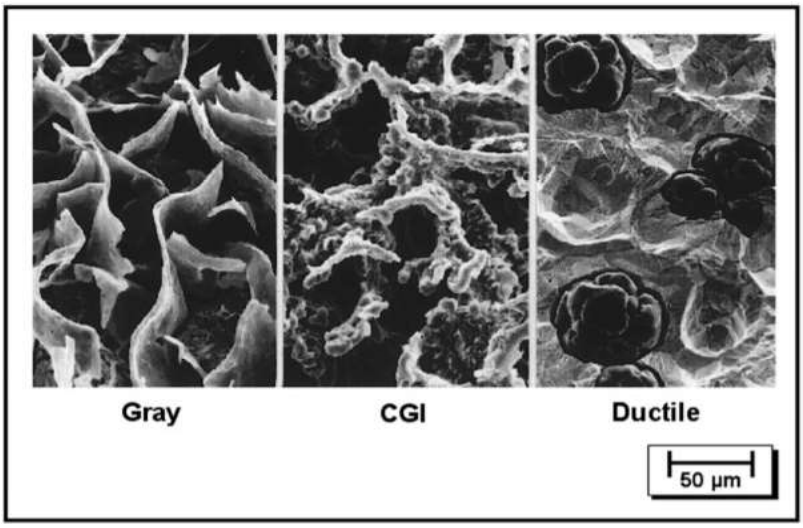

Figure 2.1 Three-dimension graphite shapes using deep-etched scanning electron micrographs

Accordance to the ISO 16112 standard ("Compacted (Vermicular) Graphite Cast Iron—Classification," 2016), CGI graphite particles are predominant in the vermicular form (equivalently type IV per ASTM A247 or form III per ISO 945-1). The spheroidal graphite content is referred to in % of nodularity detected by image analysis per the criteria mentioned in the Sinter Cast nodularity rating chart (SinterCast Nodularity Rating Charts, 1997) which depends on the roundness shape factor to quantify each particle between compacted or nodular.

The roundness shape factor is defined in Figure 2.2. The particles are classified as either vermicular or nodular if their roundness shape factor is <0.525 or >0.625 respectively; with reference to ISO 16112 international standard for CGI. The different intersection lines A-A

& B-B shown in Figure 2.3, incorrectly interpret the nodule graphite whereas C-C section reveals a well-formed CGI particle to evaluate the irregular nodules, comparable to form VI, V, or IV graphite defined in ISO 945-1. (Chuang et al., 2015).

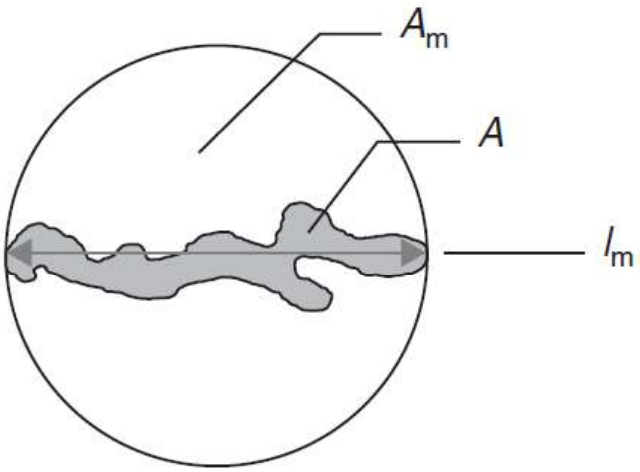

Figure 2.2 Roundness shape factor definition

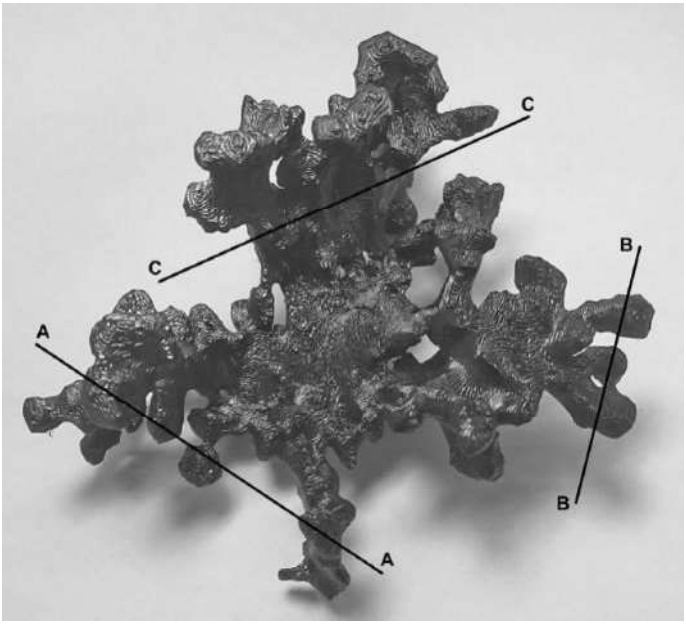

Figure 2.3 Various planes of polish which can cause improperly interpret the nodular graphite (Chuang et al., 2015)

A matrix of ferrite and graphite forms while the austenite decomposes during the eutectoid transformation (Ko & Konig, 2010). This process requires carbon reallocation, and this can be accomplished by carbon diffusion to graphite from austenite. Graphite morphology is critical for ferrite growth to determine the number of prism planes in the structure.

Microstructure formation is sensitive to various melt treatment elements, alloys, and process parameters. Stefanescu et al., (2018) have been studied the compacted graphite growth while solidification and observed the graphite platelets grown in the a-direction and stacked in the c-direction which coarser than GCI as shown in Figure 2.3.

2.3 Chemical composition

CGI microstructure stabilization range is too narrow, so it poses a great challenge to maintain a consistent microstructure for mass production in a foundry. A commercial CGI grade has been specified for 10-20% of nodular graphite particles without any graphite flakes (S Dawson, 1994), (S. Dawson, 1999), (Skaland, n.d.). Three dimension graphite shapes are used through deep-etched scanning electron micrographs (Steve Dawson & Schroeder, 2000) as shown in Figure 2.1.

However, mostly the stable range is found for approximately 0.008% Mg (Steve Dawson, 2002), as shown in Figure 2.4, which represents the condition for a typical CGI or ductile base iron with a sulfur content of 0.010 to 0.015% (Steve Dawson, 2002). However, the active magnesium fades at a rate of approximately 0.001% every five minutes as a result usable magnesium range is even lessor in reality.

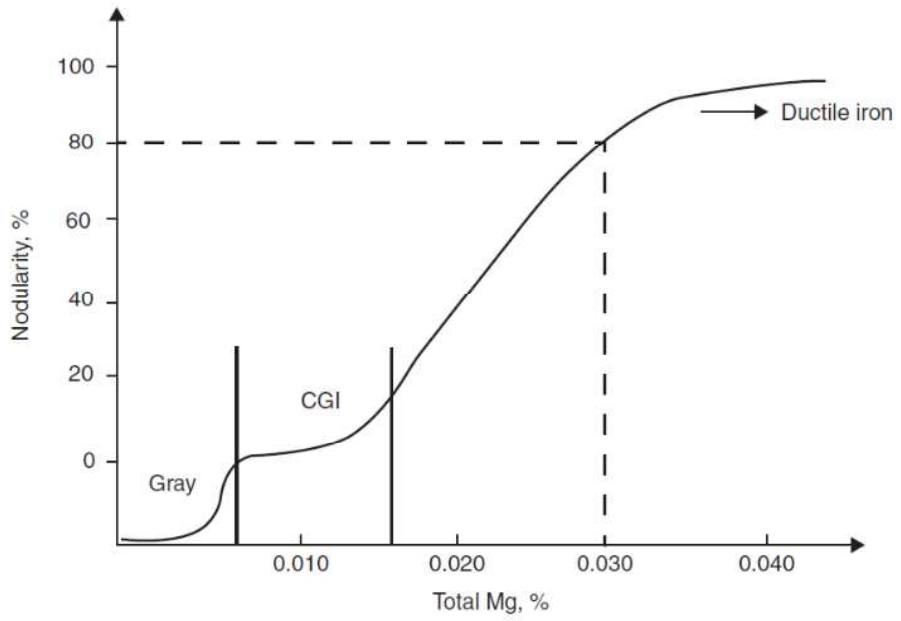

Figure 2.4 The stable CGI plateau exists over a range of approximately 0.008% magnesium and is separated from gray iron by an abrupt transition

The initial starting points must be well separated away from both the sides of plateau. This 'buffer' is critical to restrict/minimize the formation of flake or nodular graphite while pouring. Another challenge is caused by to nonstationary aspect of a stable CGI plateau. If the active oxygen and/or sulfur contents are high, It consumes the active magnesium and shifts the CGI plateau toward higher total magnesium values. Conversely, the CGI plateau shifts toward the left in case the oxygen or sulfur levels are relatively low. Such variation in the composition along with other prevalent casting process variables, make it difficult to fix the CGI chemical specification.

Figure 2.2 shows the roundness shape factor of CGI ("Compacted (Vermicular) Graphite Cast Iron—Classification," 2016) where A_m represents an area of circle of diameter equivalent to the maximum axis length of graphite particle. The "A" stands for the area of graphite particles and l_m represents the maximum length of graphite particles.

The graphite morphology transformation from flake to compacted form is accomplished through base metal treatment with the addition of graphite shape formation elements such as Rare earth, Magnesium, titanium, aluminum, and calcium. The quantity and combination of elements are the functions of the liquid treatment method and many other parameters discussed in the melting process section of "Foundry Practice for Cast Irons" (Davis, 1996). For CGI production, such element amounts are correlated as per Figure 2.5.

The tin, molybdenum, copper, and aluminum alloys used for CGI as-cast morphology change from ferrite to pearlite. Its typical quantities are 0.48% Cu or 0.033% Sn (Fowler et al., 1984), 0.5 to 1% Mo (Ziegler & Wallace, 1984), and up to 4.55% Al (Nechtelberger et al., 1970), (Cooper & C.R. Loper Jr., 1978). Figure 2.6 highlights, that although such alloys are great promoters of pearlite, those are minimally effective in CGI for the Mg content range of 0.04-0.15% (Martinez & Stefanescu, 1983) except Ti whose impact is evident for 95% pearlite generation. Saito et al., (2018) studied the Mg influence on the effect of tellurium for graphite spheroidizing inhibition and found that in Mg samples of 0.020 mass%, the spheroidal nodule shape deteriorates with excessive tellurium content because it consumes Mg which is a spheroidizing element in treatment metal.

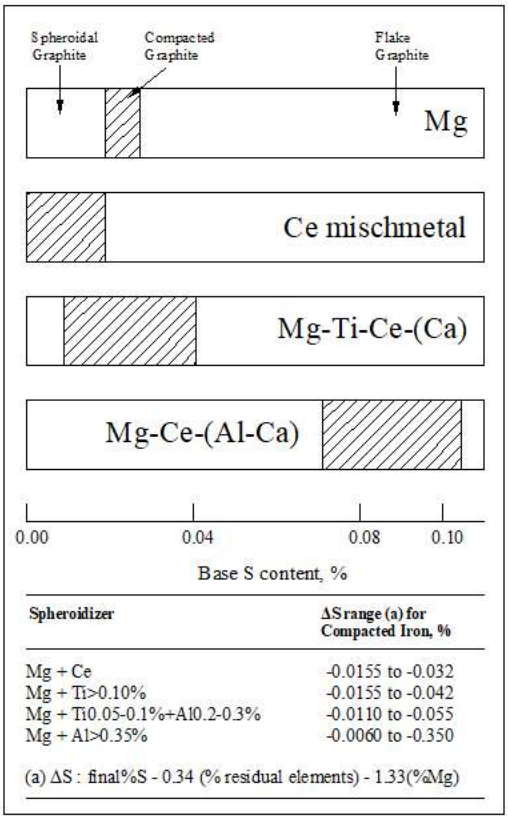

Spheroidizer	ΔS range (a) for Compacted Iron, %
Mg + Ce	-0.0155 to -0.032
Mg + Ti>0.10%	-0.0155 to -0.042
Mg + Ti0.05-0.1%+Al0.2-0.3%	-0.0110 to -0.055
Mg + Al>0.35%	-0.0060 to -0.350

(a) ΔS : final%S - 0.34 (% residual elements) - 1.33(%Mg)

Figure 2.5 Optimised initial sulfur level range as a function of other elements used for graphite compaction. The table highlights the sulfur range, for compacted iron formation with different spheroidizers in an iron composition of 3.5% C, 2.1% Si, 0.75%, Mn, and 0.0.1 to 0.08%

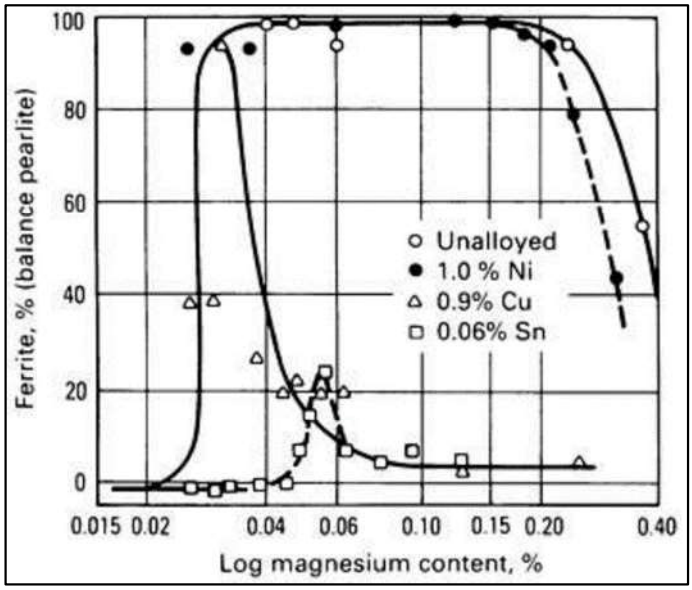

Figure 2.6 The effect of nickel, copper, and tin on composition matrix ranging from CGI to GCI for 25 mm (1in.) wall thickness

Traditionally, it is practiced to produce stable CGI by Ti addition (Renfang et al., 1994) for lower precision and low-volume production. Ti addition prevents nodule formation which widens the stable CGI plateau range. As researched by Schelling R.D., (1969) 0.2% Ti addition stabilizes CGI formation for 50% nodular content. This method is fair where limited machining is required because Ti reacts with carbide which reduces the machinability and tool's life. To overcome the challenges of Ti addition, the researchers (Nechtelberger et al., 1982), (Stefanescu et al., 1979), (QIU & Chen, 2007) have also explored the alternative approach to develop CGI using the addition of Rare Earth (RE) metals instead of Mg. Many salient advantages are using RE metals. Like, i) those are not aggressive in promoting spheroidal graphite formation, ii) Reduce fade rate (Skaland, n.d.) through its more stable oxides and sulphides and, iii) Make molten metal highly reproducible rather volatile Mg added metal. However, RE raw metal prices are costlier than those of Mg. also these are prone to carbide formation, especially for rapid cooling.

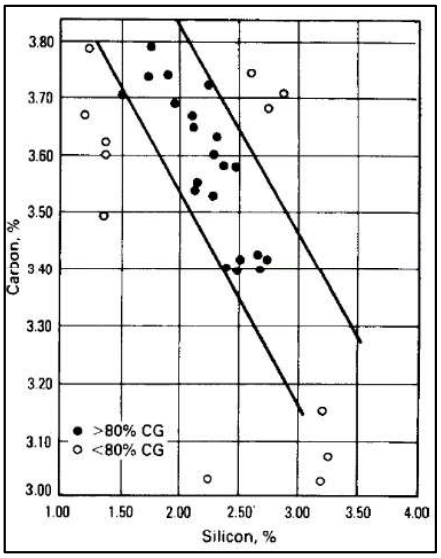

Figure 2.7 The optimum range for carbon and silicon contents for CG iron

Compacted graphite iron characteristics are stated, from hypoeutectic carbon equivalence of 3.7 to hypereutectic carbon equivalence of 4.7, along with silicon of 1.7 to 3.0% and 3.1 to 4.0% of carbon content (Evans et al., 1976), (Sergeant & Evans, 1978), (Cooper & C.R. Loper Jr., 1978). For a given section size, the reciprocal behavior of carbon and silicon influences the casting properties. H.H. Cornell and C.R. Loper Jr., (1985) have investigated optimum carbon and silicon range content as shown in Figure 2.7. Eutectic composition is favorable to achieve the optimum casting properties for the specimen of 10 to 40 mm of thickness.

Typically, CGI is being produced with sulfur with 0.07-0.12% (Ruff & Vert, 1979) content. With such a higher sulfur content, it needs more alloys for metal treatment to balance the residual sulfur in the range of 0.01–0.02% after the treatment (Cooper & C.R. Loper Jr., 1978).

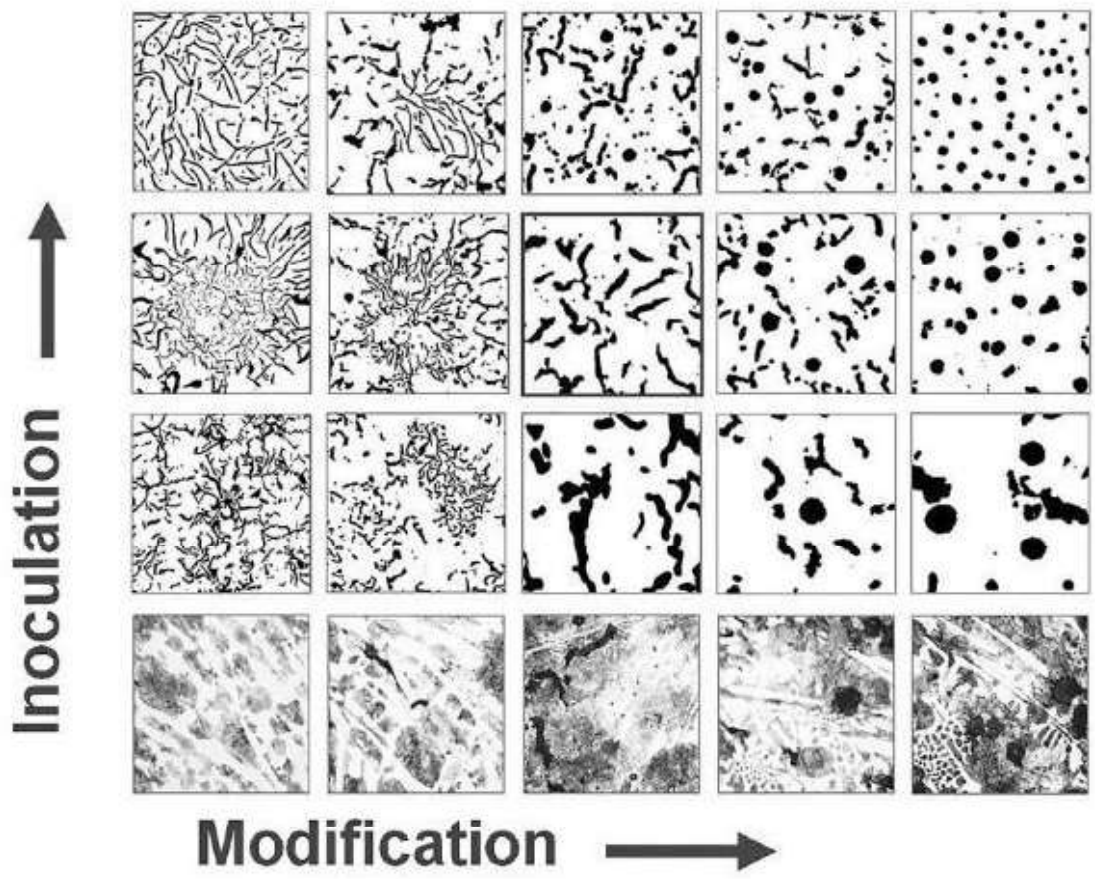

Figure 2.8 The microstructure chessboard per inoculation variation and modification

The inoculant helps to promote graphite precipitation and growth along with iron solidification. Similar to Mg addition, the CGI plateau is also sensitive to the addition of inoculant. The increment of 0.08% of inoculation shifts the CGI plateau toward higher nodularity to gain as much as>30% nodular graphite and conversely forms flakes formation at depleting inoculation. The graphite microstructure change in iron is illustrated in Figure 2.8, which reflects the criticalness of simultaneous control of inoculant and requisite adjustment of chemical elements (magnesium, cerium, lanthanum, calcium, sulfur, oxygen) to ensure reliable CGI production at the industry scale. Hence for reliable CGI production, it is essential to control inoculants simultaneously along with the controlling of graphite

shape-forming chemical elements. S. Dawson, (2002) highlights the iron microstructure behavioural change as a function of inoculation and modification over the CGI stable range as shown in Figure 2.8.

The continuous monitoring of molten metal chemical composition is crucial to control the desired microstructure formation. Traditional foundries are lively in monitoring molten metal composition using spectrometers and controlling the recipe. However, the spectrometer shows the weightage % of each respective chemical; but it has limitations either to extracting the information regarding chemical compounds prevailing for graphite morphology formation or to determining the influence of active oxygen and sulfur content over the resultant behavior of metal with the production process and raw material mixture variation. Conversely, thermal analysis is primarily based on the feedback of the solidification behavior of 200g (7 oz) of a batch iron sample. For precision and high-volume casting production, the chemical analysis technique is not favourable due to defined limitations. Hence, the thermal analysis techniques have been widely adopted (Steve Dawson, 2002), (Anjos et al., 2009).

2.4 Mechanical strengths

The mechanical and physical properties of cast materials are determined by metallurgical characteristics such as chemical composition, graphite shape, the proportion of nodules, and the perlite/ferrite ratio. The increment in nodularity percent enhances both strength and stiffness but has a negative influence on castability, machinability, and thermal conductivity. The intermediate mechanical strength and stiffness exposure by CGI in comparison to GCI and DI are principally promoted by the interconnection bond strength between vermicular graphite, worm shape, and ferrite to perlite transformation (S. Dawson & S. Dawson, 2014). Such typical ranges of ASTM A842 CGI mechanical properties are compared in Table 2.1 with reference to ASTM A48 Class 40 GCI (pearlitic) (“Standard Specification for Gray Iron Castings,” 2022), ASTM A842 (“Standard Specification for Compacted Graphite Iron Castings,” 2018) and ASTM A536-77 (“Standard Specification for Ductile Iron Castings,” 2019) Grade 100-70-03 (pearlitic), and Grade 60-40-18 (ferritic) for DI.

Many standards (“Compacted (Vermicular) Graphite Cast Iron—Classification,” 2016), (“Standard Specification for Compacted Graphite Iron Castings,” 2018), (European Committee for Standardization, 2011) have categorized CGI material grades based on their

mechanical strengths, which are primarily determined by their ferrite to pearlite matrix transition. Their material properties are listed in Table 2.1, with a reference to ASTM 842 ("Standard Specification for Compacted Graphite Iron Castings," 2018) and equivalent BS EN 16079:2011 (European Committee for Standardization, 2011), a European grade.

It is important to note that an increment in pearlite causes a rapid gain in hardness and an increase in nodularity percentage, so EN-GJV-500 has stronger strength than EN-GJV-300 but its machinability is compromised by the simultaneous hardness increase. In addition, the machinability of CGI is impacted by the interconnected graphite bond strength and chemical alloy of magnesium and sulfur (MgS). Therefore, while designing a product for a particular application, it is important to select the appropriate CGI material grade as well as the CGI material itself over GCI.

Table 2.1 Comparative mechanical properties of Cast Irons ASTM A48, ASTM A842, and ASTM A536

Material Standard	Material Grade	Matrix Structure	Tensile (MPa)	Modulus (GPa)	Fatigue (MPa)	Hardness (Brinell)	Ther. Cond. [(W/(m.K)]
ASTM A48	GCI, Class-40	Pearlitic	230-300	105-115	95-115	170-220	45-52
ASTM A842	CGI, 300 (EN-GJV-300)	Ferritic	330-400	135-145	155-185	140-180	40-50
	CGI, 450 (EN-GJV-450)	Pearlitic	410-580	140-150	195-225	200-250	31-40
ASTM A536	DI, 60-40-18	Ferritic	400-550	160-170	180-210	150-190	32-38
	DI, 100-70-03	Pearlitic	550-700	165-175	240-290	240-300	25-32

As experimented by Shao et al., (1998), the 0.2% yield and ultimate tensile strengths of predominant pearlitic cast irons gradually improve with nodularity increment as shown in Figure 2.9, 20-25% sudden drop in the strengths evident in the presence of even small fraction of flake graphite. In Figure 2.9, a negative amount of nodularity represents the flake graphite content of 20% with each -1% of the value and fully flake graphite microstructure with -5% of nodularity. Svensson I., et. al. (2009) have also studied the mechanical properties variation with the change in graphite morphologies.

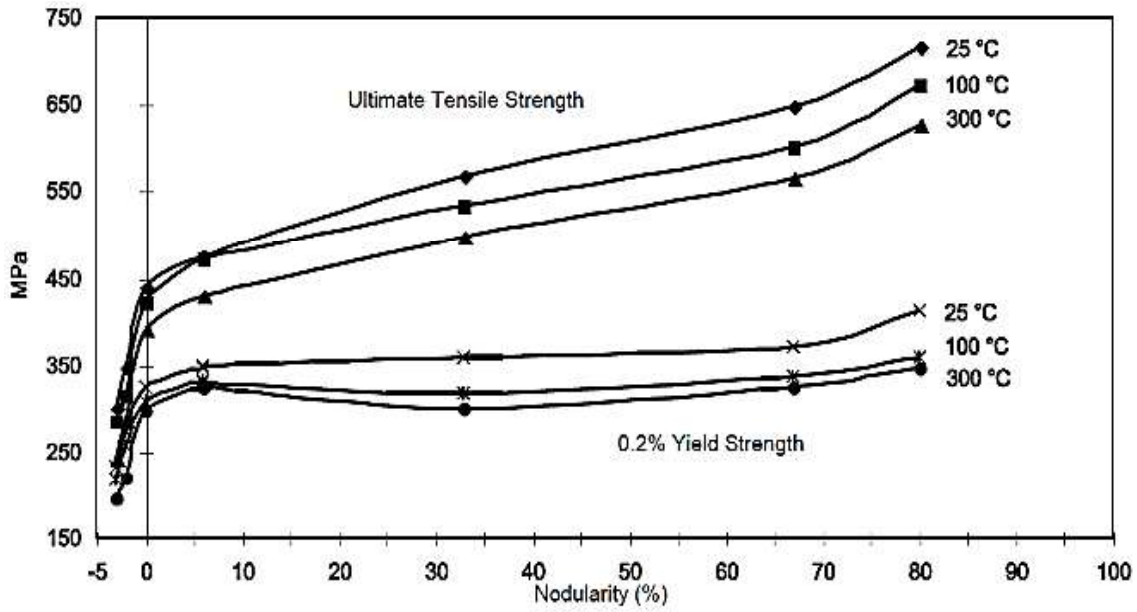

Figure 2.9 85–100% pearlitic cast irons ultimate tensile and yield strengths. Nodularity content <0% denotes the presence of 100% flake graphite in proportion to -5%

The behavior through flake graphite morphology has been studied that tensile strength is deteriorating by 10% for the increment of every 0.1% of carbon equivalent of GCI class-30 (Walton & Opar, 1981). CGI properties in accordance with ISO 16112 grades and ASTM A-842 are tabulated in Table 2.2 and Table 2.3 respectively. It has been studied that the tensile properties of CGI are not as sensitive to variation in carbon equivalent (CE) as for GCI Sergeant & Evans, (1978) but it is evident that strength increases with silicon addition.

Moreover, the variation in tensile to compressive strengths is also being observed in the cast iron material family which is primarily caused by the material stiffness posed through the geometrical shape of graphite content. DI consists of more spheroidal graphite so tensile and compressive strength are almost similar, but CGI shows somewhat dominating compressive strength than tensile, but such difference doesn't vary to a greater extent when compared to GCI. Stefanescu et al., (1983), have studied the tensile-compressive strengths behavior and outlined the comparative data as in Table 1.3. Shao et al., (1998), have conducted experiments to determine the compressive properties of CGI with variation in pearlite content, and its finding are tabulated in Table 2.4. These data suggest that unalloyed pearlite CGI compressive yield strength is approximately 20% higher than GCI (GG 30).

Table 2.2 CGI properties accordance with ISO 16112

Grade	Tensile Strength (MPa)	Yield Strength (MPa)	Elongation (%)	Modulus of Elasticity (GPa)	Thermal Conductivity (W/m°K)
GJV-300	300-375	210-260	2.0-5.0	130-145	47
GJV-350	350-425	245-295	1.5-4.0	135-150	43
GJV-400	400-475	280-330	1.0-3.5	140-150	39
GJV-450	450-525	315-365	1.0-2.5	145-155	38
GJV-500	500-575	350-400	0.5-2.0	145-160	36
For All Grades : Poisson's ratio = 0.26, CTE = $11x10^{-6}$ /K, Specific heat capacity = 0.475 J/g °K (100°C)					

Table 2.3 CGI properties accordance with ASTM A 842

Grade[a]	Min. Tensile Strength (MPa)	Min. Yield Strength (MPa)	Elongation in 50mm (%)	Hardness[b] (HB)	BID[b] (mm)
250[c]	250	175	3.0	179 max	4.50 min
300	300	210	1.5	143-207	5.0-4.2
350	350	245	1.0	163-229	4.7-4.0
400	400	280	1.0	197-255	4.3-3.8
450[d]	450	31.5	1.0	207-269	4.2-3.7

(a) Grades are specified according to the minimum tensile strength requirement given in MPa.
(b) Hardness range is non-mandatory information. Brinell impression diameter (BID) is the diameter of the impression of a 10mm diameter ball at a load of 3000kgf.
(c) The 250 grade is a ferritic grade. Heat treatment to attain required mechanical properties and microstructure shall be the option of the manufacturer.
(d) The 450 grade is a pearlite grade usually produce without heat treatment with addition of certain alloys to promote pearlite as a major part of the matrix.

Pearlite content in iron is one of the critical constituents to define impact strength. It has been observed that at low pearlite (<10%) component has great toughness which drastically reduces with the increment of pearlite, so higher pearlitic CGI offers impact strength close to DI. Charpy impact energy measurement highlights that CGI which has been developed from the base iron of DI has better impact energy absorption than that developed from GCI (Cooper & C.R. Loper Jr., 1978).

Table 2.4 Compressive properties of various CGI configurations (Shao et al., 1998)

Sample	Sample Description	Hardness (BHN 5/750)	E-Modulus (GPa)	0.2% Y.S. (MPa @20°C)	0.2% Y.S. (MPa@400°C)
1	GG 30	190	119	349	297
2	70% Pearlite CGI	207	136	409	332
3	100% Pearlite CGI	240	156	437	370
4	60% Pearlite Mo CGI	190	146	385	312
5	100% Pearlite Mo-CGI	255	148	478	394
6	90% Pearlite Cr-Mo CGI	235	150	432	360

Crack initiation under impact loading generally proceeded in ferritic graphite fracture at its interface by trans-granular cleavage. The graphite fracture predominately occurs along the boundaries of graphite crystallites (Heiber, 1979). Figure 2.10, shows that the ferritic structure absorbs the highest energy over pearlite and austempered structure (Gregorutti & Grau, 2014).

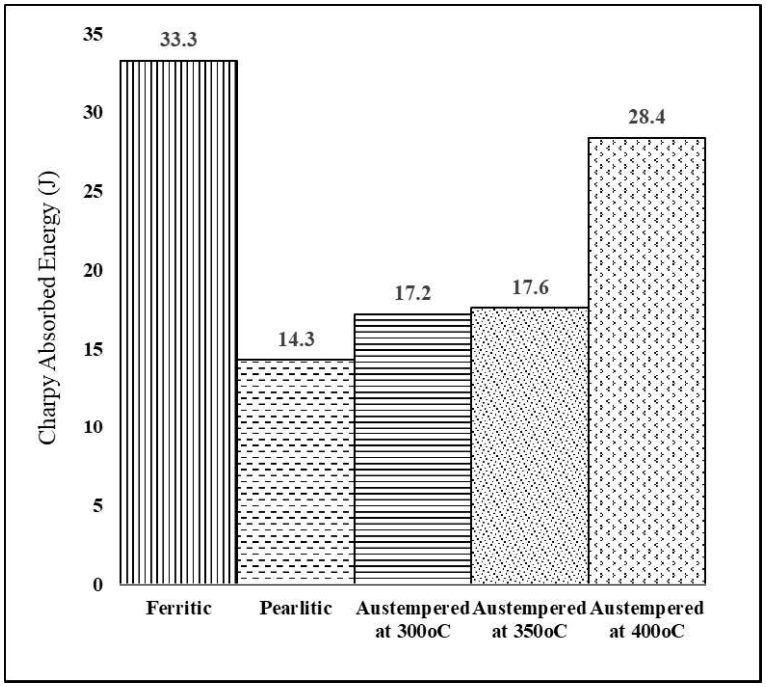

Figure 2.10 Charpy absorbed energy obtained for different metrics

The underlying fatigue behavior is due to repetitive & reversal tension-compression loadings, which prompts premature failure of the substance. The wormed graphite shape of CGI shows prominence against notch sensitivity than flakes graphite. As a result, CGI reveals better fatigue strength than GCI. The pearlitic CGI fatigue limit at room temperature

is close to 200 MPa which degrades further to 155 MPa at 400°C. Such a limit is almost double that of a class 30 GCI. As CGI has excellent thermal capacity, it helps to gain the thermal fatigue strength too to improve the fatigue life which is 200-400% higher than GCI (Y.J. Park et al., 1987). These virtues make CGI the preferred choice for engine cylinder block manufacturing.

Table 2.5 shows the fatigue strengths of CGI with various matrix structures (E. Nechtelberger, 1980). The highest fatigue strength & endurance ratio have been observed in as-cast CGI with >90% ferrite. Superior fatigue strength was evident in un-notched pearlitic structures (Shikida et al., 1986) which have been compared with notched structures in Figure 2.11, which is relatively 25% better than ferritic CGI. The fatigue endurance ratio has been studied to 0.44 -0.46 for a ferritic to a pearlitic higher-nodularity CGI (Loper et al., 1980). CGI & DI were equally notch sensitive for fatigue notch factors of >1.71 whereas GCI is minimally notch sensitive for a notch factor <1. 5 (E. Nechtelberger, 1980). The fatigue behavior of pearlitic CGI is similar to ferritic ductile iron. Whereas, ferritic CGI torsional fatigue limit under fully reversed loading matches DI and has a good correlation with the bending loading behavior (Sumimoto et al., n.d.).

Table 2.5 CGI fatigue properties from rotating-bending tests

Matrix Structure	Graphite Type	Tensile Strength (MPa)	Fatigue Strength (MPa)	Fatigue Endurance Ratio	Hardness HB
As-cast ferrite (>90% ferrite)	95% CG	336	211	0.63	150
As-cast ferrite	CG	388	178	0.46	184
As-cast pearlite	CG	414	185	0.45	205
As-cast pearlite	CG+SG	473	208	0.44	217
As-cast pearlite (70% pearlite)	CG	386	186	0.48	…

The modulus of elasticity (Elastic modulus) of predominate pearlite varies with nodularity content as shown in Figure 2.12 (S. Dawson, 1999). Here as well, the presence of flake graphite deteriorates the elastic modulus like the strength. Nechtelberger et al., (1982) also studied that CGI & DI elastic modulus remains linear at initial loading due to their ductility but this was not true for GCI through its poor ductility due to flake graphite. The pearlitic and ferritic matrices of CGI exhibit a modulus of elasticity, E of 144 GPa, as shown in Figure 2.13 which was slightly lower than DI. This is justified through the shaper & wormed

graphite morphology of CGI than that of spheroidal graphite of DI (Nechtelberger et al., 1982).

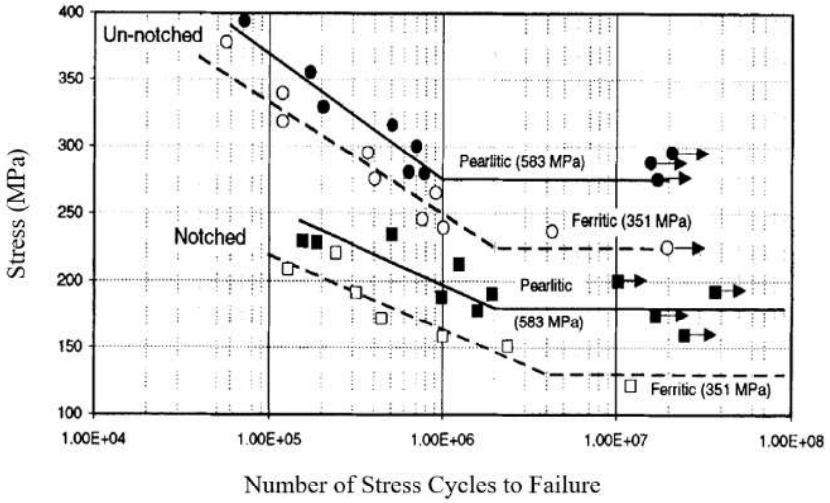

Figure 2.11 Ferritic, pearlitic, and higher-nodularity CG fatigue curves with reference of Table 2.5 data

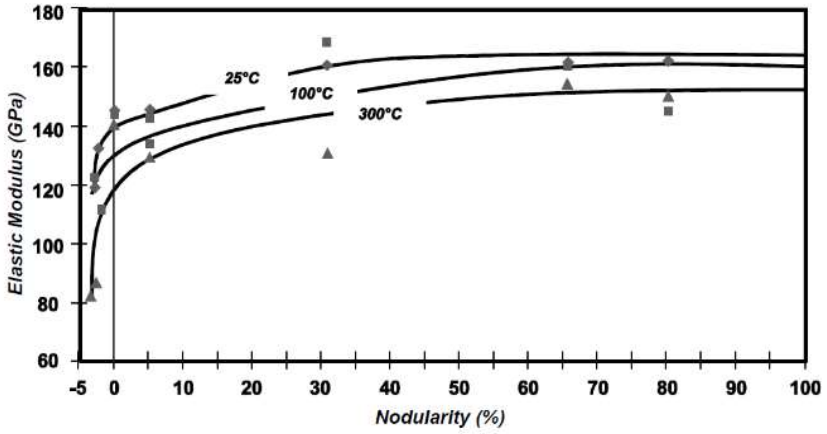

Figure 2.12 85-100% pearlite cast irons elastic modulus with reference to nodularity and temperature

2.5 Physical properties

During the solidification of CGI ferritic matrices formation happens, rather than pearlite due to graphite growth and diffusion. So, to promote pearlite formation, some of the stabilizing elements like copper and tin have to be added in base iron which gains 10-15% superior hardness than GCI. As shown in Figure 2.14, the hardness increment rate is in a linear proportion to the rate of change of pearlite structure with the presence of chromium,

manganese, and titanium, along with other trace elements in the raw materials (Shao et al., 1998). The Brinell hardness remains constant until 90% nodularity.

In GCI, manganese sulfide (MnS) is formed by a sulfur reaction which lubricates the cutting surface whereas, CGI forms the MgS by a reaction of sulfur with faded Mg in molten metal. Such MgS content gains superior hardness over MnS. As a result, machinability is more difficult in CGI than GCI (Ulrich, 2000). A Titanium (0.1-0.2%) is added in CGI as a graphite stabilizer which forms a hard cubic of titanium carbonatite that leads to tool wearing increases subsequently (S. Dawson, 1994). Titanium content increases the drill thrust by 50% relatively for non-titanium bearing (Murthy & Seshan, 1984).

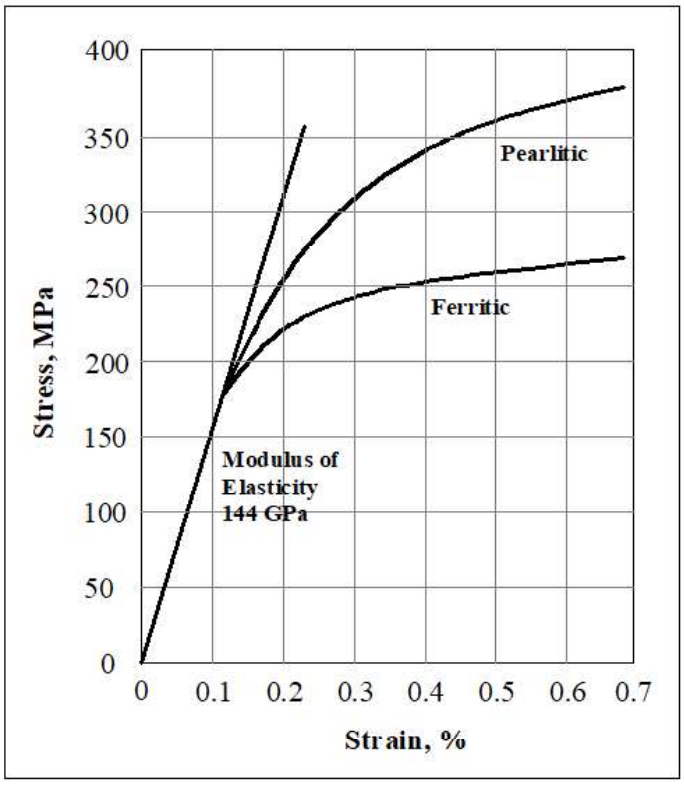

Figure 2.13 Pearlitic and Ferritic compacted graphite iron castings Stress-strain, Image recreated from Nechtelberger et al., (1982)

The damping capacity is the inherent material capacity to absorb the energy of the vibratory body upon impacting force. This is one of the critical properties to expedite its industry-wide application relevance to noise, vibration, and harshness domains. Damping capacity is primarily reliant on graphite shape, nodularity, and forms of microstructures. The dense graphite presence in GCI acts as a damper against vibration and continuously reflects in

flakes. Once flakes of graphite transform to patch, the damping capacity decreases rapidly for CGI and DI (Shao et al., 1998). Relative damping capacities are 1.0:0.35:0.14 for GCI:CGI: DI. Damping capacity also relies on elastic modulus (Kurikuma et al., 1998) but it's not influenced by carbon and pearlite content (Shao et al., 1998). However, this can vary within 5-10% with a change in graphite size and density (Sergeant & Evans, 1978).

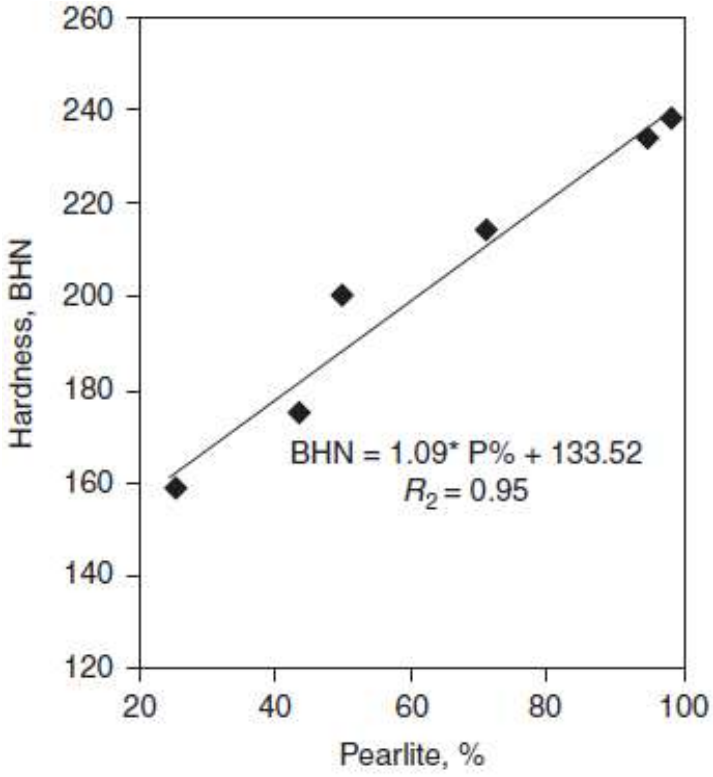

Figure 2.14 0-20% nodularity CGI Brinell hardness with reference to pearlite

The molten cast iron fluidity is widely dependent on the carbon, silicon contents, and instantaneous temperature. However, the morphology of the structure also matters on top of these variables. Flake graphite iron has superior fluidity as compared to spheroidal graphite iron. CGI can be easily poured into thin sections with higher carbon equivalent.

CGI casting offers better shrinkage and eliminates the porosity as compared to DI because of wall movement tendency during its preparation Figure 2.15, shows a comparative study among various irons. The shrinkage volume is 4.1% for FGI, 4.8% for CGI, and 7.0% for SGI for eutectic cast irons (Sergeant & Evans, 1978). Dimension change due to solidification expansion is 4.4 for SGI, and 1.0-1.8 for CGI with reference to 1.0 of FGI (Stefanescu et al., 1979). Generally, CGI has a greater casting yield because of the riserless gating system.

The cooling zone develops at the interfacing of the superheated metal and cold mold wall. Metal is rapidly solidifying near the cooling zone. There is a broader opinion that CGI has an intermediate chilling tendency but as shown in Figure 2.16, it has the highest chilling tendency because its effect intensifies for 6 to 64% of nodularity (Stefanescu et al., 1983).

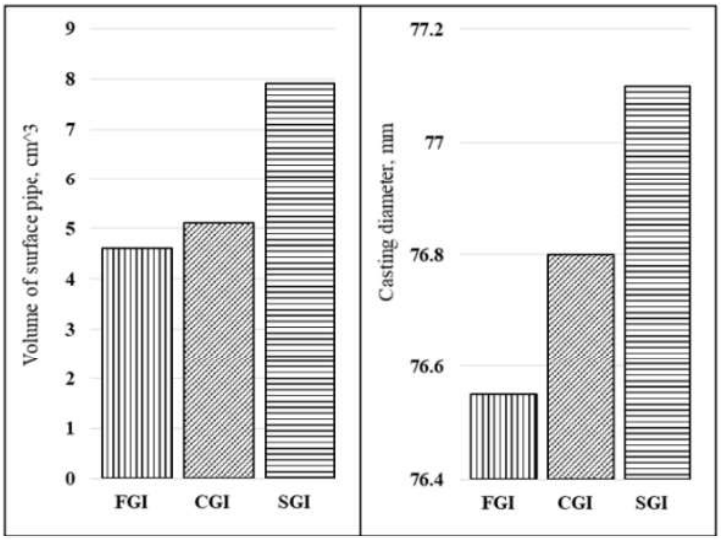

Figure 2.15 Volume shrinkage and Dimensional change comparison for irons poured in green sand molds. Image recreated from Sergeant & Evans, (1978)

The study extends a microstructure-based thermal conductivity model from pearlitic LGI to CGI and ferritic–pearlitic LGI. It uses a thermal resistance network to represent heat flow through eutectic cells and their boundaries, emphasizing the role of graphite connectivity and hydraulic diameter. The model accurately predicted thermal conductivity across samples with varying nodularity, with less than 4% deviation from experimental data. Silicon segregation was found significant at low Si content. The model's applicability to both LGI and CGI highlights its general relevance, offering valuable insights for optimizing cast iron microstructures to achieve desired thermal performance (Belov et al., 2024).

Influence of cutting parameters and graphite morphology on surface quality of compacted graphite iron, highlighting the role of cutting speed and tool wear in defect formation and plastic deformation behavior during face milling (Niu et al., 2025).

Influence of cutting-induced stresses outweighs microstructural differences in CGI; thick CVD coatings enhance tool life, highlighting the need for an integrated approach to tool selection under extreme roughing conditions (Esposito et al., 2025)

2.6 Production process

There are approaches to ensure CGI production either using spheroidizing element Mg in GCI as a base iron or using anti-spheroidizing element Ti in DI - to develop the intermittent CGI microstructure. Steve Dawson, (2002) has studied that addition of 0.001% Mg in base metal, the flake patch structure can be transformed into a fully compacted microstructure, which enhances ultimate tensile strength to 450 MPa from 320 MPa by conversion of fully pearlitic from flake patch microstructure.

Residual Mg% promotes nodularity in the thinner section but in the thicker section, the solidification rate deteriorates which fades residual Mg% effectiveness for nodularity. The empirical formula Eq. (1) has been derived to estimate the nodularity in the produced alloys of 10–50 mm of section thickness (Kim et al., 2009).

$$Nodularity\ \% = 3091.4 \cdot Mg\% + 50 \cdot Mg\% \ (x - 30) - 9.5 \qquad (1)$$

For 0<Mg%<0.03

Where,

Mg %= Residual Mg content

x *= Casting thickness in mm*

Titanium, Ti acts as an anti-spheroidizing element to promote compacted graphite shape along with pearlite content. Ti is capable of forming carbide; as a result, pearlite content also gains simultaneously. It is studied that 0.15wt% of Ti addition improves 10% of the compacted graphite content while 5-10% of pearlite content (Shy et al., 2000). However, pearlite content reduces with specimen thickness increases. Ti addition helps to widen the CGI stable range for Mg for successful CGI production. An anti-spheroidizing element is a reliable approach for CGI development, it has limited exposure for certain precision manufacturing applications because Ti tends to form carbide and nitro-carbide which makes the metal very hard and impacts the machinability and tool life. Alonso et al., (2020) have been studying how the graphite nucleation is influenced by the addition of Ti in CGI formation by restricting the growth of Mg–Ca sulfide.

The inoculant helps to promote graphite precipitation and growth along with iron solidification. Hence for reliable CGI production, it is essential to control inoculants simultaneously along with the controlling of graphite shape forming elements (magnesium,

sulfur, lanthanum, calcium, cerium, oxygen). Figure 2.8, highlights the iron microstructure behavioral change as a function of inoculation and modification over the CGI stable range. Regordosa et al., (2019) have studied the impact of inoculation and other chemical composition on CGI microstructure change while solidification.

The spheroidizing element addition practice is quite crucial to ensure the minimal fading of the element post-metal treatment. Because such elements are highly volatile and fade rapidly. There are primarily sandwich and injection treatment methods practiced for Mg addition in molten metal. The sandwich method is quite reliable over the injection method because it helps to prevent the evaporation of Mg to intact its influence on nodule formation.

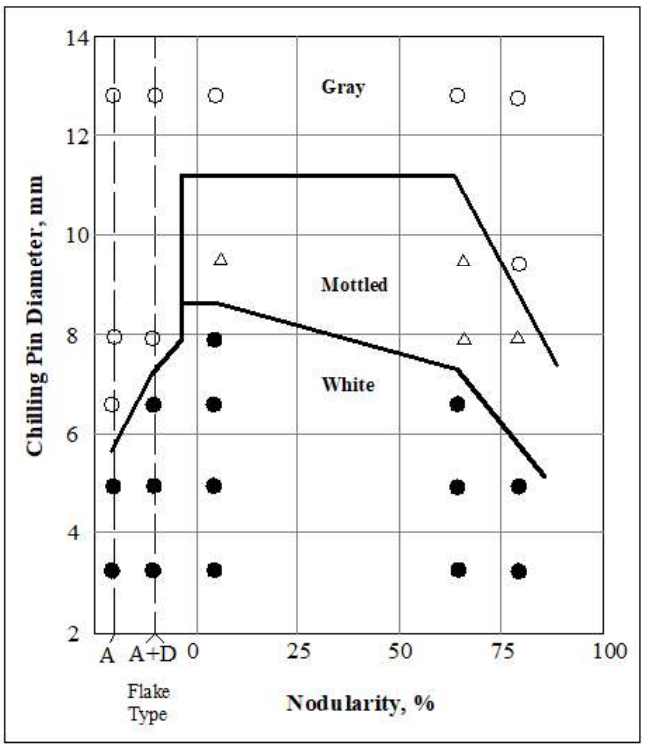

Figure 2.16 Graphite shape influence on cast iron chilling tendency. Type A uniformly distributed and randomly oriented graphite flakes. Type D, Inter-dendritic segregated and randomly oriented graphite flakes. Image recreated from Stefanescu et al., (1983)

The CGI has better castability than DI due to lower Mg content so the chances of having casting defects such as cold shuts, misruns, and any defects pertinent to shrinkage and porosity, are significantly reduced. The porous defects are desirable for some of the special applications where they need high strength and greater energy absorption capacity at a lightweight. S. Dawson et al. (2009) have proposed a method to develop porous CGI

castings. The shrinkage sensitivity is quite progressive with increments of nodular & Mg content for GCI to DI transformation.

Re-melting of base material has high nodularity (around 96%) and high residual percentage of Mg (≈ 0.065%). With residual Mg control, the nodules transit to CGI with increased holding time. Figure 2.17 shows vermicular graphite follows linear development along with holding time.

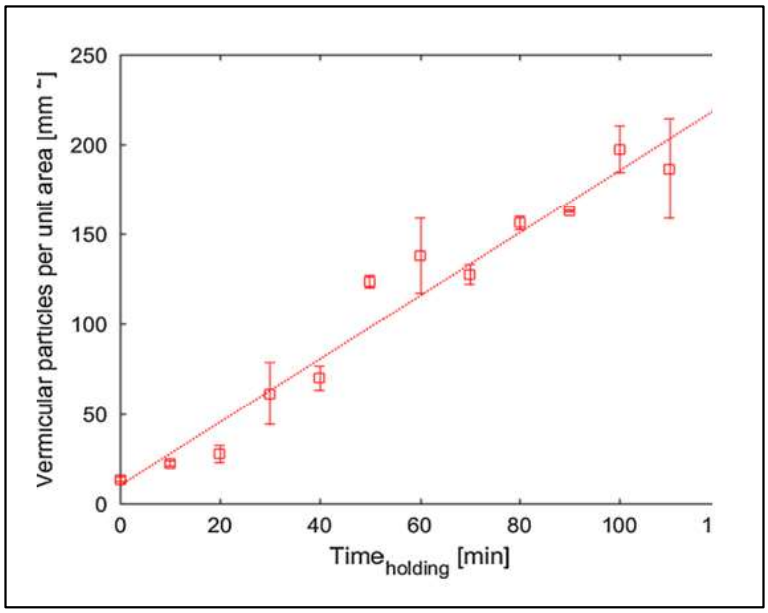

Figure 2.17 The effect of holding time on nodularity (Hernando, 2017)

2.7 Production process control

Apart from appropriate chemical addition as a part of metal treatment, it is simultaneously crucial to ensure the adoption of rigorous real-time process monitoring and control philosophy. Typically, foundries need to focus on two aspects, i) Appropriate base metal treatment approach, and ii) Base metal treatment monitoring & control while establishing the CGI production process.

Traditionally, it is practiced to produce stable CGI by Ti addition (Renfang et al., 1994) for lower precision and low-volume production. Ti addition prevents nodule formation which widens the stable CGI plateau range. As researched by R.D Schelling (1969), 0.2% Ti addition stabilizes CGI formation for 50% nodular content. This method is fair where limited machining is required because Ti reacts with carbide which reduces the machinability and tool's life. To overcome the challenges of Ti addition, the researchers (Nechtelberger et al.,

1982), (Stefanescu et al., 1979), (QIU & Chen, 2007) have also explored the alternative approach to develop CGI using the addition of Rare Earth (RE) metals instead of Mg. Many salient advantages have been found in using RE metals. Like, i) those are not aggressive in promoting spheroidal graphite formation, ii) Reduce fade rate through its more stable oxides and sulfides and, iii) Make molten metal highly reproducible rather volatile Mg added metal. RE raw metal prices are costlier than those of Mg and also these are prone to carbide formation, especially for rapid cooling.

The continuous monitoring of molten metal chemical composition is crucial to control the desired microstructure formation. Traditional foundries are lively in monitoring molten metal composition using spectrometers and controlling the recipe. However, the spectrometer shows the weight percentage of each respective chemical. It has limitations in extracting information about the chemical compounds involved in graphite morphology formation. Additionally, it cannot determine the influence of active oxygen and sulfur content on the resultant behavior of the metal, considering variations in the production process and raw material mixture. Conversely, thermal analysis is primarily based on the feedback of the solidification behavior of 200g (7 oz) of a batch iron sample (Shao et al., 1998). For precision and high-volume casting production, the chemical analysis technique is not favorable due to its defined limitations. Hence, the thermal analysis techniques have been widely adopted (Steve Dawson, 2002), (Anjos et al., 2009).

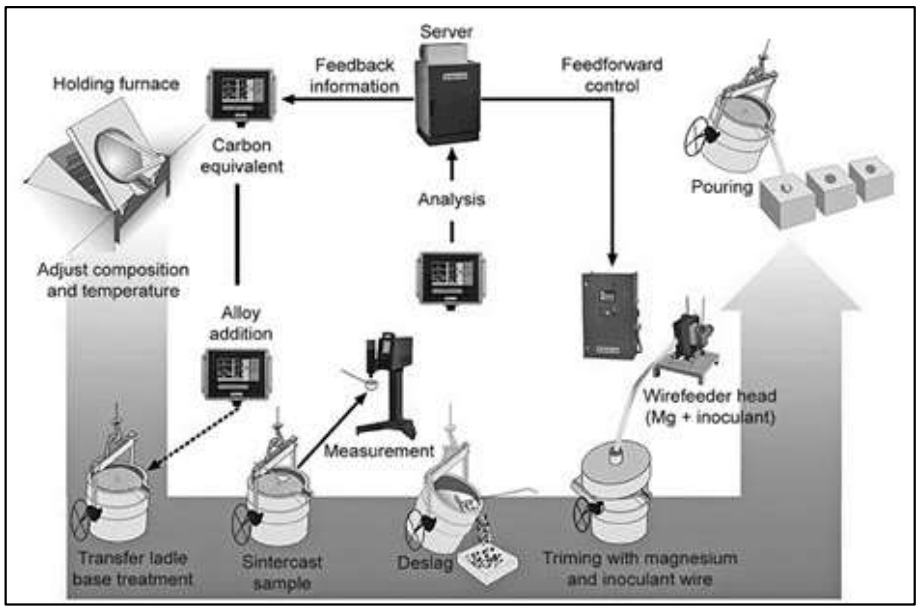

Figure 2.18 Typical CGI production process flow

This technique works on thermal analysis measurement of molten metal after the addition of inoculant and modifying (Mg, RE, Ti) elements. Upon feedback of thermal analysis, magnesium and/or inoculant is added in the form of core wire as a corrective action, before pouring. The SinterCast has innovated a state-of-the-art thermal analysis control system that works on tightly integrated feedback-enabled process flow as shown in Figure 2.18 (Steve Dawson, 2002). In this process, the microstructure is correlated with reference to graphite growth and latent heat released by solidifying samples in the bespoke (Guesser et al., 2001) container. The SinterCast thermal analysis sample is obtained by immersing the steel-walled sampling device shown in Figure 2.19 into the molten metal after the base treatment.

D. Stefanescu (2015) has explained the conventional cooling curve-based direct thermal analysis technique using a sand cup. Unlike sand cups, metallic cup device helps to avoid oxidation during iron pour-in and lead for precise measurement of undercooling. A reactive material has been layered on the inner surface of a sampler to enable Mg fading measurement. The sampling device has been built with a couple of reusable thermocouples which have been placed at the bottom and thermal center. The thermocouples placed at the bottom predict the iron behavior after 0.003% of Mg fading whereas the central one determines the treated base iron. As shown in Figure 2.20 (Guesser et al., 2001), The etched cross-section of SinterCast samples, and undercooled D-type flake graphite formation took place due to loss of active magnesium. The flake graphite content impacts the thermal analysis cooling curve which is referred to by the bottom thermocouple. This brings uncertainty to outline the abrupt transition between CGI and GCI.

2.8 Product simulation

The simulation of compacted graphite iron (CGI) products using ANSYS Inc., (2022), a powerful finite element analysis (FEA) software, has been extensively employed for simulating and analyzing various engineering applications (Wu et al., 2019), (Lei et al., 2011), including the behavior of product made of CGI materials. The focus of ANSYS-aided simulation remains to assess the opportunity to optimize the product using CGI material as compared to GCI and DI to evaluate the cost-saving possibilities – in a way to determine the competitiveness.

Optimization studies have been conducted to enhance the design and performance of CGI components. ANSYS provides a platform for parametric analysis and optimization, enabling

researchers to identify the most influential design parameters and their impact on the final product's performance. This approach facilitates the development of CGI materials with improved mechanical strength, thermal stability, and overall efficiency.

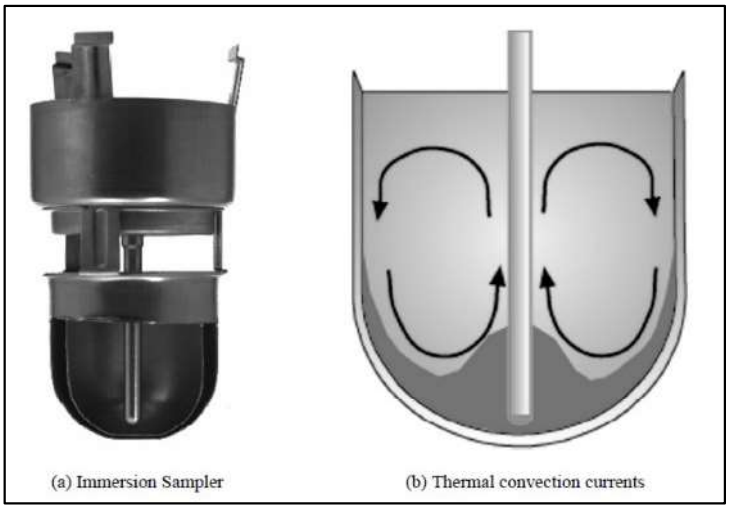

Figure 2.19 The immersion-type sampler

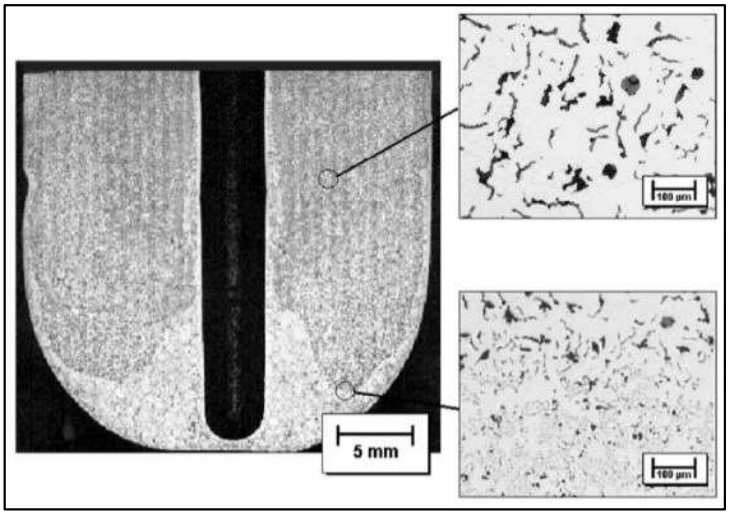

Figure 2.20 SinterCast probe and Mg reaction

2.9 Literature summary

Despite a lengthy history of ferrous material production in foundries, the graphite transition features from flakes to vermicular to spheroidal, or vice versa, are still a very sensitive criterion. The production of CGI mandates the need for accurate metal treatment processes which presents a critical challenge to achieve optimal microstructure and maintain quality production. The problem is defined in terms of the correct balance of magnesium (Mg) in

the iron to create the desired compacted graphite vermicular microstructure maintain the same balance throughout the process and mitigate the issues associated with high Mg-content.

The CGI quality is ensured by an appropriate quantity of magnesium in addition to the desulfurized base iron. A precise amount has been required to stabilize the CGI within a Mg-range of 0.008%. When the magnesium content is too low, flake-type graphite has been formed which reduces the strength and stiffness by 20-30%. When the magnesium content is too high, it induces high nodularity which increases the strength and stiffness of iron. It reduces thermal conductivity & machinability and also worsens issues related to shrinkage. Magnesium fading presents an additional problem. During production, the magnesium content may decrease due to the evaporation of 0.001% Mg every five minutes, which forces the foundries to avoid working too close to the low-Mg side of the CGI range.

The foundry process has evolved through the integration of continuous monitoring and control technologies (thermal analysis) by SinterCast, Sweden, especially for CGI production. There is great potential to investigate the intrinsic behavior of CGI microstructure formation under monitoring casting parameters such as chemical composition, holding time, and temperature using traditional foundry processes.

Therefore, the quality and mass production of CGI is hampered by the inherent difficulty of maintaining the magnesium balance and the resulting microstructural issues. Traditional foundry practices have somewhat lack off required precision, consistency, and real-time monitoring capabilities to ensure the optimal magnesium content throughout the process. A robust solution to maintain the right balance of magnesium to achieve the ideal microstructure and maintain quality production of CGI is a significant opportunity for research in a step to make CGI a viable material for the industry's needs.

2.10 Research gap

It is observed that there is great consensus among the researchers about the CGI microstructure, chemical composition, and production process sensitivity. However, limited efforts have been made to overcome the known production challenges. During such research study, it has been attempted to survey the feedback from many reputed foundries and foundry experts for CGI casting development and noticed the confidence level deficiency for same.

This may be due to limited exposure and uncertain process control. Still, some of the market players only could succeed in establishing thermal analysis feedback-based process control technology and very limited information is available to the public about intrinsic working philosophy. Apart from this technique, there is no credible alternative process that has been innovated so far. Such production limitations restrict the industry's enthusiasm to expand the CGI application base.

Hence, a great opportunity exists to conduct an extensive investigation to bring insight into existing process control technology. This process knowledge may help further to innovate a viable CGI production process and its control philosophy which can be afforded by traditional metal foundries across the globe.

2.11 Objectives of present work

The objective of this research is to gain a greater insight into CGI microstructure formation and innovate the production process which enables access to the traditional foundry practices in a direction to make viable materials to tap the abundance of opportunities lies for many of the industrial applications.

The main objectives of this research are:

- To explore the intrinsic behavior of CGI microstructure transformation due to its crystalline restructuring.
- To establish casting monitoring and control process, while enabling CGI production utilizing a traditional foundry setup.
- Realize the sensitivity of CGI microstructure transformation in the presence of various chemical additives and foundry process parameters.
- Product design assessment using CGI to unveil the potential design optimization opportunities for cost-effective product development in comparison to GCI and DI.

2.12 Scope of present research work

The scope of work of current investigation are:

1) A comprehensive literature review to understand the intrinsic behavior of CGI

microstructure transformation under prevailing boundary conditions and recent advancements in CGI production unveils the potential of the research gap.

2) Experiment investigation for potential production approaches to develop CGI and establish a reliable & viable production process, to enable the traditional foundry practices and setup.

3) Characterization of developed CGI.

4) Commercial evaluation of created CGI for cost-effective centrifugal pump volute product creation through comparison studies with GCI and DI.

CHAPTER 3

COMPACTED GRAPHITE IRON PRODUCTION USING TRADITIONAL FOUNDRY PRACTICES

This research focuses on thoroughly investigating and establishing the manufacturing process of Compacted Graphite Iron (CGI) using traditional foundry practices. The main goal is to evaluate and establish a consistent and cost-effective procedure for CGI production within a traditional foundry setup. The researcher has explored various molten metal treatment methods, adjustment of chemical compositions, spheroidizing element concentrations, holding time, pouring temperature, and operating procedures. The aim is to understand the impact and identify necessary adjustments for the formation of CGI microstructure.

3.1 Production process

CGI microstructure stabilization range is too narrow, so it poses a great challenge to maintain a consistent microstructure for mass production in a foundry. A commercial CGI grade has been specified for 10-20% of nodular graphite particles without any graphite flakes. The stable range is found for approximately 0.008% Mg. But in reality, Mg content is even lower because active Mg fades at a rate of 0.001% per five minutes. The active oxygen and/or sulfur content consumes the active Mg which moves the Mg stable range to the higher side.

The inoculant helps to promote graphite precipitation and growth along with iron solidification. Similar to Mg addition, the CGI plateau is also sensitive to the addition of inoculant. The increment of 0.08% of inoculation shifts the CGI plateau toward higher nodularity to gain as much up to>30% nodular graphite and conversely forms flakes formation at depleting inoculation.

Apart from accurate chemical composition, there are many uncertain variables like foundry process control, and workmanship plays a crucial role in producing consistent CGI. Hence, it is not advisable to rely only on the sandwich method, a one-step base metal treatment process for spheroidal Mg element addition has been tried in the current investigation. It is preferred to adopt a measure-and-control kind of two-step-controlled treatment approach to mitigate the risk posed by defined uncertainty. In this procedure, it is essential to comprehend the solidification behavior of molten metal after the completion of the initial treatment process. The residual nodular-controlling elements have been then introduced to achieve the desired solidification behavior. Ultimately, this two-step treatment process effectively mitigates the risk of graphite flake formation. Implementing real-time monitoring and control of base metal elements requires the adoption of state-of-the-art control technologies, which proves challenging for traditional foundries.

3.2 Experimental procedure

The current experimental investigation requires specific equipment and materials have be managed according to requirements. The establishment of a foundry setup for conducting the proposed experiments is costly as well as time-consuming. Therefore, the experiments have been carried out at well-established foundries such as Himcast, Halol, and Nodule cast-Vadodara to alleviate these resource-intensive requirements.

- Basic foundry setup: Furnace, sandwich ladle, Crucible, molds, K-type thermocouple, Graphite stirrer, casting tools, etc.

- Raw materials: Cold rolled close annealed (CRCA) scrap, High-quality pig iron, Foundry return (FR), Iron sulfide (FeS), FeSiMg (Ferrous silicon magnesium) and Cold-rolled coil (CRC) chips

- Inoculant: CaSi (Calcium Silicon)

- Analytical tools: Spectrometer for chemical composition analysis, Optical microscope for microstructure and image analysis, Scanning Electron Microscope (SEM) for 3D image, hardness tester, tensile strength tester (UTM)

3.2.1 Material selection

- Assemble all the necessary materials and ensure that safety equipment is worn at all

times throughout the experiment.

- Clean the furnace and ensure it's in proper working condition.

- Prepare the charge materials according to the mixture ratio for CGI: CRCA, FR Pig Iron, FeS, CRC chips, FeSiMg. Figure 3.1 (a) shows Ferrous Sulphide (FeS) powder, it acts as a nucleating agent for the formation of CGI during solidification and which is encourages the formation of CGI rather than FGI.

(a) (b)

(c) (d)

(e) (f)

Figure 3.1 Experiment preparation: (a) Ferrous Sulphide (FeS), (b) Pig Iron, (c) FeSiMg, (d) CRC Chips, (e) FR, and (f) CRCA

3.2.2 Experimental setup

In the current investigation medium frequency Induction furnaces have been used. Heat the induction furnace and add the prepared mixture of raw materials. The temperature has been closely monitored using a pyrometer, aiming for a melting temperature around 1350°C to 1550°C. The molten metal is stirred periodically to ensure uniform melting and mixing of the charge materials. Once the temperature reaches a suitable temperature, molten metal is ready for sandwich treatment using a compliant ladle.

Such sandwich treatment technique is utilized to ensure adequate magnesium recovery post magnesium alloy addition in molten metal. For this technique, partitions bottom creates pockets where magnesium alloy is placed and covered through CRC chips (2-3% of metal weight) before metal treatment. The molten base metal out of the furnace poured into a ladle away from the pocket. Once the sandwich treatment has taken place, the entire mixture is stirred well through a graphite stirrer to ensure appropriate mixing. During such a treatment process, it is critical to control the appropriate quantity of Magnesium alloys in addition to ensuring the desired graphite morphology formation. Figure 3.2 (a) shows the experiment setup at Himcast foundry, Halol and Figure 3.2 (b) and (c) show the sandwich crucible and graphite stirrer respectively. For the melting process ensure a range of temperature remains between 1350°C to 1550°C. The prepared molten metal has been used for sandwich treatment by using a compliant sandwich ladle. After the alloying process, the nodulizing elements FeSiMg have been added in appropriate proportion. This is to foster nucleation sites for graphite precipitation.

The nodulizing process should transform the graphite flakes in the iron into rounded, compacted shapes. The amount of magnesium added in the alloying step is crucial in controlling the shape of the graphite precipitates. Figure 3.3 (a), (b), and (c) shows heated charge material, measured temperature with a pyrometer, and prepared crucible for preheating respectively.

(a) (b) (c)

Figure 3.2 Melting of the molten metals (a) Melting in induction furnace, (b) Partitioned ladle, and (c) Graphite stirrer

The sand mold cavities have been prepared by industry-standard procedure. The prepared molten CGI has been poured into it and allowed to solidify to prepare button sample size specimens as shown in Figure 3.4 (a), (b), and (c) show the sand mold preparation and pouring the molten CGI into molds and allowing it to solidify respectively. The molten metal solidifies, and samples have been removed from molds and cleaned for further treatment.

(a) (b)

(c)

Figure 3.3 Melting of the molten metals (a) Heating of molten metal (b) Realtime temperature measurement and (c) Prepare crucible for heating

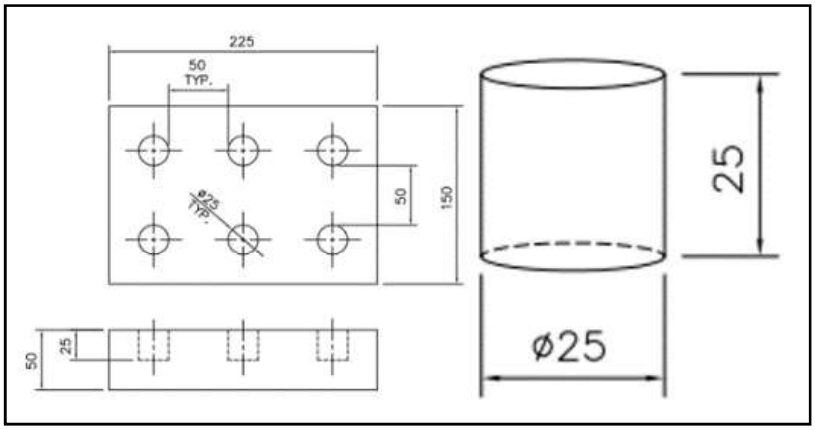

(a)

(b) (c)

Figure 3.4 Melting of the molten metals (a) Button sample size, (b) Sand mold preparation, and (c) Poured specimens

Testing and analysis

After the CGI cooled, a spectrometer is utilized to perform a chemical composition analysis to verify if the metal meets the required specifications. The cast specimens have been reformed for microstructure examination using a metallurgical microscope. This allows you to assess the shape of the graphite and the iron matrix. The hardness test and a tensile strength test to assess the mechanical properties of the CGI have been performed. Later, compared the results quality with CGI standards specifications.

Data recording

Record all measurements, observations, and results in a lab notebook, ensuring comprehensive documentation of all aspects of the experiment. This includes detailing the quantity and ratios of raw materials and additives used, as well as the temperatures at various stages of the process. Additionally, include results from the microstructure analysis, noting the shape and size of graphite particles and the condition of the matrix. Mechanical properties, such as hardness and tensile strength, should also be recorded. Furthermore, document any difficulties or issues encountered during the experiment, along with any deviations from the planned procedure, to ensure a thorough and accurate account of the experimental process.

Acceptance criteria

Achieving the desired quality of CGI through conventional foundry practices is essential to meet industry standards. The CGI should exhibit a well-balanced microstructure featuring compacted graphite nodules accordance to ASTM A247-19 Type IV ("Standard Test Method for Evaluating the Microstructure of Graphite in Iron Castings," 2019), along with favourable mechanical properties such as tensile strength and hardness inline to ISO 16112 ("Compacted (Vermicular) Graphite Cast Iron—Classification," 2016) and equivalent ASTM A842 ("Standard Specification for Compacted Graphite Iron Castings," 2018). The production process must be both cost-effective and efficient. To enhance the overall quality parameters, it is essential to consider improvement in the casting process for optimization.

3.3 Metal treatment approaches

3.3.1 Experimental iterations

Hereby various experiments have been conducted by exploring many of the potential molten metal treatment methodologies by making variations in chemical composition, metal treatment process, and operating procedure, to assess their impact and required essential adjustment enabling CGI microstructure formation.

Iteration 1: Pure sulfur addition in ductile iron

In this investigation initially experiment had been performed at Parvati Techno Cast Pvt. Ltd., Vadodara. CGI was produced using a process similar to that of ductile iron, maintaining 0.008% Mg based on the empirical formula per Eq. (2):

$$\%Mg = 16.2\ \%\ S + 0.25(+/-\ 0.1)\ \% \qquad (2)$$

According to this formula, 0.01% sulfur was added to 1 kg of prepared molten metal to achieve the target residual Mg range of 0.008%. In this process, Ductile Iron 400-15 grade charge material have been heated in an induction furnace at 1350ºC. Once the molten metal reaches the desired temperature it goes through sandwich treatment. After sandwich treatment pure sulfur was added and thoroughly stirred. The treated molten metal was then poured into a chilled mold for chemical analysis and microstructure examination.

The cast samples were tested at Met Heat, Vadodara. The results comparing samples cast with sulfur and without sulfur indicated a fading effect. Microstructural analysis at 200X magnification revealed an interdendritic pattern of austenite and carbide.

Iteration 2: Iron sulfide (FeS) addition in ductile iron

Charge iron was heated in an 800 kg/500 Hz induction furnace at Himgiri Casting Pvt. Ltd., Halol. The charge consisted of 40% scrap iron and 60% ductile iron returns, with a maximum sulfur content of 0.02%. The iron was treated with 5-6% FeSiMg nodularizer using the sandwich technique, followed by ladle inoculation with 0.8% CaSi. After the pre-inoculation process, 0.002% sulfur was added to the crucible along with 4 kg of treated molten metal at 1420°C, which was then stirred well for 1-2 minutes. The molten metal was cast into round pieces (1 inch diameter by 1 inch length) in sand molds. The holding time between the Mg

treatment and pouring into the molds did not exceed 9 minutes.

The results of the cast samples indicate that increasing the holding time decreases the temperature of the molten metal. Chemical analysis of the cast samples shows that the residual Mg content was in the range of 0.03% to 0.088%. These results did not meet our target residual Mg range.

Once iteration 1 and 2 results do not comply with the rated material specification while performing further iteration 3, the sandwich method and simultaneous measure-and-adjust treatment strategy have been adopted to preserve the critical chemicals like. active Mg, and Sulfur. Such methodologies are classified as Method-1, 2, and 3. Apart from this, during all phases of molten metal treatments charge material temperature changes have been keenly observed. All such material treatments have been performed at a laboratory scale using a batch of 50kg of base iron material which had chemical specifications as mentioned in Table 3.1, Table 3.2, and Table 3.3. The base iron material has been melted until 1550^{o}C using a 500Hz induction furnace. During the melting over the furnace, periodic chemical composition and instantaneous temperature have been closely monitored.

Here, three different metal treatment methods have been explored by following the process flow depicted in Figure 3.5.

Such methods follow:

i. Method 1: Mg addition by sandwich treatment
ii. Method 2: Sulfur addition in ductile iron post Mg treatment
iii. Method 3: Mg and CaSi inoculant addition

3.3.2 Method-1: Mg addition by sandwich treatment

During this process, attempts have been made to produce CGI using the least magnesium alloy addition to the sandwich treatment process because magnesium is suitable for deoxidation treatment which causes flake to spheroidal graphite formation while utilizing cast iron base metal. The material's chemical composition is shown in Table 3.1.

The base iron material composition is primarily of ductile iron nature so that Mg addition makes sense to desulfurize base iron to produce CGI. It is known that Mg fades rapidly while molten metal treatment as a result, the availability of active Mg varies for 40-60% (Simmons, 1976) of initial addition post-recovery.

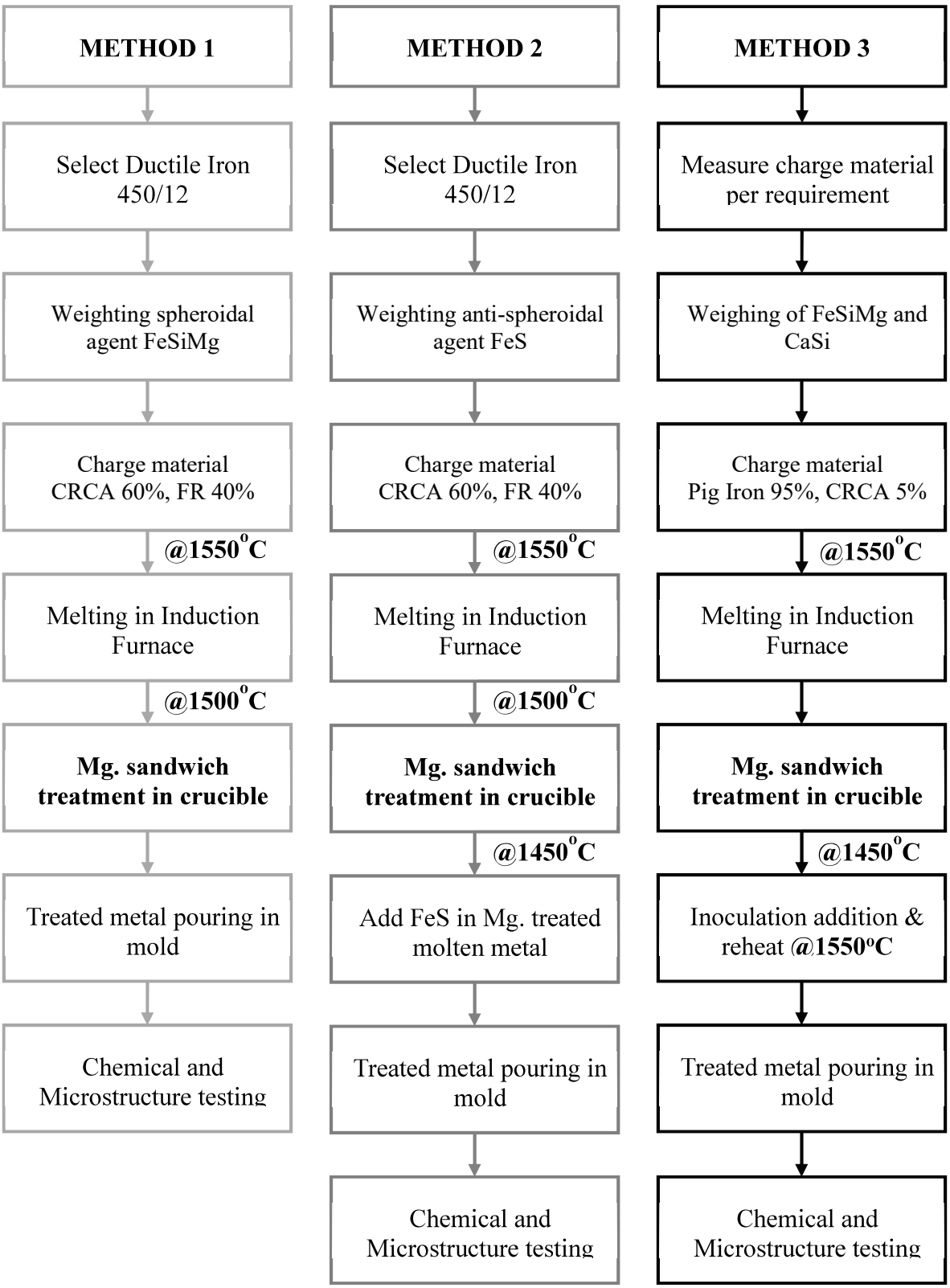

Figure 3.5 Metal treatment process flows

Table 3.1 Chemical composition of base iron material for method-1

Material Type	Chemical Composition (%)										
	C	Si	Mn	P	S	Mg	Cu	Sn	Cr	Ni	Fe
CRCA (60%)	1.4	0.37	0.25	0.025	0.002	---	0.003	0.008	0.016	0.039	Bal.
Foundry Return (40%)	3.26	2.66	0.299	0.0267	0.020	0.0386	0.052	0.017			Bal.
FeSiMg		46.2				9.9					Bal.

So, to achieve a stable plateau of ~0.008% of active Mg post metal treatment, initially pure Mg was added in variations of 0.014%, 0.016%, 0.018%, and 0.020% through sandwich treatment in the form of 10%MgFeSi. As a part of the sandwich treatment, the molten metal was poured into a pre-heated 5kg of the sandwich ladle as shown in Figure 3.6(a), where the prescribed amount of Mg and CRC chips have been(Simmons, 1976) pre-placed on one side of partitioned bottom created using refractory brick. CRC chips control the Mg fading by covering it. Once the Mg reaction with molten metal is accomplished, button samples as shown in Figure 3.6 (b), (c), and (d), have been cast to investigate the chemical analysis and microstructure.

The chemical analysis has been accomplished through a spectrometer; the process of a spectrometer is explained in Sec. 1.5.3. The microstructure of the specimen has been examined using an optical microscope at different magnifications. Additionally, a 2% nital solution has been employed to reveal and study the grain boundaries and phases present in the specimens. The results of varying magnesium percentage specimens have been discussed in the result and discussion chapter.

3.3.3 Method-2: Mg + Sulfur addition

As explored earlier, a great limitation for CGI production lies in balancing the stable Mg plateau with no flakes or excessive nodule graphite formation. Several methods have been explored experimentally for CGI production. It is also viable to re-sulfurize magnesium-treated iron during the production of compacted graphite iron (CGI) and considering the initial sulfur content of the base iron, it becomes possible to regulate and control the nodularity of the graphite as studied by Riposan et al. (2003).

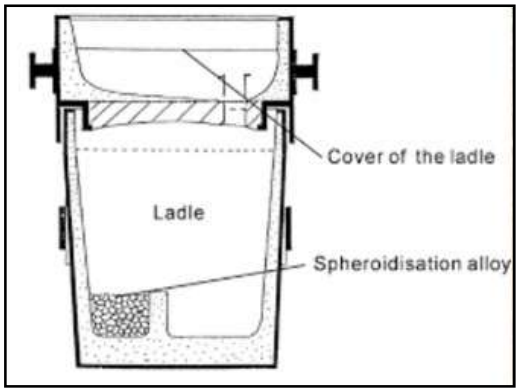

(a)

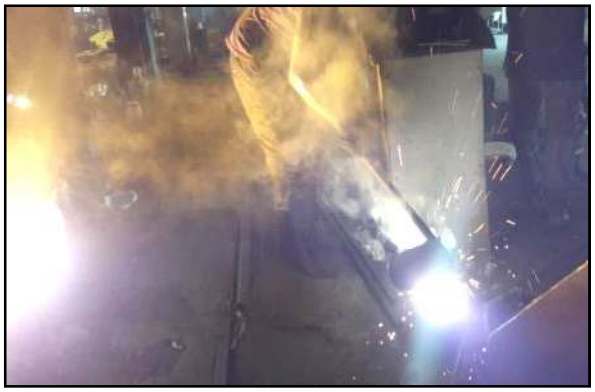

(b) (c)

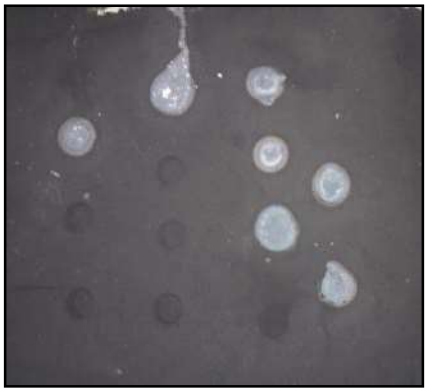

(d) (e)

Figure 3.6 CGI production (a) Ladle for Sandwich treatment through MgFeSi, (b) Base metal treatment, (c) Casting pouring, (d) Poured specimen, and (e) Specimen policing for chemical and microstructure testing

In the production of spheroidal graphite iron (SGI) or ductile iron elements like magnesium (Mg) and Titanium (Ti) have been added into gray cast iron to facilitate the formation of spheroidal graphite. The presence of sulfur can potentially interfere with this process. Sulfur

has an affinity for magnesium, forming compounds that reduce the effectiveness of magnesium in promoting the desired spheroidal graphite morphology. This interference leads to the formation of graphite structures like compacted graphite iron (CGI).

Sulfur is generally considered a detrimental element in the production of spheroidal graphite iron (SGI) or ductile iron. In the context of iron metallurgy, sulfur can lead to the formation of compacted graphite iron (CGI) rather than spheroidal graphite iron. However, sulfur can counteract the nodularising effect of magnesium. Sulfur tends to form compounds with magnesium, reducing its effectiveness in promoting spheroidal graphite morphology. This can result in the formation of compacted graphite morphology. A secondary controlling factor, denoted as the Mg(fin) / S(fin) ratio (Chisamera, 2002) plays a crucial role in shaping the ultimate structure of the castings morphology. When maintained within the range of 1.0 to 2.0 of final Mg/S ratio it contributes to the production of compacted graphite iron (CGI).

In this method, researchers have selected charge material as 60% CRCA and 40% pig iron for balance sulfur. The charge materials have been heated in medium frequency induction furnace. The molten metal treated with both spheroidizing and re-sulfurizing elements, such as Mg and sulfur S provides better results. However, it is to be noted that Ti has strong carbide, and nitro-carbide TiC formation tendency which severely impacts the machining tool life. So sulfur in iron reduces the risk of carbides as well as promotes graphite nodularity in compacted forms. As shown in Table 3.2, the chemical composition of base iron where sulfur is ~0.02%, the Mg addition has been made to base iron using sandwich treatment to ensure the expected ~50% recovery of active Mg. The Mg has been added in the form of 0.041% of MgFeSi in 50kg of molten metal to secure 0.025% of residual Mg. Now, to promote the graphite compacting in molten metal sulfur was added in the form of 10%FeS at the level of 0.015%, 0.020%, 0.025%, 0.030%, and 0.035% at delayed time after Mg treatment.

The molten metal with varying sulfur levels was poured into a button sample with the selected parameter in Table 3.3. Further, all specimens have been analysed for chemical analysis and microstructure through a spectrometer and microscope at TCR, Vadodara.

Table 3.2 Chemical composition of base iron for Method-2

Material Type	Chemical Composition (%)										
	C	Si	Mn	P	S	Mg	Al	Sn	Cr	Ni	Fe
CRCA (60%)	0.05 Min	0.20 Min	0.35 Max	0.05 Max	0.02 Max	---	---	0.008	0.016	0.039	Bal.
Pig Iron (40%)	4.065	2.47	0.55.	0.08	0.03		---	0.017			Bal.
MgFeSi		44.73				7.1	0.59				Bal.
FeS					10						Bal.

Table 3.3 Experimental parameters

Parameter	Detail
Mg treatment	Sandwich
Residual Mg	0.025%
Sulfur in base metal	0.022%
Pouring time	5 min
Treatment temperature	1450°C
Maintain Mg/S	0.5 – 2
Graphite stirrer	Φ8mm, L 30mm

3.3.4 Method-3: Mg addition + CaSi inoculant treatment

The inoculant addition is also similarly sensitive for stable CGI plateau because the addition of 0.08% of inoculation promotes CGI nodularity from <5% to >30% as studied by S. Dawson (2002). Higher inoculation promotes the formation of nodular graphite and stable plateau simultaneously whereas effect is conversely with low inoculation. Therefore, it is important to control Mg addition and inoculant simultaneously by continuous measurement. During this method of metal treatment, Mg as well as CaSi inoculant elements are poured in controlled manners by following a two-step approach to have stable microstructure transformation.

The 50kg of base iron charge material (mixture of 95% sorel pig iron and 5% CRCA) has been utilized and its chemical specifications are mentioned in Table 3.4. The charge material has been melted until 1550ºC using a medium frequency induction furnace. As a part of the sandwich treatment, the molten metal has been poured into a pre-heated 5kg sandwich ladle where 7.1%MgFeSi and CRC chips have been pre-placed at the partitioned bottom created through refractory brick. The MgFeSi has been added 0.0375% at 1550 ºC to achieve the residual Mg in the range of 0.009% by assuming 40% of active Mg recovery. After Mg addition, the molten metal mixture was stirred well utilizing a carbon graphite stirrer. During this transition, temperature and chemical composition have been measured, where temperature drop was realized to ~1360ºC. Before CaSi inoculant addition, the entire molten metal mix was repoured into a ladle to heat up further to ~1540ºC. Later, 0.55% of metal weight CaSi inoculant was added in a pre-heated crucible. Such mixture was poured into button test samples at 1- 1.5 mins of solidification time intervals as shown in Figure 3.7 to note the change in graphite morphology against solidification time. All samples were examined for microstructure and volume fraction through an optical microscope, chemical analysis through a spectrometer, and observed morphology structure through a scanning electron machine.

3.4 Experimentation validation

Validation experiments are a pivotal stage in the transition from laboratory-scale experimentation to full-scale industrial production, especially in the context of Compacted Graphite Iron (CGI) production. Its role is multifaceted, bridging the gap between research and real-world applications. It also validates the effectiveness and feasibility of the production methodologies. Initially, the objectives of these trials are stringently set. This could involve stipulating the desired graphite morphology within the iron, affirming the mechanical properties, or ascertaining the economic viability of the process. Validation runs as an intermediary stage; it inherently operates on a scale that is larger than lab experiments but not as extensive as full-scale production. This scale has been judiciously selected to ensure meaningful data acquisition while optimizing costs.

The actual production phase experiments were closely emulating the expected conditions of a full-scale operation. The casting process has been iterated three times to see the process

variance while manufacturing tensile specimens, with rigorous oversight of key parameters. During this approach, the volume fraction and microstructure assessment of samples 1-3 indicate a conspicuous presence of compacted graphite in the range of 65-72%. This observation is likely attributed to the favorable existence of Mg% well within its optimal range.

Table 3.4 Chemical composition of base metal

Material Type	Chemical Composition (%)												
	C	Si	Mn	P	S	Mg	Cu	Sn	Cr	Ca	Ba	Al	Fe
CRCA	0.05 Min	0.20 Min	0.35 Max	0.05 Max	0.02 Max	---							Bal.
Sorel Pig Iron	4.065	2.47	0.55.	0.08	0.03		0.003	0.008	0.016				Bal.
FeSiMg		44.73				7.1						0.59	Bal.
CaSi		71.95								1.62	2.47	1.16	Bal.

Figure 3.7 Poured molten metal in button sample

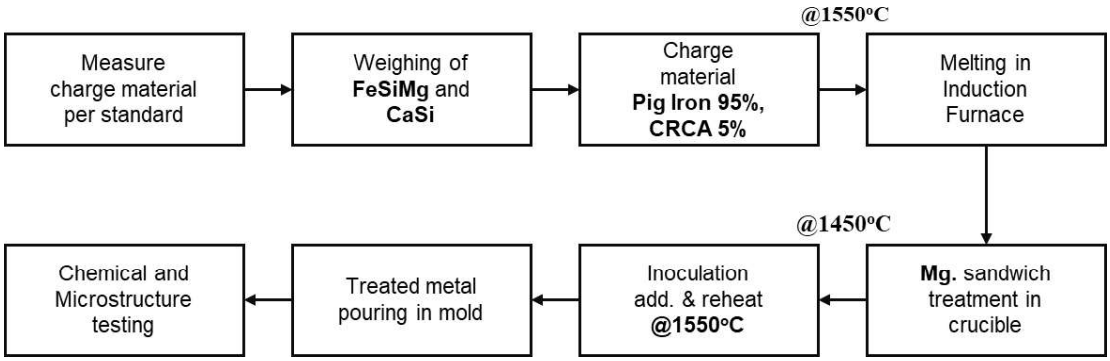

Figure 3.8 Metal treatment process followed while pilot trials, per Method-3

The base metal undergoes a metal treatment process by repeating method 3 as described in Figure 3.5 and Figure 3.8, designed to foster the creation of compacted graphite consistently. The chemical composition of base metal is determined as mentioned in Table 3.5. Its primary objective is to validate and ensure the reliability of the overall traditional foundry process. The careful control of these parameters and the repetitive nature of the casting process collectively contribute to the consistent material quality of tensile specimens.

Table 3.5 Chemical composition of base metal for pilot trials

Material Type	Chemical Composition (%)												
	C	Si	Mn	P	S	Mg	Cu	Sn	Cr	Ca	Ba	Al	Fe
CRCA	0.05 Min	0.20 Min	0.35 Max	0.05 Max	0.02 Max	---							Bal.
Sorel Pig Iron	4.06	2.49	0.56.	0.09	0.04		0.003	0.008	0.016				Bal.
FeSiMg		43.27				7.5						0.55	Bal.
CaSi		73.25								1.74	2.52	1.19	Bal.

3.5 Metallurgical characterization

Metallurgical characterization of compacted graphite iron (CGI) involves a detailed analysis of its microstructure, chemical composition, and SEM to understand and optimize its performance for various applications. This characterization process is crucial for ensuring CGI meets the specific requirements of its applications.

3.5.1 Chemical assessment

The purpose of a chemical composition assessment for casted metals is to determine the types and composition of elements present in the metal. This allows the verification of material specifications and identification of the material. It also assesses the properties such as hardness, corrosion resistance, and tensile strength.

The chemical analysis has been conducted at Aadhya Engineering Services, Vadodara. An Optical Emission Spectrometer (OES) of GNR-Italy has been used as shown in Figure 3.9. The testing method follows the ASTM E1999-18 standard method for optical emission spectroscopy analysis.

Figure 3.9 Optical emission spectrometer

3.5.2 Microstructure assessment

In the pursuit of a great insight into the material's characteristics, microstructure and image analysis have been systematically conducted using an optical microscope instrument. During this, the researcher meticulously examined key aspects, including grain boundaries, phases, and the impact of inoculation. To facilitate such microstructure assessment, the specimens underwent a series of well-defined preparatory steps encompassing cutting, polishing, and etching. These preparatory measures were essential for unveiling the intricate details of the microstructure, ensuring a thorough exploration of the material's internal features.

The microstructure assessment is critical to understand morphology of graphite structure, shape, etc to determine the material class and expected mechanical properties. The quality of CGI should be made upon achievement of the microstructure along with graphite nodules and its shape well within expectation set per the ASTM A247-19 Type IV ("Standard Test Method for Evaluating the Microstructure of Graphite in Iron Castings," 2019) standard.

The microstructure of the cast samples has been observed at Aadhya Engineering Services, GIDC, Vadodara, a NABL-certified ISO testing lab. The microstructure examination has been performed using a metallurgical microscope as shown in Figure 3.10, following the ASM Handbook Vol 9: 2004 test method. Simultaneously the volume fraction was also done through inbuilt image analyzer software.

Figure 3.10 Metallurgical microscope

3.5.3 Scanning electron microscope (SEM)

Scanning electron microscope (SEM) images of cast samples tested in TCR, Vadodara. The SEM images of cast samples have been observed in various magnifications such as 300X, 800X, 1000X, and 2000X. Figure 3.11 shows the SEM instrument with its specification as follows.

Make : Pemtron Corporation, Korea

Model : SEMART SS– 100

Resolution : 3 nm

Filament : Tungsten

Max Magnification : 20x -100000X

Axis Manual Stage movement - (X, Y, Z, Tilt and Rotation)

3.6 Mechanical characterization

Mechanical characterization of compacted graphite iron (CGI) is essential for determining its suitability and performance in various applications, involving tests that measure hardness, and tensile strength. Hardness tests, such as Brinell, assess the material's resistance to deformation and wear, while tensile tests measure its strength and ductility, indicating its ability to withstand tensile forces without breaking. This characterization is critical as it predicts the material's behavior under operational stresses, ensuring the reliability, safety, and longevity of CGI components. Without thorough mechanical characterization, there is a risk of unexpected failures, costly repairs, and potential safety hazards.

Figure 3.11 Scanning Electron Microscope

3.6.1 Tensile strength testing

Mechanical tensile testing stands as a foundation for evaluating the inherent properties of materials. The mechanical strength of a material such as uniaxial strength using the universal tensile machine as well as small punch test technique as studied by P. Patel et.al, (2023), (2022). As far as, there is not crunch of specimen material volume, a uniaxial tensile test based on ASTM E8 ("Standard Test Methods for Tension Testing of Metallic Materials," 2010) followed where a standardized specimen, often shaped as a cylindrical bar or a dog-bone as Figure 3.12 (a), have prepared and mounted on a universal tensile testing machine (UTM) as Figure 3.12 (b). This machine then exerts a progressively increasing pulling force on the specimen, recording the force applied and the specimen's resultant deformation. This data has been used to plot a stress-strain curve, from which critical mechanical attributes like the Elastic Modulus, Yield Strength, Ultimate Tensile Strength, and Elongation have been derived. Within the context of CGI production, tensile testing serves multiple roles. Firstly, it acts as a robust verifier of CGI quality, ensuring the material aligns with preset standards. Discrepancies in tensile properties might flag potential inconsistencies in the production procedure, possibly linked to variations in graphite morphology. Furthermore, the insights gleaned from these tests guide iterative refinements in the production process. If, for instance, CGI doesn't meet stipulated strength or ductility benchmarks, modifications can be made to the production parameters, such as altering the magnesium treatment or adjusting cooling rates. Regular tensile testing also acts as a guardian of consistency, ensuring that as CGI production scales, the material's properties remain steadfast. Lastly, for a nascent CGI

production process, tensile testing offers a validation mechanism, confirming the process's integrity and assuring that the resultant CGI adheres to industry or application-specific criteria. In essence, the role of mechanical tensile testing in CGI production is both diagnostic and prescriptive, offering both a snapshot of the material's current properties and a roadmap for future process optimization.

All three specimens have been casted accordance with geometrical dimensions set in ASTM E8M standard as shown in Figure 3.12, to perform the tensile testing in accordance to ASTM E8 (“Standard Test Methods for Tension Testing of Metallic Materials,” 2010) at Aadhya Engineering Services, Vadodara. Such specimens have been utilized for comprehensive investigations, encompassing microstructure analysis, image analysis, chemical composition assessment, tensile testing, and hardness evaluation. This multi-faceted examination ensures a thorough understanding of the specimens' characteristics and properties, aligning with established standards for robust and comprehensive material assessment. There were three samples to underwent testing for repeatability to nullify the process compliance error of the material made of chemical composition mentioned in Table 3.5.

The assessment of material properties included the determination of hardness using a Brinell hardness tester. Additionally, the tensile strength of all specimens has been also evaluated utilizing a universal testing machine. This test helps to unveil comprehensive insight into the mechanical characteristics of the material, providing valuable data on both hardness and tensile strength. Such dual assessments contribute to a holistic understanding of the material's performance under tensile mechanical loads and offer insights into its suitability for specific applications.

3.6.2 Hardness testing

A hardness test has been conducted at Aadhya Engineering Services in GIDC, Vadodara. The Brinell Hardness Testing machine employed loads of 62.5 and 187.5 kgf, utilizing 2.5 and 5.0 mm steel ball indenters for Brinell hardness assessment as referred to in Figure 3.13. To facilitate this testing, a CGI sample was prepared of appropriate size and shape. Ensure that the surface to be tested is smooth, and polishing has been done.

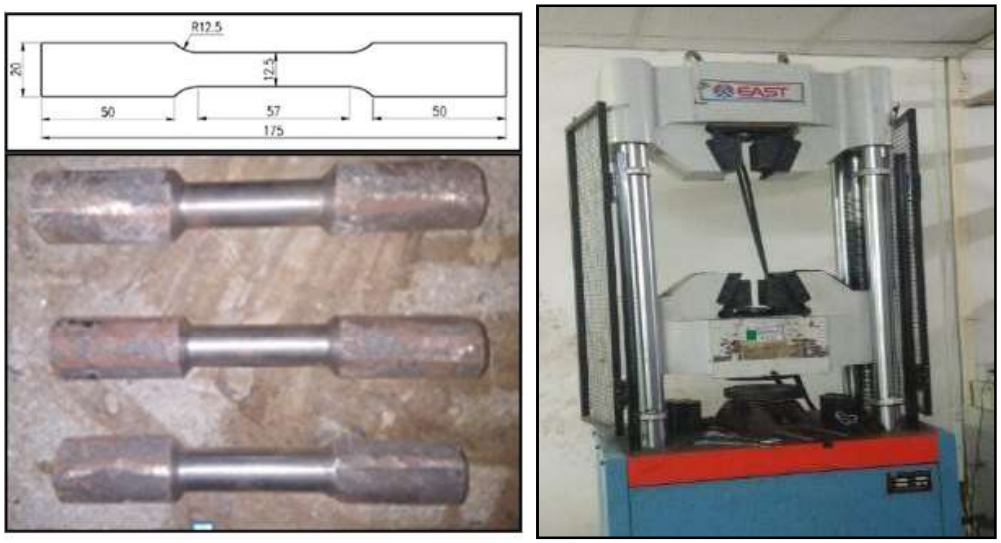

(a) (b)

Figure 3.12 (a) ASTM-E8 standard specimen dimensions (units in mm), and (b) Universal tensile machine

Figure 3.13 Brinell Hardness tester

3.6.3 Density of material

Density measurement of metal involves determining the mass per unit volume of the metal sample. The process starts with volume determination, either geometrical measurements are used for regular-shaped samples or the water displacement method for irregular shapes as shown in Figure 3.14 for measured mass. Later, the density is calculated by dividing the mass by the volume. This measurement has taken place in the fluid mechanics lab at Government polytechnic, Godhra.

The weighted mass of the casted sample was 139 gm, which displaces a water volume of 20 cm^3 So calculated density seems to be 6.95 gm/cm^3 ~ 7000 kg/m^3

Figure 3.14 Density measurement

CHAPTER 4

RESULT AND DISCUSSION

4.1 CGI production process

The multiple metal treatment methods have been explored to bring greater insight into microstructure formation at instantaneous molten metal chemistry and understand their potential impact on CGI graphite morphology. It is well known that CGI development is critical through the achievement of worm-shaped graphite formation which makes them distinct among GCI and DI. However, it is worth noting that CGI graphite formation takes place through a narrow window of graphite shape modification from flakes for GCI to nodules for DI. Such a narrow window only establishes surrounding to active Mg% of 0.008% and little separation from that range makes rapid transformation in graphite shape.

4.1.1 Production method-1: Mg addition by sandwich treatment

While exploring method-1, one-step Mg addition through the sandwich treatment process, it has been noticed that Mg% recovery was quite inconsistent even though following the identical treatment process as referred from the chemical composition results outlined in Table 4.1. The microstructure has been tested at TCR laboratory, Vadodara, and chemical analysis and nodularity content have been analyzed using in-house laboratory at Himcast foundry, Halol where casted samples have been examined using 2% nital etchant at 200X magnification through optical microscopy and chemical analysis using a spectrometer. Figure 4.1, the microstructure of sample-1 shows a graphite flake in the matrix of pearlite with the presence of ferrite. Similarly, sample-2 microstructure shows graphite nodules surrounded by ferrite in the presence of pearlite. Sample 3 shows nodular graphite and a few compacted graphite surrounded by ferrite with the presence of pearlite and carbide. Sample 4 shows nodular graphite surrounded by more ferrite in the presence of pearlite. Table 4.1 results confirm that the Mg% closer to the requisite 0.008% is observed only in sample-3 for 0.0093% while achieving 51.7% recovery of active Mg post metal treatment. While doing

the microstructure assessment of all 4 samples, vermicular graphite is evident in the range of 12-15% in sample 3 only as shown in Figure 4.1. This may be due to the existence of Mg content closer to a stable plateau. However, one of the greatest challenges is to ensure consistent active Mg recovery in the range of 0.008% post sandwich treatment repeatedly by means of such a one-step molten metal treatment process to get quality CGI. It has been studied that CGI formation is quite sensitive to Mg addition. Even 0.001% Mg addition, can transform flakes of graphite into compacted graphite (Steve Dawson, 2002).

The outcome of such a method concludes that the residual magnesium range achieved closer to the desired range, however, the percentage of compacted morphology falls short of rated worm graphite which compels alteration in chemical composition.

Table 4.1 Chemical composition and microstructure remark

Sample	Mg%	Temp ± 10° C	Chemical Composition			Mg % Recovery	Nodule %	Graphite formation Remark
			C	S	Mg			
1	0.014	1370	3.39	0.025	0.0041	29.3	23	carbides and flake
2	0.016	1370	3.24	0.023	0.0054	33.1	43	Flake/nodular
3	0.018	1370	3.31	0.020	0.0093	51.7	74	12-15% worm graphite visible
4	0.020	1370	3.26	0.020	0.0119	59.5	85	Nodular

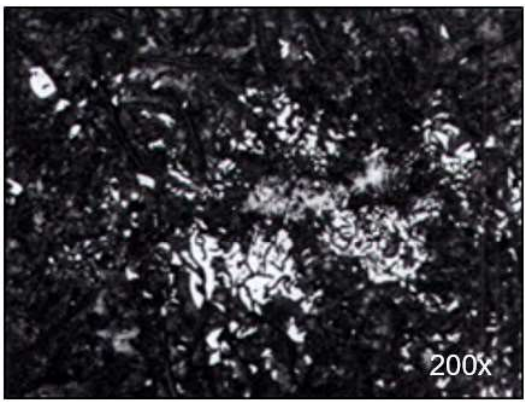

Sample 1: 0.014% Mg

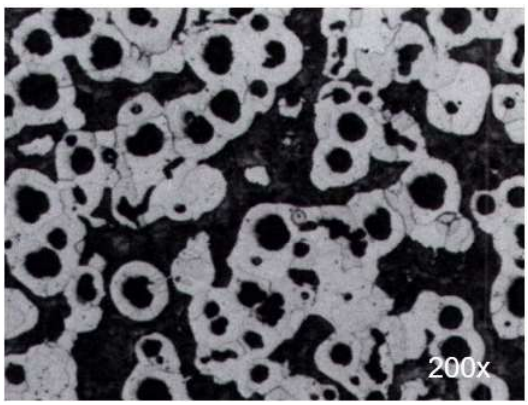

Sample 2: 0.016% Mg

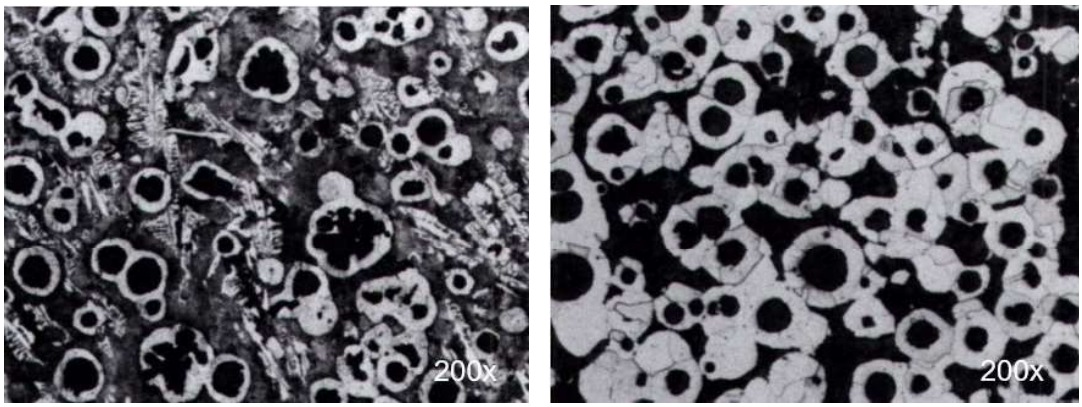

Sample 3: 0.018% Mg Sample 4: 0.020% Mg

Figure 4.1 Microstructure of casted samples with 2% Nital

4.1.2 Production method-2: Mg + Sulfur addition

The microstructure assessment has been examined at TCR, Vadodara using an optical emission spectrometer in accordance to ASTM E-415-17, IS 1188-98 method whereas chemical composition and nodularity content has been assessed in-house laboratory at Himcast foundry, Halol. The results of all the samples are reflected in Table 4.2. It shows that the percentage of Sulfur increases in molten metal residual Mg decreases and the final ratio of Mg/S also decreases. At the least residual Mg observed to 0.023% for final Mg/S ratio of 1.04, only 2-4% graphite worms are visible whereas largely graphite is in nodular form. However, to increase the narrow %Mg window causing vermicular graphite formation for CGI, sulfur in the form of FeS is added post-Mg treatment to promote the nodularity and graphite in a compacted shape.

Table 4.2 Chemical composition post-metal treatment

Sample	Mg%	FeS%	Pour time (Sec)	Temp ± 10° C	Chemical Composition			Mg/S	Nodule %	CGI Remark
					C	S	Mg			
1	0.041	0.015	56	1370	3.28	0.014	0.025	1.78	57	-
2	0.041	0.020	64	1370	3.24	0.018	0.024	1.33	46	-
3	0.041	0.025	71	1370	3.39	0.022	0.023	1.04	79	2-4% worm graphite visible
4	0.041	0.030	79	1370	3.48	0.031	0.023	0.74	67	-

The microstructure was examined through an optical microscope using the ASTM E407-07 method and etchant 2% nital. All samples of microstructure are shown in Figure 4.2 at 200X, in a sample-1 and 2, the microstructure shows few graphite nodules surrounded by a ferrite with the presence of pearlite and carbide, whereas sample 3 shows 2-3% compacted graphite surrounded by ferrite in a presence of pearlite and sample 4 shows the microstructure of nodule graphite surrounded by ferrite in a presence of pearlite. Table 4.2 results confirm that the final Mg/S ratio of 1.04 times with sample-3. It also reveals that much of the volume fraction is not enough to qualify for rated CGI-grade material. It seems that CGI formation through this approach is neither promising nor consistent.

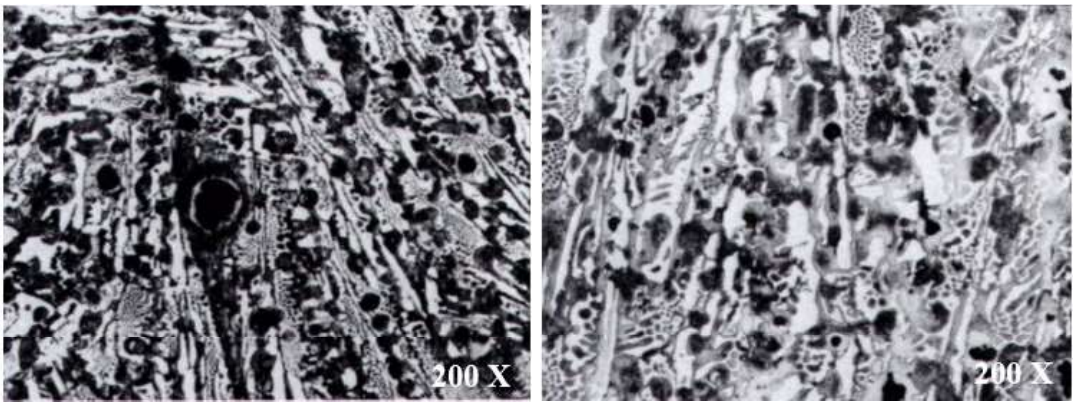

Sample 1: Final Mg/S ratio = 1.48 Sample 2: Final Mg/S ratio = 1.33

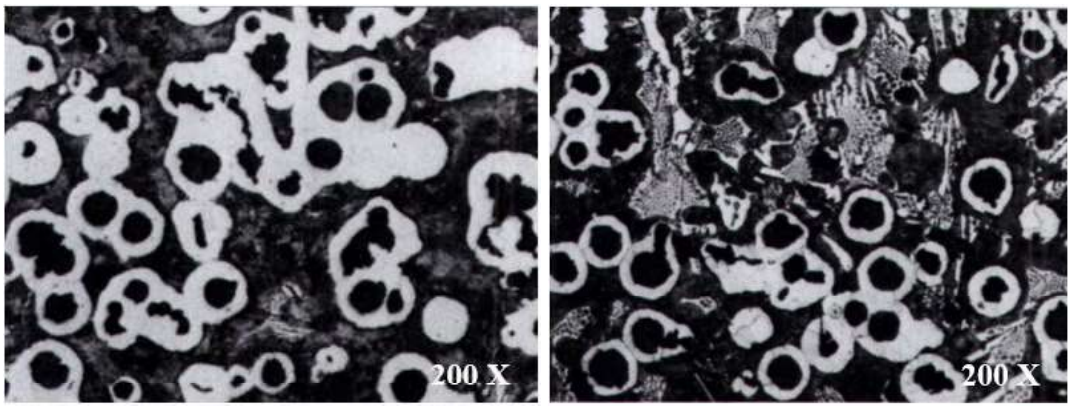

Sample 3: Final Mg/S ratio = 1.04 Sample 4: Final Mg/S ratio = 0.74

Figure 4.2 Microstructure using 2% Nital

4.1.3 Production method-3: Mg addition + CaSi inoculant treatment

The chemical composition and image analysis have been performed at Aardhya Testing Lab,

Vadodara on the samples of production method-3. The tested samples underwent preparation in accordance with standard metallographic procedures. Specifically, samples extracted from casted molds have been mounted in Bakelite, followed by grinding and polishing. Subsequently, the samples have been etched using a Nital solution with a concentration of 2%, a choice made for its consistent and uniform results.

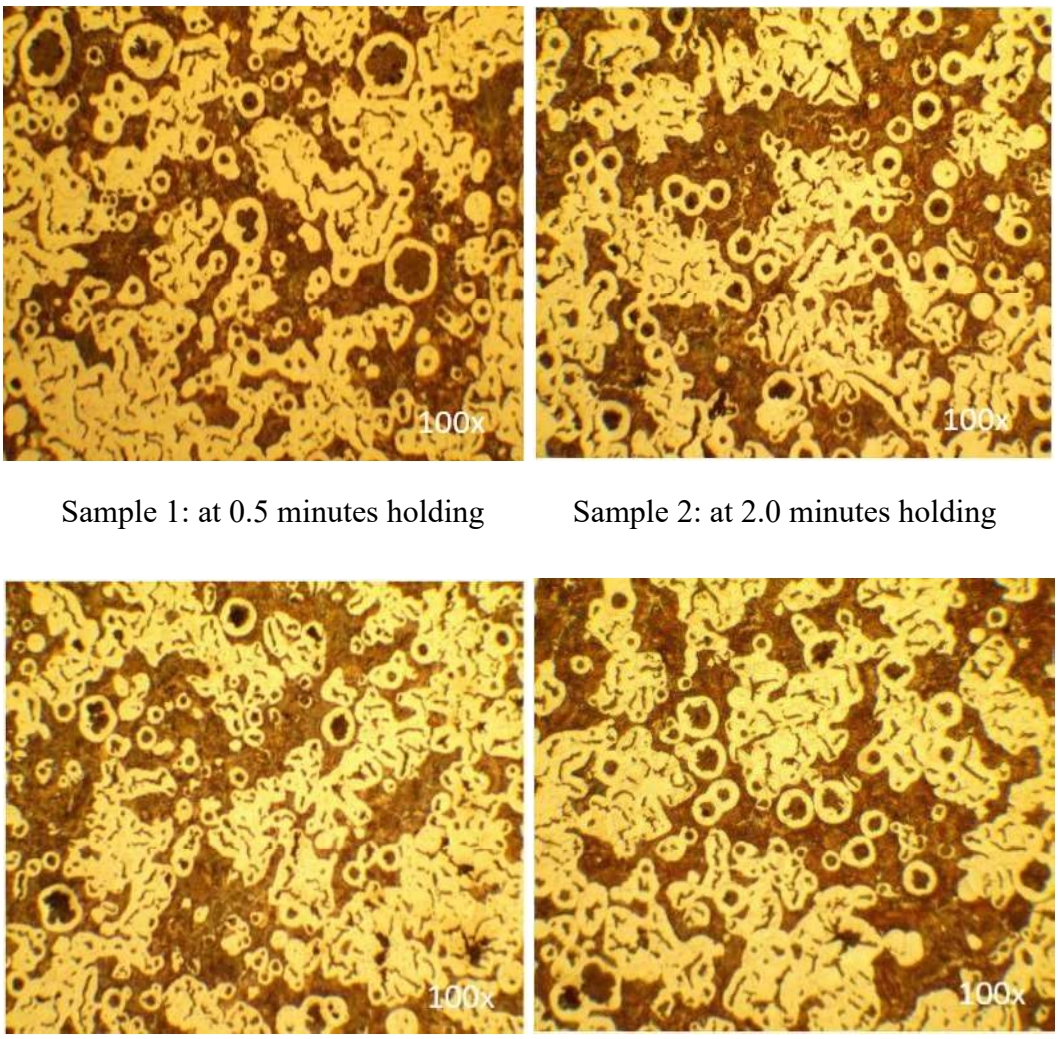

Sample 1: at 0.5 minutes holding Sample 2: at 2.0 minutes holding

Sample 3: at 3 minutes holding Sample 4: at 4.2 minutes holding

Figure 4.3 Microstructure of samples with 2% Nital

Microstructure photographs of the CGI samples have been taken using an optical microscope employing the AES/E/09 method. The microstructural analysis of all specimens is shown in Figure 4.3.

It reveals a microstructure featuring the presence of nodules of graphite /compacted graphite, enclosed within a ferritic matrix with the presence of pearlite. Additionally, this

microstructure is characterized by the concurrent presence of pearlite and eutectic carbides. The volume fraction of the microstructure as per Figure 4.4 confirms that there is a gradual increase in the percentage of compacted graphite iron and a simultaneous decrease in nodule counts in samples 1, 2, and 3 but sample 4 shows decreasing CGI due to the material starts to become solidify. This trend is associated with an increase in holding time, resulting in a decrease in the residual magnesium content.

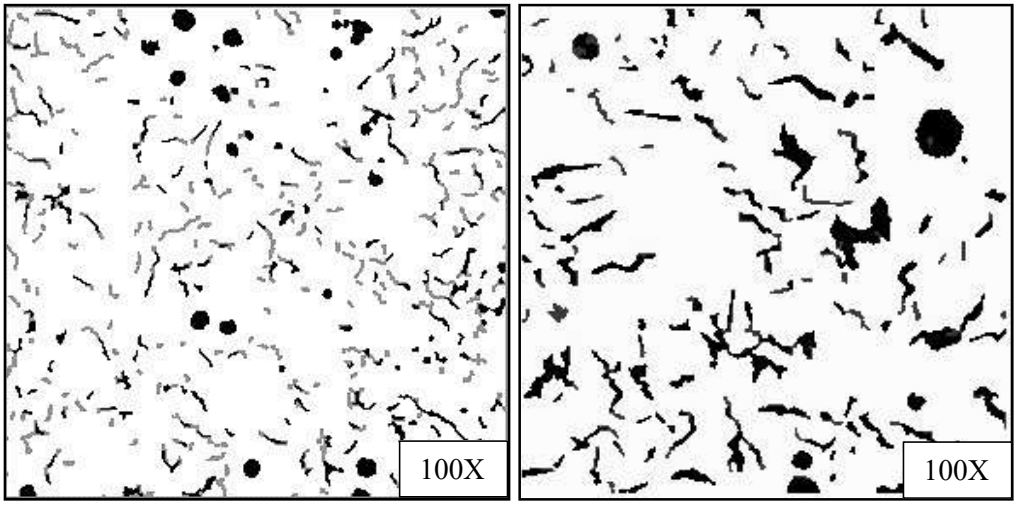

Sample 1: 41% CGI - 59% nodules Sample 2: 53% CGI - 47% nodules

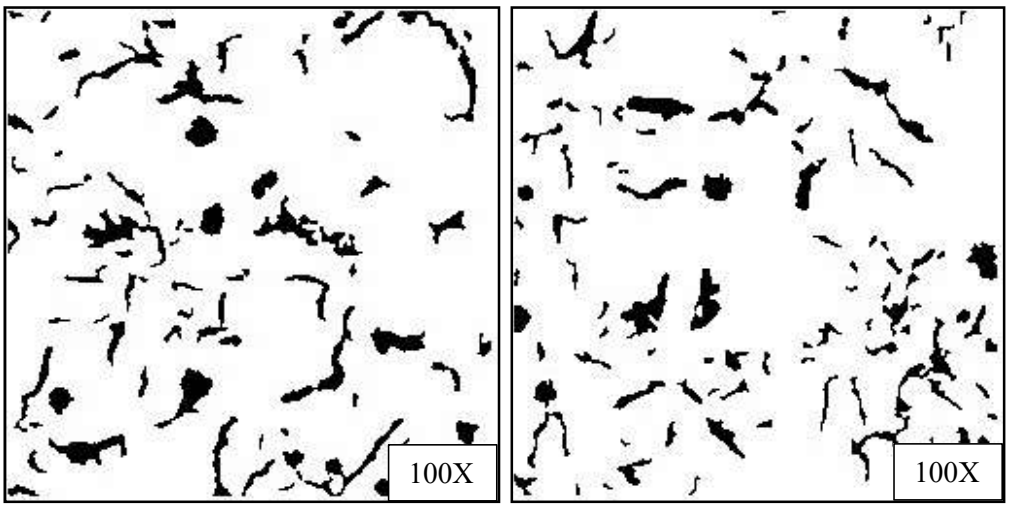

Sample 3: 65% CGI - 35% nodules Sample 4: 48% CGI - 52% nodules

Figure 4.4 Volume fraction of all Samples

The spectrometer testing, as outlined in Table 4.3, reveals that an extended holding time of molten metal results in a noticeable reduction in residual magnesium content. Consequently, it is inferred that a desirable residual Mg content within the narrow range of 0.008% was

successfully attained with a holding time of 3.5 minutes following inoculation at a pouring temperature of 1540°C (sample 3). This particular sample exhibited 65% compacted graphite, along with the remaining portion consisting of nodule graphite within a ferrite and pearlite matrix. The implications of this methodology suggest that as the holding time at a constant temperature post-inoculation increases, there is a consistent decrease in residual Mg levels, accompanied by fluctuations in the volume of vermicular graphite.

Table 4.3 Assessment of chemical and graphite composition at varying holding times of casted samples

Sample No.	Holding Time ± 0.5 (min.)	Temp. ± 20 (°C)	Chemical Composition (%)							Nodule %	CGI %
			C	S	Si	Mn	Mg	P	CE		
1	0.5	1540	3.55	0.016	2.46	0.41	0.013	0.011	4.29	59	41
2	2.0		3.56	0.014	2.42	0.42	0.011	0.011	4.35	47	53
3	3.5		3.62	0.011	2.36	0.38	0.009	0.010	4.17	35	65
4	4.2		3.31	0.012	2.21	0.39	0.006	0.010	4.43	52	48

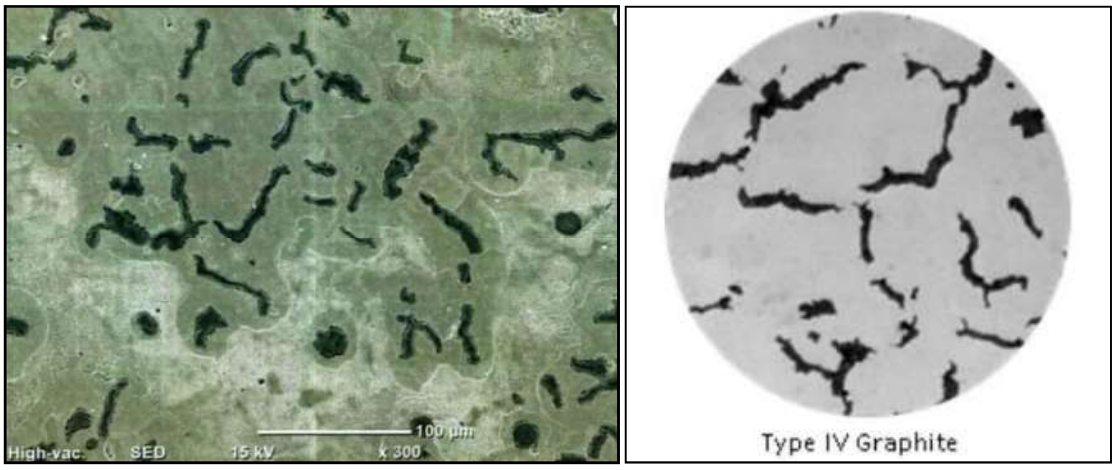

Figure 4.5 Deep-etched scanning electron micrographs show shorter, thicker, and rounded edges at 300X

An examination of vermicular morphology in sample 3 has been done through Scanning Electron Microscopy (SEM) at TCR lab, Vadodara at 300X magnification, utilizing the ASM volume 9 method. Figure 4.5 illustrates the vermicular graphite, showcasing characteristics such as shorter, thicker, and rounded edges in accordance with ASTM A247-19, Type IV graphite standards. It

is noteworthy that the production of Type IV compacted graphite, as depicted in Figure 4.5, can be achieved through a multistage metal treatment method in a conventional casting setup. This involves controlling the pouring temperature at 1440 °C, maintaining a holding time of 3.5 minutes, and ensuring a carbon equivalent (CE) of 4.17%. A convincing outcome confirms that achieved compacted graphite iron (CGI) falls within proximity to the ASTM A247-19 ("Standard Test Method for Evaluating the Microstructure of Graphite in Iron Castings," 2019) standard CGI specifications.

4.2 Results of validation experiments

To validate CGI production process conformance, three experimental repetitions have been conducted by adopting identical chemical composition and methodology that have been investigated as method 3. This iterative approach serves to bolster user confidence in the consistency of the methodology for producing high-quality CGI.

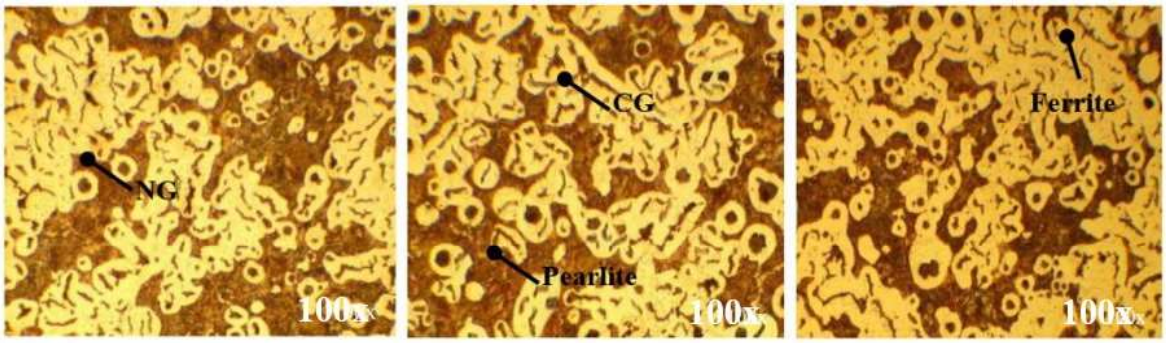

Sample-1 Sample-2 Sample-3

Figure 4.6 Microstructure at 100x magnification

The microstructures have been observed using the AES/E/09 metallurgical microscope instrument at a magnification of 100x with a 2% Nital concentration. The attainment of vermicular graphite morphology is associated with specific conditions, including a residual magnesium content of 0.008%, carbon equivalent, holding time, and the use of an inoculant. This desired range of residual magnesium can be achieved by incorporating 0.0375% magnesium alloy and 0.55% CaSi inoculant through a multi-stage metal treatment process. As illustrated in Figure 4.6, the microstructure of the CGI reveals a ferrite matrix surrounded by vermicular graphite morphology, along with pearlite exhibiting a dark appearance. The compacted graphite constitutes approximately 70% in a hypereutectic composition with a carbon equivalent ranging from 4.5% to 4.7%.

The chemical and microstructure results of Figure 4.3, and Figure 4.4 listed samples as specified in section 4.1.3, conform to the reliability of method 3 as a well-suited CGI production methodology by adopting the traditional casting setup.

As shown in Figure 4.7, the volume fraction and microstructure assessment of samples 1–3 reveal that compacted graphite is evident in the range of 65-72%, which may be primarily driven by residual %Mg existence well within its favorable range. The volume fraction of graphite was observed through the AES/E/09 metallurgical microscope at Aradhya testing lab, Vadodara.

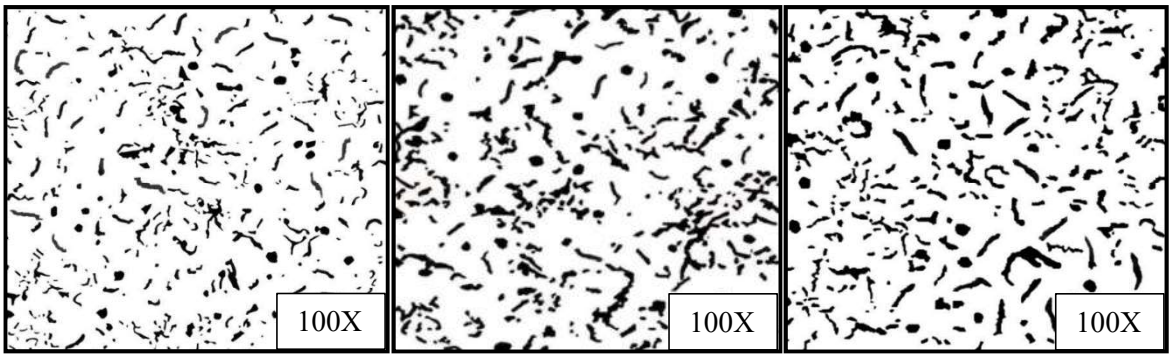

S1: 65.2%CG-34.8%NG S2:70.9% CG-29.1%NG S3:72.3%CG-27.7%NG

Figure 4.7 As polished volume fraction using a metallurgical microscope

The third multi-stage metal treatment methodology supported by Mg addition along with inoculant gives quite consistent results. During this multi-stage metal treatment process, chemical composition is measured at each stage for continuous chemical adjustment to achieve the desired Mg. Such measured data are outlined in Table 4.4, where the chemical composition of the material after the final treatment was precisely measured as presented in Table 4.5. This tabulated data serves as a comprehensive reference for understanding the elemental makeup of the treated material, providing crucial insights into its composition post-treatment. The test samples have been formed from an on-going batch of treated metal as well as finally treated molten metal. Before going for SEM testing, the samples have been polished to make them defect-free. All such SEM tests have been performed in-house facility of Himcast, Halol foundry. The identified key chemical compositions are already included in sections 3.3.2, 3.3.3, and 3.3.4 whereas other sample reports are included in Annexure 1.

Table 4.4 Chemical composition of pre-inoculant treated metal

Sp. No.	Holding Time (min.)	Temp. ± 50 (° C)	Chemical Composition (%)								
			C	Si	Mn	P	S	Cr	Mg	Cu	Sn
1	2	1450	3.46	2.50	0.25	0.022	0.022	0.015	0.015	0.018	0.007
2	2		3.45	2.47	0.29	0.021	0.027	0.016	0.017	0.017	0.006
3	2		3.51	2.42	0.27	0.022	0.025	0.011	0.012	0.020	0.006

Table 4.5 Chemical composition of final treated metal

Sp. No.	Holding Time (min.)	Temp. ± 50 (o C)	Chemical Composition (%)									CE*	CG %	Nod. %
			C	Si	Mn	P	S	Cr	Mg	Cu	Sn			
1	3.40	1440	3.571	2.502	0.402	0.011	0.011	0.030	0.013	0.410	0.039	4.40	65.2	34.8
2	3.59		3.680	2.671	0.370	0.031	0.010	0.030	0.010	0.361	0.098	4.58	70.9	29.1
3	4.15		3.671	2.672	0.371	0.028	0.019	0.021	0.009	0.371	0.035	4.57	72.3	27.7

*%CE=C + 1/3 (Si + P)

Figure 4.8 Broken specimens after the test

The production of three tensile test samples adhered to the standards outlined in ASTM E8 ("Standard Test Methods for Tension Testing of Metallic Materials," 2010) has been done. The tensile test has been performed at room temperature over three specimens for repeatability to nullify the process compliance error until specimens are broken as shown in Figure 4.8 and measured results are tabulated in Table 4.6. The harness test was performed over the same specimens before testing them over UTM.

The culmination of extensive research and validation has confirmed that the established CGI production process is well efficient. Analysing the results yielded through rigorous tensile tests provides a profound understanding of the material's mechanical attributes, reinforcing the success of the devised production methodology. The derived elastic modulus showcases the developed CGI stiffness which aligns with the prevailing ASTM 842 ("Standard Specification for Compacted Graphite Iron Castings," 2018) and equivalent BS EN 16079:2011 (European Committee for Standardization, 2011), a European grade. Apart from this, the evaluated other mechanical parameters like yield and ultimate strengths and corresponding strain rate also confirm the specification of standard CGI material.

Table 4.6 Mechanical and metallurgical properties of samples of Table 4.5

Properties	**Sample 1**	**Sample 2**	**Sample 3**	**ISO 16112** ("Compacted (Vermicular) Graphite Cast Iron— Classification," 2016)	**ASTM A842** ("Standard Specification for Compacted Graphite Iron Castings," 2018)
% Elongation	2.94	3.26	2.73	1-3.5	1
Ultimate strength N/mm^2	471	486	465	400 – 475	Min. 400
Yield strength N/mm^2	292	322	298	Min. 280	
Elastic modulus N/mm^2	146000	161000	149000	140000-150000	
Hardness (HBW)	138	148	136.7	-	197-255
CGI %	65	71	72	80	
Nodularity%	35	29	28	20	
Pearlite%	76	72	68	100	

However, beyond these material strengths, the real testament to the CGI production process viability lies in its efficiency. The production process demonstrated remarkable repeatability, ensuring consistent quality across different batches, which is crucial for large-scale industrial applications and mass production. A crucial aspect of process viability is cost-effectiveness. The methodologies employed in the developed process leverage existing foundry

infrastructures with minimal modifications, ensuring feasibility to do close monitoring and control.

The quality assessment results of the established CGI production process, underscore the mechanical superiority as well as endorses the commercial and operational viability of our production process. By merging technical excellence with efficient production process parameters, the developed CGI production process stands poised as a pioneering benchmark, offering both quality and scalability in a cost-effective framework.

CHAPTER 5

TECHNICAL VIABILITY ASSESSMENT OF DEVELOPED COMPACTED GRAPHITE IRON

5.1 Materials selection

Many standards ("Compacted (Vermicular) Graphite Cast Iron—Classification," 2016), ("Standard Specification for Compacted Graphite Iron Castings," 2018), (European Committee for Standardization, 2011) have categorized CGI material grades based on their mechanical strengths, which are primarily determined by their ferrite to pearlite matrix transition. The material properties are listed in Table 5.1, with a reference to ASTM 842 ("Standard Specification for Compacted Graphite Iron Castings," 2018) and equivalent BS EN 16079:2011 (European Committee for Standardization, 2011), a European grade. As a part of this research, developed CGI is developed using traditional foundry techniques; the CGI material properties are presented in Table 5.2, and its mechanical strength is around 471 MPa, which is quite similar to ASTM A842 CGI-450 or EN-GJV-450.

This study aims to do a technical as well commercial (techno-commercial) viability assessment of developed CGI by designing a centrifugal pump volute under the prevalent hydrostatic pressure. Typically, pump volutes are made of GCI for low pressure whereas DI is used for high pressure application. Here, it is attempted to replace or bridge the material strength gap that exists in-between GCI and DI through CGI for cost-effective product development without compromising the prevalent strength requirement.

The developed CGI material properties are determined with reference to UTM mechanical testing using three different specimens as per Figure 4.8 and the least properties among Table 4.6 have been considered for current assessment which is in the range of commercially available CGI grade as outlined in Table 5.1. The GCI of ASTM A48 Class-40 ("Standard Specification for Gray Iron Castings," 2022) and DI of ASTM A536 60-40-18 ("Standard

Specification for Ductile Iron Castings," 2019) grades are used, as shown in Table 5.2 – to make a holistic comparison.

Table 5.1 Compacted graphite iron material grades per ASTM 842 and BS EN 16079:2011

ASTM 842 Material Grade	BS EN 16079 Material Grade	Matrix Structure	Ultimate Strength (MPa)	Yield Strength (MPa)	Elongation (%)	Elastic modulus (GPa)	Thermal Cond. (W/m^{o}K)
300	EN-GJV-300	Ferritic	300-375	210-260	2.0-5.0	130-145	47
350	EN-GJV-350	Ferritic-Pearlitic	350-425	245-295	1.5-4.0	135-150	43
400	EN-GJV-400	Pearlitic-Ferritic	400-475	280-330	1.0-3.5	140-150	39
450	EN-GJV-450	Predominantly Pearlitic	450-525	315-365	1.0-2.5	145-155	38
---	EN-GJV-500	Pearlitic	500-575	350-400	0.5-2.0	145-160	36

Table 5.2 GCI, CGI, and DI materials properties

Material	Density (kg/m^3)	Poisson's ratio	Elastic modulus (GPa)	Yield Strength (MPa)	Strain at Yield	Ultimate Strength (MPa)	Strain at Break
GCI, ASTM A48 Class- 40	7150	0.26 (Comp.)	145	520 (Comp.)	0.1% (Comp.)	1200 (Comp.)	4.9% (Comp.)
		0.04 (Ten.)		112 (Ten.)	0.01% (Ten.)	400 (Ten.)	0.5% (Ten.)
CGI, Developed	7000	0.26	146	292	0.41%	471	2.9%
DI, ASTM A536 60-40-18	7100	0.275	169	276	0.36%	414	18.0%

As shown in Figure 5.1, Ramberg & Osgood (1943) relationship, Eq. (3) is utilized to outline the multilinear elastic-plastic stress-strain properties of GCI, CGI, and DI with reference to mechanical properties data points listed in Table 5.2 which follows the strain hardening co-efficient of 4.43-2.44, 3.86 and 9.61 respectively. It is critical to note that GCI is inherently brittle for tensile whereas ductile for compressive loading; unlike equal tension-

compression behavior posed by other metals including CGI and DI so Figure 5.1 shows separate stress-strain curves for GCI whereas unique curves for CGI and DI to demonstrate tensile-compressive behavior.

$$\text{Ramberg-Osgood Equation, } \epsilon = \frac{\sigma}{E} + K\left(\frac{\sigma}{E}\right)^{n} \quad (3)$$

5.2 Product designing

Designing a cost-effective centrifugal pump involves consideration of several factors out of which material selection is one of the critical aspects because of the choice of materials that offer the best balance between cost, durability, and performance. For example, GCI is used over DI for adequate pressure application giving greater saving opportunities through cheaper raw material costs as well as manufacturing costs due to castability and machinability. Similarly, CGI can fit well as an alternative to GCI and DI for specific pressure applications. Here, a comparative strength assessment has been made by designing a centrifugal pump volute for permissible yielding and breaking pressures while utilizing available adjacent strengths of material grades of GCI, CGI, and DI. This study is made over the virtual model of pump volute. The 3D CAD model has been prepared in Creo software. The structural strength validation and design optimization have been carried out by leveraging Finite Element Analysis (FEA), a numerical simulation approach powered by ANSYS Mechanical (ANSYS Inc., 2022) FE simulation tool.

The FE simulation has been performed over pump volute using calibrated FEA methodology and boundary conditions. The proposed pump volute product specifications are as:

a. Geometry (Sen.) : Hollow pipe, OD/ID = 317.5mm/303.3mm, Length = 3048mm

b. Geometry (Final): 6x4x8-inch – central discharge end-suction centrifugal pump

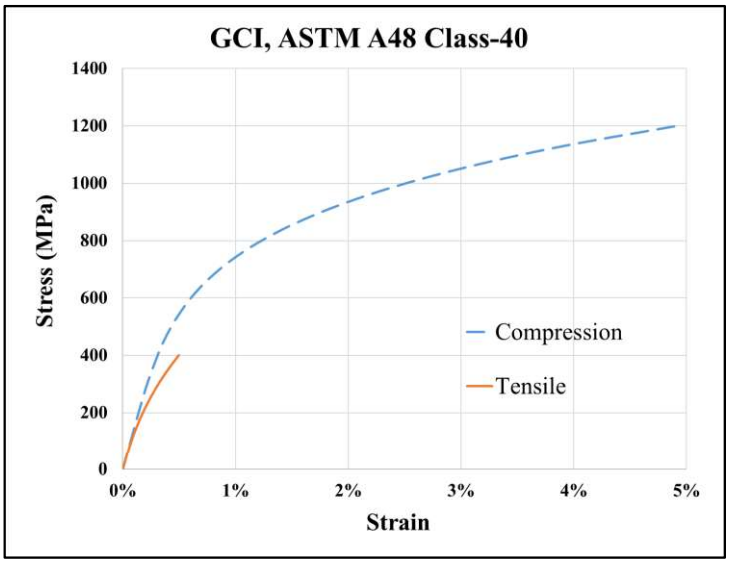

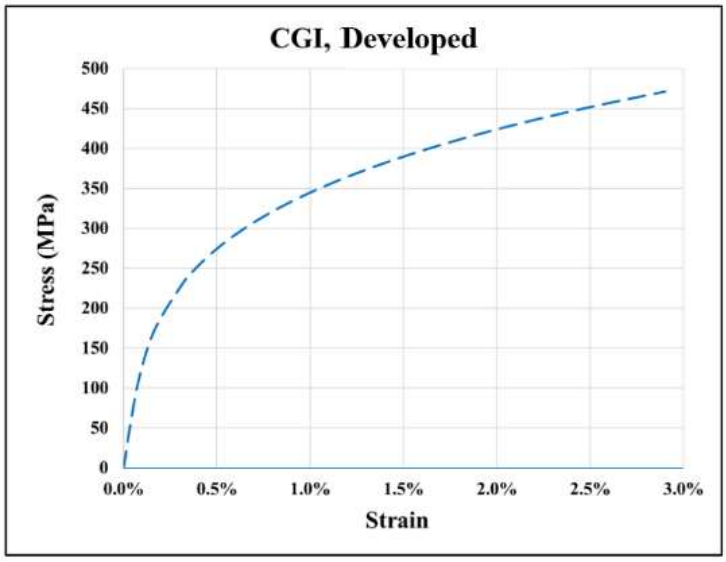

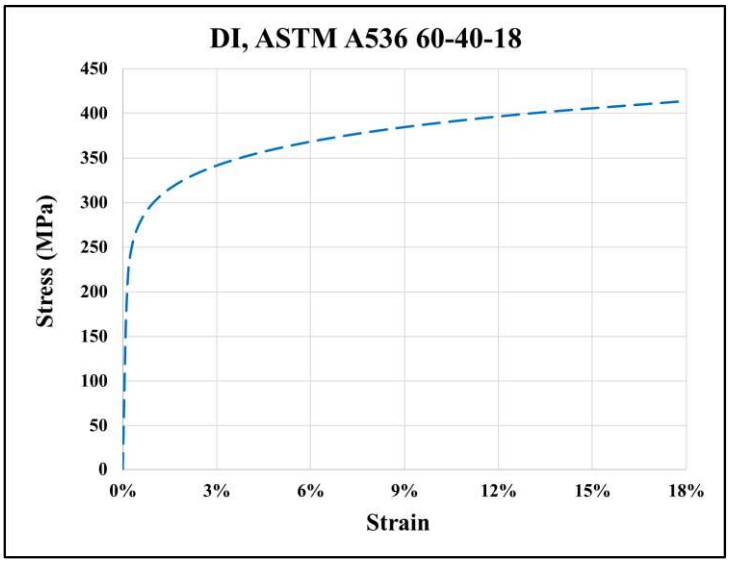

Figure 5.1 Multilinear stress-strain properties of GCI, CGI, and DI per Table 5.2

5.2.1 FEA simulation approach

Finite Element Analysis (FEA) is a powerful simulation tool used by engineers to predict the behavior of physical systems under various conditions. It involves the creation of a computational model of a physical system and the application of forces with constraints so system behavior can be determined before manufacturing. FEA can be used to analyse problems related to structural analysis, heat transfer, fluid dynamics, and many more. The FEA simulation process involves various steps such as:

Model geometry creation: the first step in an FEA simulation is creating the geometry of the model. This is usually done using Computer-Aided Design (CAD) software. The geometry should accurately represent the physical system to analyse.

Meshing: The geometry is divided into smaller, simpler shapes called elements. This process is known as meshing. Each element is connected to its neighbours at points called nodes. The density and distribution of the mesh can significantly impact the accuracy of the simulation. More complex areas of the model usually require a denser mesh.

Material properties: The material properties of each element must be defined. This includes properties such as density, modulus of elasticity, Poisson's ratio, thermal conductivity, and more, depending on the type of analysis.

Boundary conditions: It is to define the boundary conditions for the simulation. These represent the constraints and loads on the system. Constraints could include fixed points where the model can't move, while loads could be forces, pressures, temperatures, etc., that are applied to the model.

Solving: FEA software then solves the governing equations for each element, considering the material properties and boundary conditions. The results at each node are then compiled to create a full picture of how the model behaves under the given conditions. The software typically uses a variety of numerical methods and algorithms to solve these equations.

Post-processing: Finally, the results are analysed and visualized. FEA software usually includes tools for viewing the results in various ways, such as contour plots, vector plots, deformation plots, etc. This step is crucial for interpreting the results and making design decisions.

FEA is a numerical method, and its accuracy depends on several factors. These include the quality of the geometry, mesh types, the accuracy of the material properties and boundary conditions, and the appropriateness of the mathematical models and algorithms used by the software. Therefore, it's important to validate FEA results with experimental data whenever possible.

5.2.1.1 FEA methodology calibration

Since the present work solely relies on FEA-aided virtual testing for product strength validation, it is crucial to establish a well-calibrated simulation methodology in order to eliminate the simulation compliance error. For the same, sensitivity studies have been performed to verify the FEA result accuracy and its influence against critical simulation parameter variation like mesh element size, material model, simulation pre-post processing approach, etc. FE simulation-aided product design validation is widely explored over the industry as an alternative to physical tests.

5.2.1.1.1 FEA simulation set-up

The objective of this study is to design a centrifugal pump volute, the FEA methodology validation has been done using a simple hollow pipe. Because FEA results through analytical calculations under various loading scenarios, which is not feasible to match for 3D complex pump geometry. A simplified hollow pipe geometry was considered as per the specifications, while the multilinear material properties, including isotropic strain hardening, were applied in accordance to the material properties are outlined in Figure 5.1 to accurately capture the Bauschinger effect. The various types of loadings have been applied as mentioned in Figure 5.2 and among them CGI made product permissible strengths have been extracted in Figure 5.3. The designing for yield and breakage criteria are as follows

a. Material definition

   i. Materials : 1) GCI, ASTM A48 Class- 40, per Table 5.2

      2) CGI, Developed, per Table 5.2

      3) DI, ASTM A536 60-40-18, per Table 5.2

   ii. Properties : Multilinear elastic-plastic stress-strain curve

   iii. Plasticity model : Multilinear isotropic hardening

b. Meshing quality

i. Element type : Hexahedron

ii. Element size : 5mm

iii. Aspect ratio : 3

c. Loading scenario

i. Hydrotest : Until yield and breakage

ii. Tensile : Until yield and breakage

iii. Compressive : Until yield and breakage

iv. Bending : Until yield and breakage

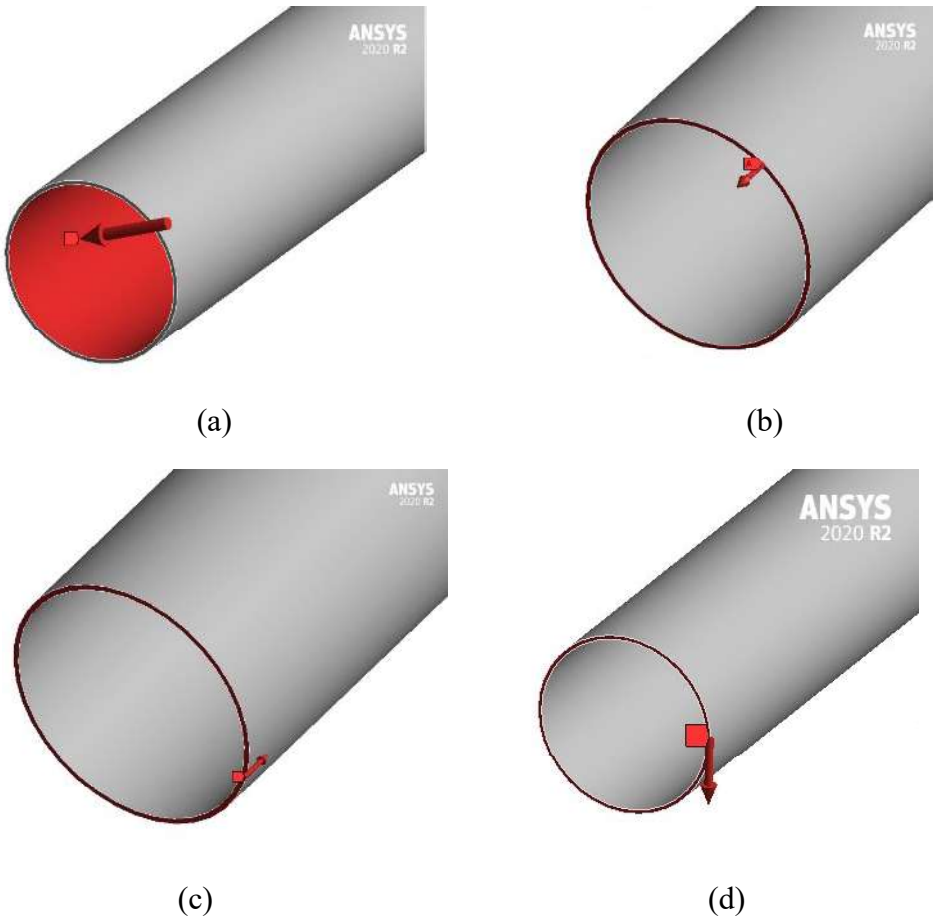

Figure 5.2 Definition of loads, (a) Hydrotest, (b) Tension, (c) Compressive, and (d) Bending

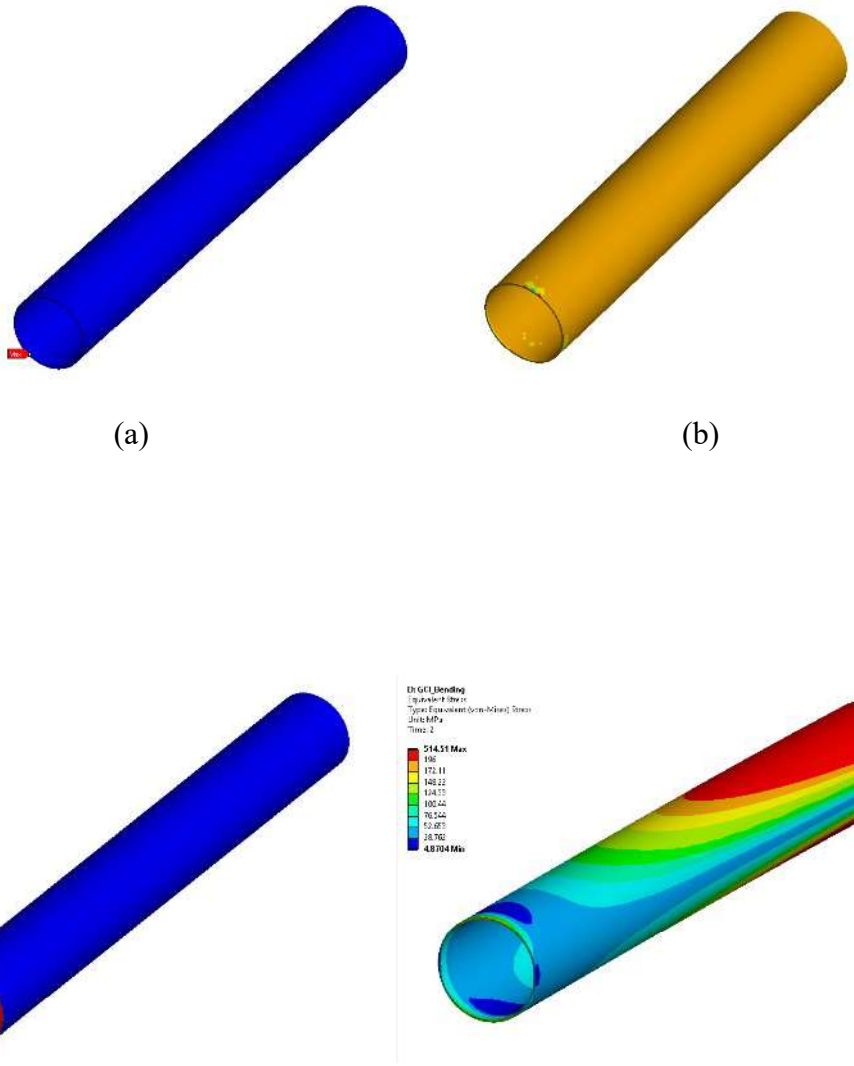

(a) (b)

(c) (d)

Figure 5.3 FEA results, (a) Hydrotest, (b) Tension, (c) Compressive, and (d) Bending, for CGI

5.2.1.1.2 Results calibration

The maximum permissible load-carrying capacities have been estimated against yielding and breakage criteria as summarized in Table 5.3. Analytical calculations have been made using the empirical analytical formulae listed in Eq. (4), (5), (6), and (7), and those are applied for validating the FEA-estimated permissible loads. The load estimation error% observed within ±3% per Table 5.4 which confirms the accuracy of the FEA methodology, such calibrated methodology has been pursued further in due course of research study.

Table 5.3 Permissible loads estimation using GCI v/s CGI v/s DI

Loading type	FEA estimated permissible load						Permissible load per Analytical calculation#					
	GCI		CGI		DI		GCI		CGI		DI	
	at Yield	at Break	at Yield	at Break	at Yield	at Break	at Yield	at Break	at Yield	at Break	at Yield	at Break
Hydrotest pressure (Bar)	49	177	129	208	122	183	49	177	129	208	122	183
Tensile force (kN)	764	2727	1991	3211	1882	2822	764	2727	1991	3211	1882	2822
Compressive force (kN)	3545	8181	1991	3211	1882	2822	3545	8181	1991	3211	1882	2822
Bending moment (kN-m)	58	207	151	243	143	214	60	205	154	239	148	210

 # Analytical calculation results are with reference to Eq. (4), (5), (6), (7)

$$\text{Hydrotest pressure (Bar)},\ P = \frac{\sigma\,(D_o - D_i)}{D_o}\,.\,10 \tag{4}$$

$$\text{Tensile force (kN)},\ F = \sigma_t\,A\,.1000 \tag{5}$$

$$\text{Compressive force (kN)},\quad F = \sigma_c\,A\,.\,1000 \tag{6}$$

$$\text{Bending moment (kN-m)},\ M = \frac{2\,\sigma\,I}{D_o}\,.\,10^6 \tag{7}$$

5.2.2 Design assessment by FEA simulation

This study aims to assess the techno-commercial viability of CGI over GCI and DI while designing industrial centrifugal pump volutes where these materials are predominantly used for non-contamination liquids application. As stated in Section 5.2.1.1.1, a 6x4x8-inch central discharge end-suction centrifugal pump is considered for designing a clean water firefighting application as shown in Figure 5.4. Along with the volute, the corresponding bearing frame and cover plate are also considered while simulation to capture their geometrical stiffnesses.

Table 5.4 Permissible loads estimation error%, FEA v/s Analytical from Table 5.3 data

Loading type	Error % (FEA v/s Analytical estimation)					
	GCI		CGI		DI	
	at Yield	at Break	at Yield	at Break	at Yield	at Break
Hydrotest pressure (Bar)	0.0%	0.0%	0.0%	0.0%	0.0%	0.0%
Tensile force (kN)	0.0%	0.0%	0.0%	0.0%	0.0%	0.0%
Compressive force (kN)	0.0%	0.0%	0.0%	0.0%	0.0%	0.0%
Bending moment (kN-m)	-3.4%	1.0%	-2.0%	1.6%	-3.5%	1.9%

5.2.2.1 Meshing and convergence

Meshing is a crucial step in FEA. It involves breaking down a complex structure into smaller, simpler parts that are easier to analyze. These smaller parts are called elements, and the entire structure is divided into a 'mesh' of these elements. There are several types of elements used in FEA meshing, including line elements, triangle, or quad elements (2D), and tetrahedral or hexahedral elements (3D).

In the current assessment, hexahedron (or hex) mesh, which has six-sided cubes, elements have been utilized. It is more computationally time-consuming than tetrahedral elements (which are four-sided pyramids), but due to certain advantages of getting higher quality results, especially for problems with complex geometry or multilinear materials is used in the current study. This is because they more accurately represent the physical behavior of the model. However, one significant disadvantage of hexahedron meshing is that it is generally more difficult and time-consuming to create, particularly for complex geometries.

The mesh element size and aspect ratio are also very important as they influence the accuracy of the solution, computational time, and memory requirements. Generally, the smaller the elements, the more accurately the actual geometry is represented. Therefore, it may be necessary to have smaller elements in areas of the model where the stress gradient is high. This captures the behavior of the model more accurately in these areas. It created an overall greater element count which increases the computational time and memory required. So, a

balance must be struck between the level of detail necessary for accurate results and the computational resources available. A common way to choose an appropriate element size is through a convergence study. This involves running simulations with different mesh sizes and comparing the results. Once the results change very little in the range of RMS 1e-3 with further refinement of the mesh, the mesh is said to be "converged". Such mesh convergence study is performed to decide the most appropriate mesh element size without compromising results accuracy and its outcome is as shown in Figure 5.5.

Figure 5.4 6x4x8 inch volute geometry

The aspect ratio of a mesh element is the ratio of its longest dimension to its shortest dimension. High aspect ratios (long, thin elements) can lead to less accurate results, particularly for stress analysis. This is because the results may be dependent on the direction of the longest dimension, leading to "stiffness" or "locking" effects also it leads to numerical instabilities and excessive element distortion, which goes against results accuracy. So, it is practiced to achieve an aspect ratio lesser than 5. Here, it followed for 3. Hence it is crucial to make a balancing approach while doing meshing, enabling controlling of computation time without compromising the quality.

Finally, the pump volute is meshed through 5mm of elemental size whereas the critical cut-water tongue area is locally refined using 1.5mm of size to enhance the accuracy as shown in Figure 5.6. There is a total element count crossed to 6.95 lacs.

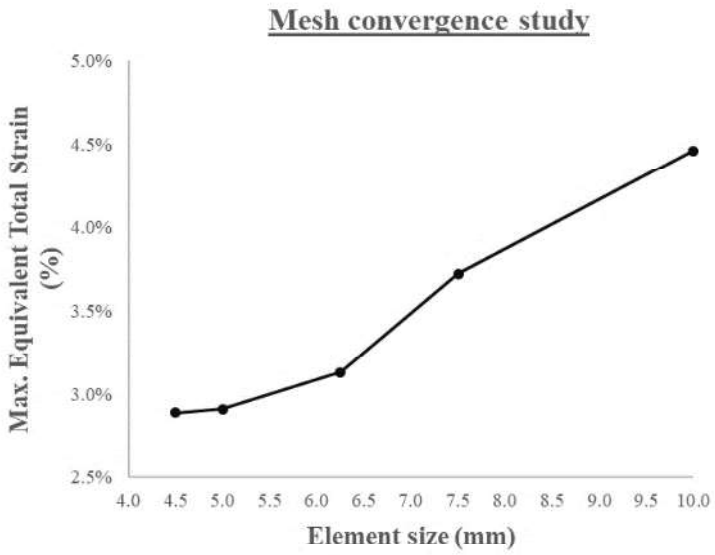

Figure 5.5 Mesh convergence study performed on CGI baseline volute geometry

5.2.2.2 Boundary conditions definition

The FEA method of structural engineering problem solves the partial differential equation of motion where underlying force, stiffness, and displacement are included so that the definition of loads and constraints are two fundamental parameters that define the boundary conditions and their accuracy to obtain a realistic simulation by mimicking real-world boundary conditions.

Loads represent the external effects acting on the system which can be defined in many nature per real application. In a pumping system, underlying hydraulic pressure is predominant which drives the fluid pumping function through impeller rotation, so such load is considered here while designing. Whereas the constraints define how the model is restricted in its movement. It also establishes the model's degrees of freedom, i.e., the directions in which each node is allowed to move. Constraints have been used to simulate the model's real-world conditions. Here, appropriate loads and constraints are considered as shown in Figure 5.7.

Due to the nature of the application, it is crucial to know the permissible yielding and breakage hydrotest pressures to be sustained using potential materials. The hydrotest pressure is the most predominant loading criterion to ensure the pump volute’s structural strength integrity therefore, this study also focused on product design validation by FE

simulation-aided hydrotest loading only as illustrated in Figure 5.7. Whereas, as shown in Figure 5.5, the mesh convergence study is performed to decide the most appropriate mesh element size without compromising results accuracy while controlling computation time.

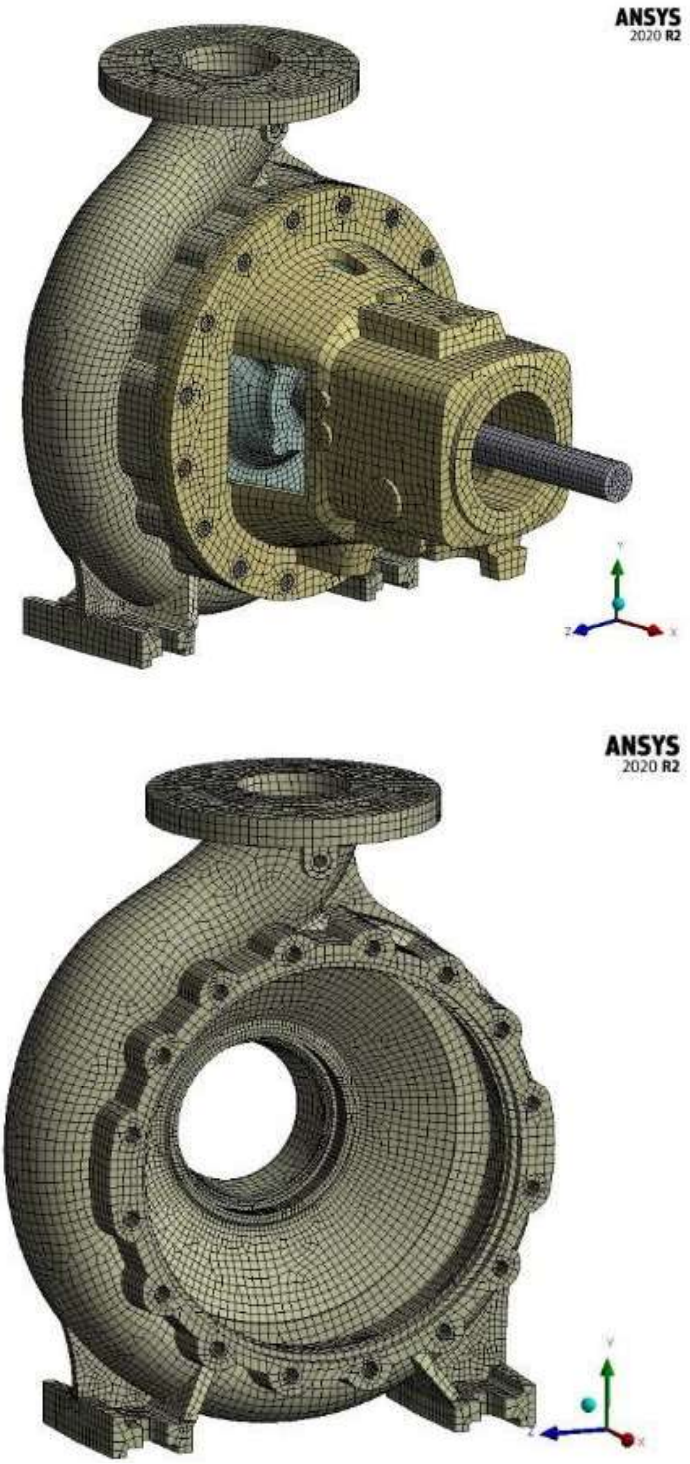

Figure 5.6 Hexahedron meshing of volute assembly

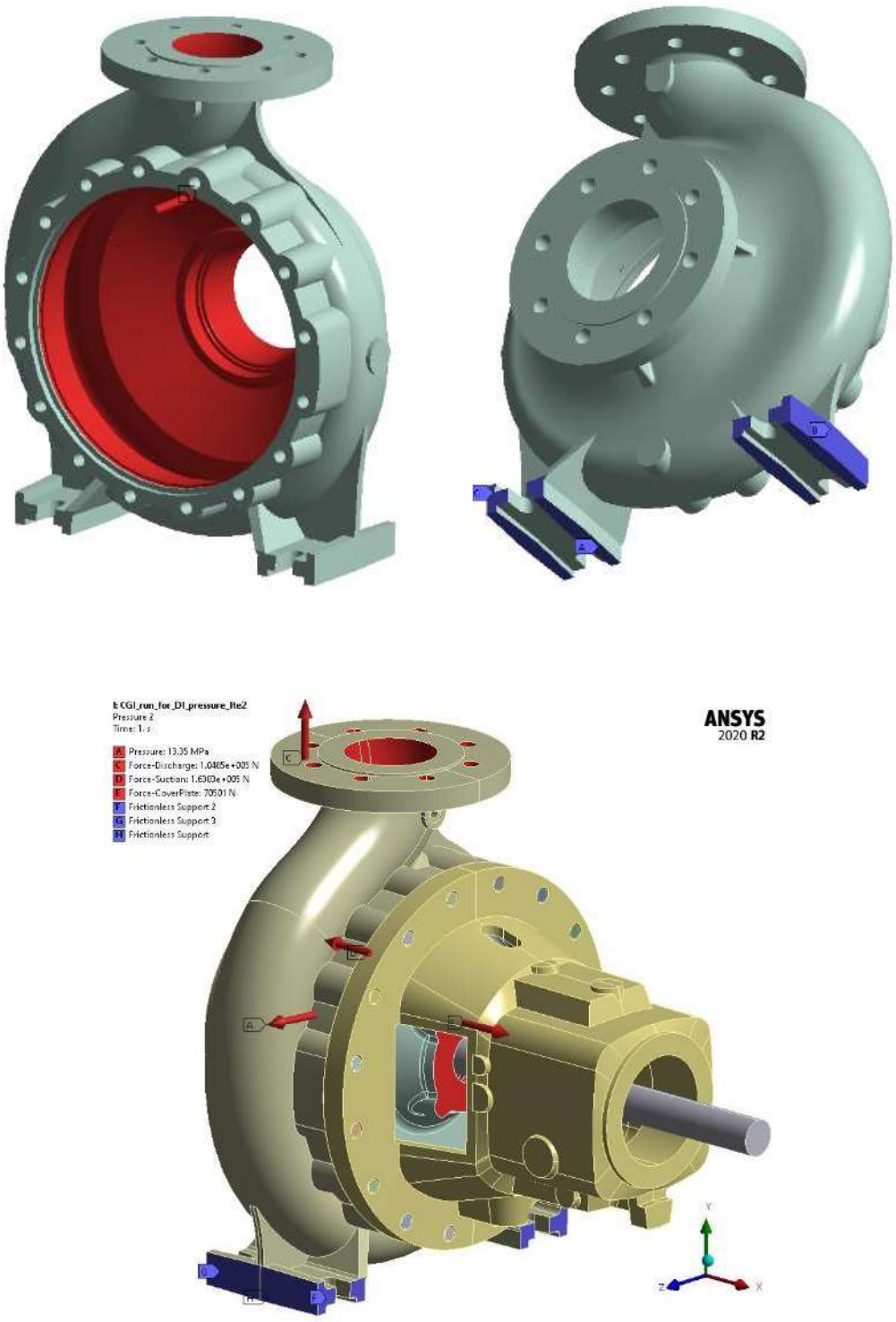

Figure 5.7 Hydrotest pressure loading, and constraint definition

5.2.2.3 Results post-processing

The post-processing is the stage where the results of an FEA simulation are analyzed and interpreted. It is a critical phase in the FEA process, as the insights gained here drive

decision-making and potential design changes. Post-processing often involves result analysis by extracting and analyzing the result plots of essential parameters like stress, strain, deformation, and intensity of distribution across products. It also ensured the FEA models and derived results accuracy as a part of verification and validation. Finally, after making all sorts of checks the decision is made whether the product design is safe to operate, or potential changes are to be made. In many instances, it is also industry-wide practice to look for an opportunity to go for design optimization to reduce the product cost if the existing design offers more than adequate design safety margin.

Here, volute design qualification and optimization comparison are supposed to be made with reference to respective maximum pressure carrying capacity so that those are manually back calculated with reference to averaged elemental equivalent total stain exposure per permissible yield and ultimate criteria pertinent to particular material of construction. The equivalent total strain results are presented in Figure 5.8, and evaluated maximum permissible loads are summarized in Table 5.5 for all of the potential materials under consideration.

Table 5.5 Max. permissible pressure carrying capacities and design margin for baseline volute geometry

Geometry Volume (m^3)	**Volute Mass (Kg)**	**GCI, Class-40**		**CGI, Developed**		**DI, 60-40-18**		**Design Margin using CGI over GCI**		**Design Margin using CGI over DI**	
		Y	**B**	**Y**	**B**	**Y**	**B**	**Y**	**B**	**Y**	**B**
1.0155e-2	GCI = 72.6 CGI = 71.1 DI = 72.1	1.2	38.4	27	81	28.5	135	2150%	111%	-5%	-40%

* *Y = At permissible yield limit*
B = At permissible breakage (ultimate) limit

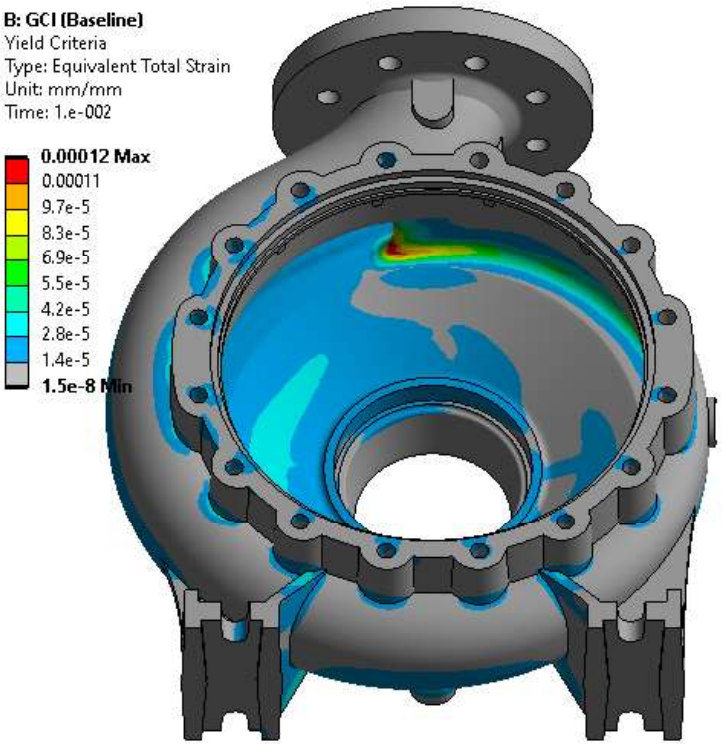
B: GCI (Baseline)
Yield Criteria
Type: Equivalent Total Strain
Unit: mm/mm
Time: 1.e-002
0.00012 Max
0.00011
9.7e-5
8.3e-5
6.9e-5
5.5e-5
4.2e-5
2.8e-5
1.4e-5
1.5e-8 Min

(a)

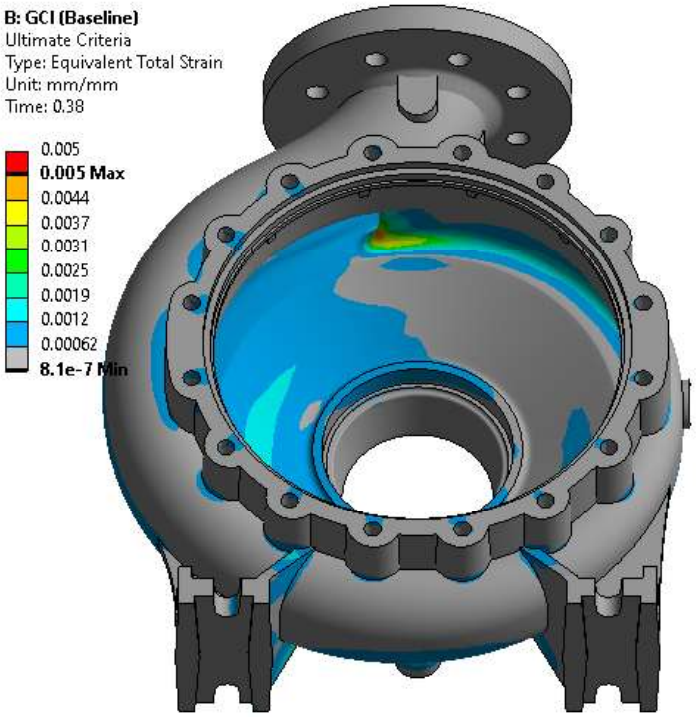
B: GCI (Baseline)
Ultimate Criteria
Type: Equivalent Total Strain
Unit: mm/mm
Time: 0.38
0.005
0.005 Max
0.0044
0.0037
0.0031
0.0025
0.0019
0.0012
0.00062
8.1e-7 Min

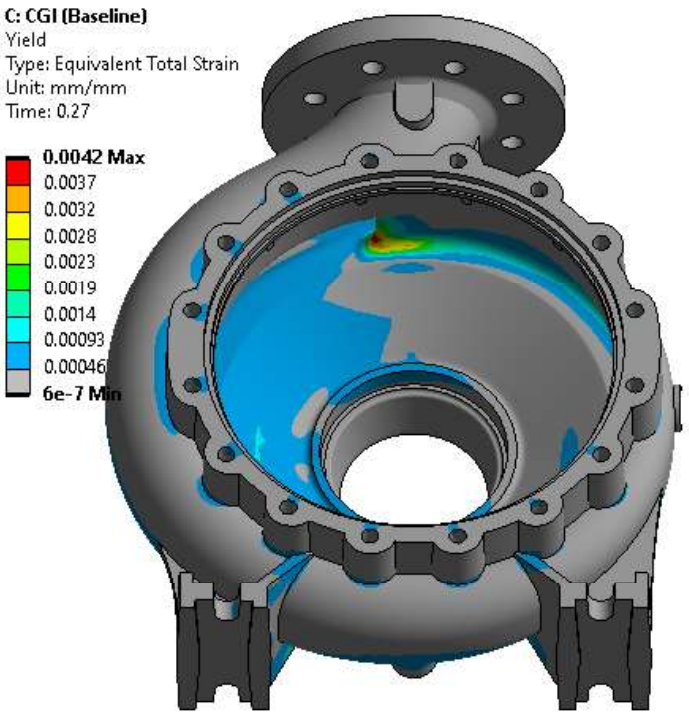
C: CGI (Baseline)
Yield
Type: Equivalent Total Strain
Unit: mm/mm
Time: 0.27
0.0042 Max
0.0037
0.0032
0.0028
0.0023
0.0019
0.0014
0.00093
0.00046
6e-7 Min

(b)

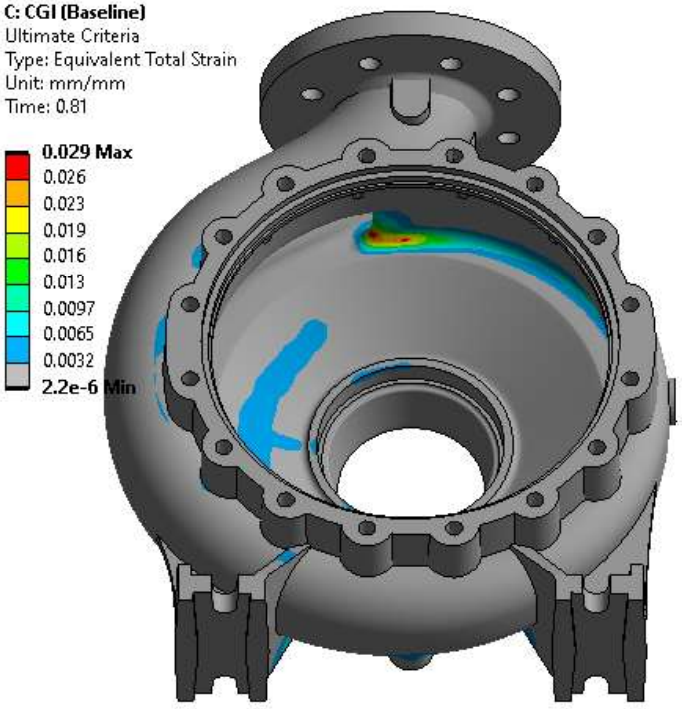
C: CGI (Baseline)
Ultimate Criteria
Type: Equivalent Total Strain
Unit: mm/mm
Time: 0.81
0.029 Max
0.026
0.023
0.019
0.016
0.013
0.0097
0.0065
0.0032
2.2e-6 Min

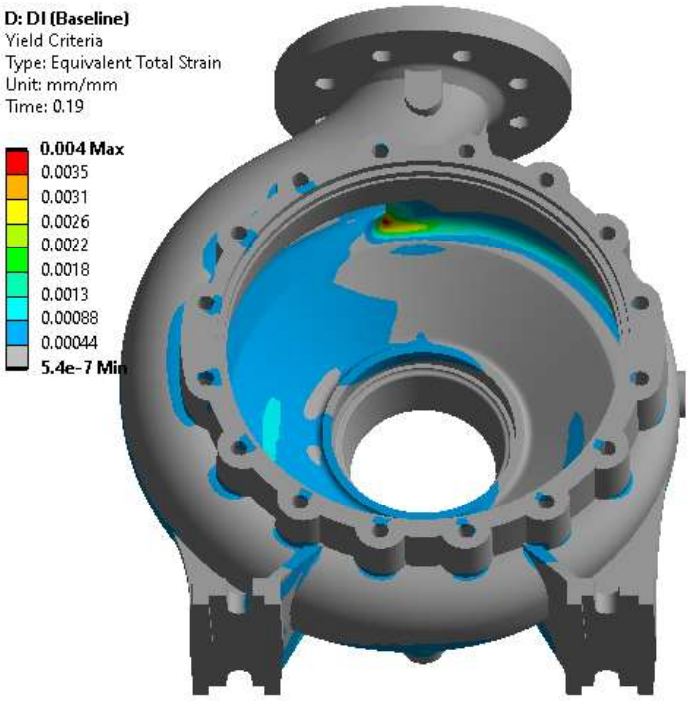

(c)

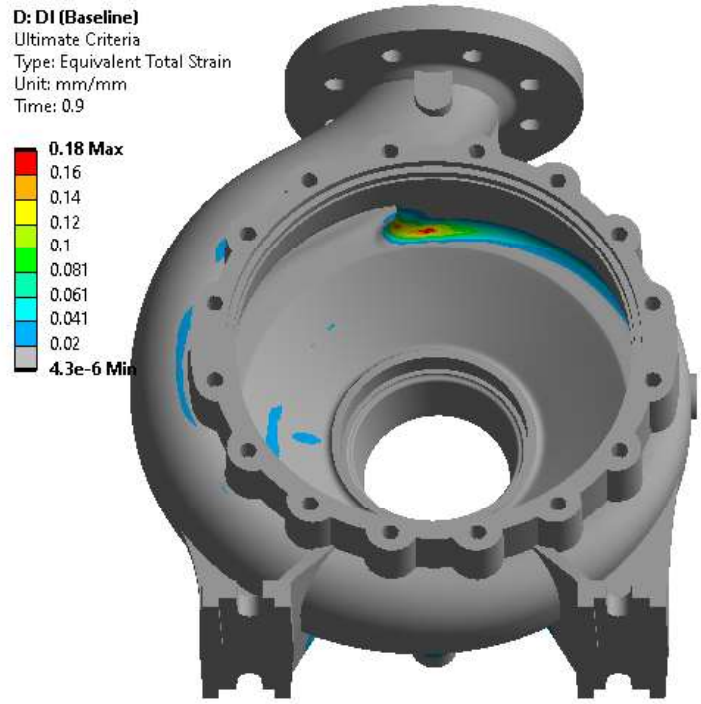

Figure 5.8 Yield and Ultimate total strain results of baseline volute geometry using (a) GCI, (b) CGI, (c) DI

5.3 Design optimization

Product design optimization involves making improvements to a product design so that it better meets its intended purpose or meets its purpose more cost-effectively. The goal could be to improve the product's functionality, manufacturability, durability, or aesthetic appeal, among other factors. It requires a careful understanding of the product's requirements, the needs and preferences of the product's users, and the technical and economic constraints of production. Here the prime objective of product design optimization is to reduce the product weight without compromising its reliability and durability. Reduction in product weight leads to a reduction in manufacturing cost to make the product cost competitive.

It is important to note that design optimization opportunity is primarily driven by cumulative stiffnesses of material as well as geometry. Table 5.5 shows available design margin is led by material stiffnesses only, which may not yield the full expected product mass and cost reduction while optimizing product geometry simultaneously. It is similar to what the design optimization opportunity realized in the case of simplified pipe during the FEA methodology calibration study. The design margin using potential materials for simplified pipe is tabulated in Table 5.6 and it's interesting to note that utilizing CGI over GCI improves the design margin by ~160% and ~17% while it is designed for yielding and breakage respectively. It is except for compressive load-case, due to GCI's excellent compressive strength among other materials posed by flakes graphite particles. The developed CGI also performs better over DI by ~6% and ~14% while designing for yielding and breakage respectively but this advantage may not be realized while using most superior grades of DI. This superior performance of CGI is primarily attributed to its elastic stiffness and plastic strain hardening.

The CGI volute geometry is optimized until the limit of rated permissible pressure of GCI and DI baseline geometries to assess the net design and cost optimization opportunities by capturing discussed cumulative stiffnesses. While doing the design optimization, the critical geometrical dimensions are varied systematically to see their overall impact on the strength and load-carrying capacity.

There are a total of 9 design iterations that have been simulated by adopting the virtue of parametric design exploration. During such a parametric design exploration, critical geometrical dimensions that are supposed to be varied are set as a parameter. So that volute CAD geometry is automatically updated. Later it synchronizes to FEA software and gets it imported as an FEA simulation model and all the default simulation steps are followed

intuitively including reporting of the desired FEA result parameters. Such intuitive simulation process flow along with the list of design iterations are displayed in Figure 5.9. The optimized CGI volute results are plotted in Figure 5.10.

Table 5.6 Design margin using CGI over GCI and DI for simplified pipe geometry

Loading type	Design margin using CGI, Over GCI		Design margin using CGI, Over DI	
	at Yield	at Break	at Yield	at Break
Hydrotest pressure (Bar)	163.3%	17.5%	5.7%	13.7%
Tensile force (kN)	160.6%	17.7%	5.8%	13.8%
Compressive force (kN)	-43.8%	-60.8%	5.8%	13.8%
Bending moment (kN-m)	160.3%	17.4%	5.6%	13.6%

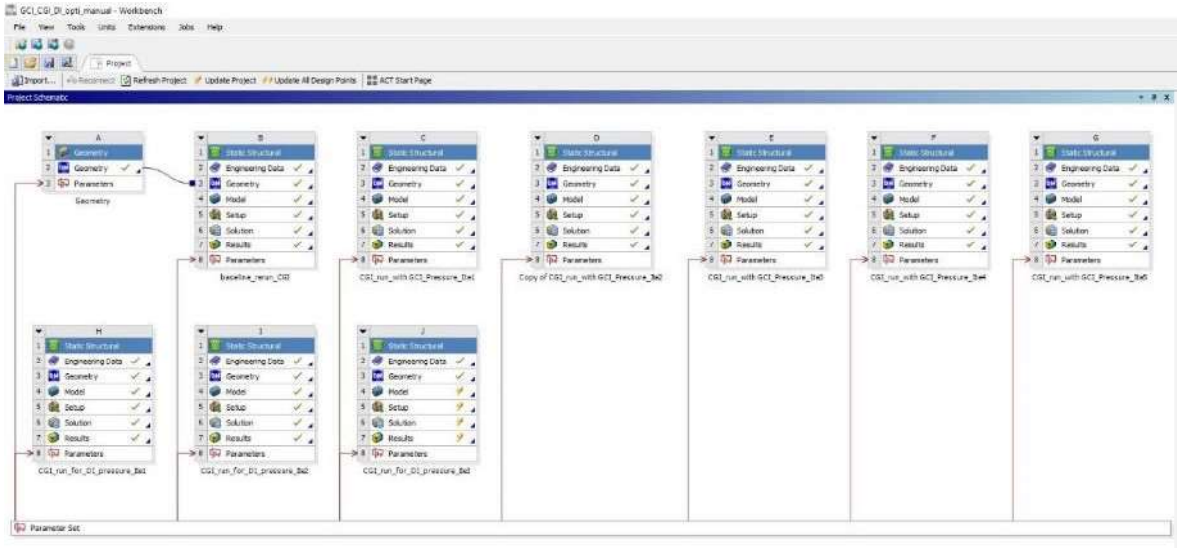

Figure 5.9 FEA simulation design exploration using ANSYS while design optimization

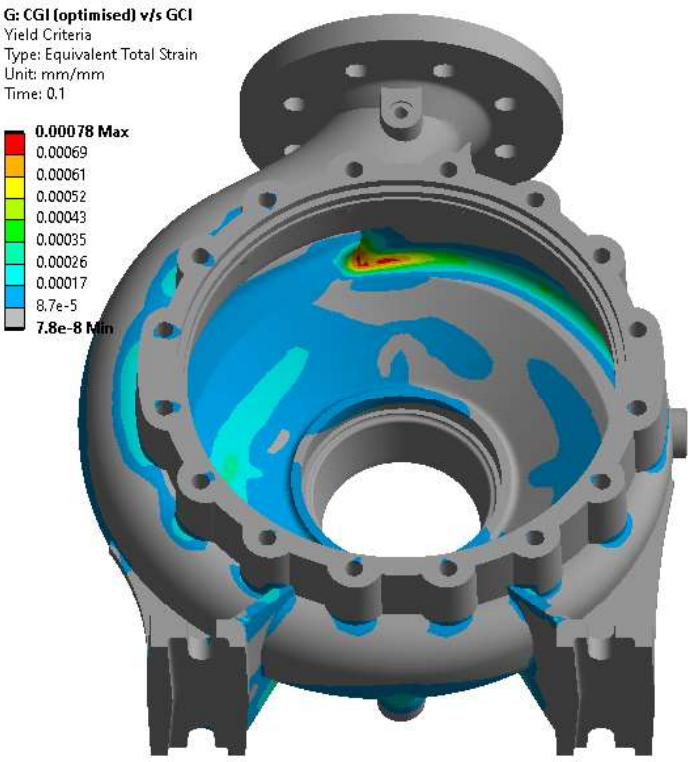
G: CGI (optimised) v/s GCI
Yield Criteria
Type: Equivalent Total Strain
Unit: mm/mm
Time: 0.1
0.00078 Max
0.00069
0.00061
0.00052
0.00043
0.00035
0.00026
0.00017
8.7e-5
7.8e-8 Min

(a)

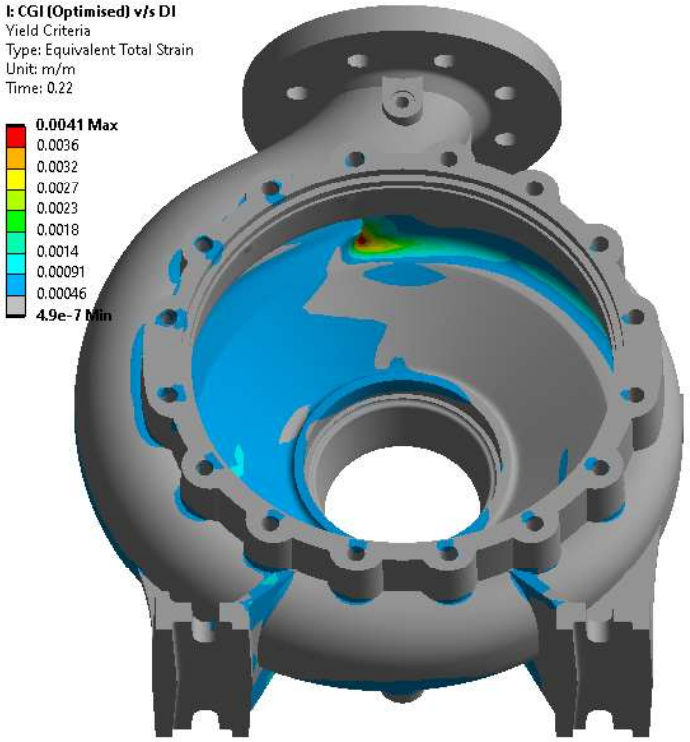
I: CGI (Optimised) v/s DI
Yield Criteria
Type: Equivalent Total Strain
Unit: m/m
Time: 0.22
0.0041 Max
0.0036
0.0032
0.0027
0.0023
0.0018
0.0014
0.00091
0.00046
4.9e-7 Min

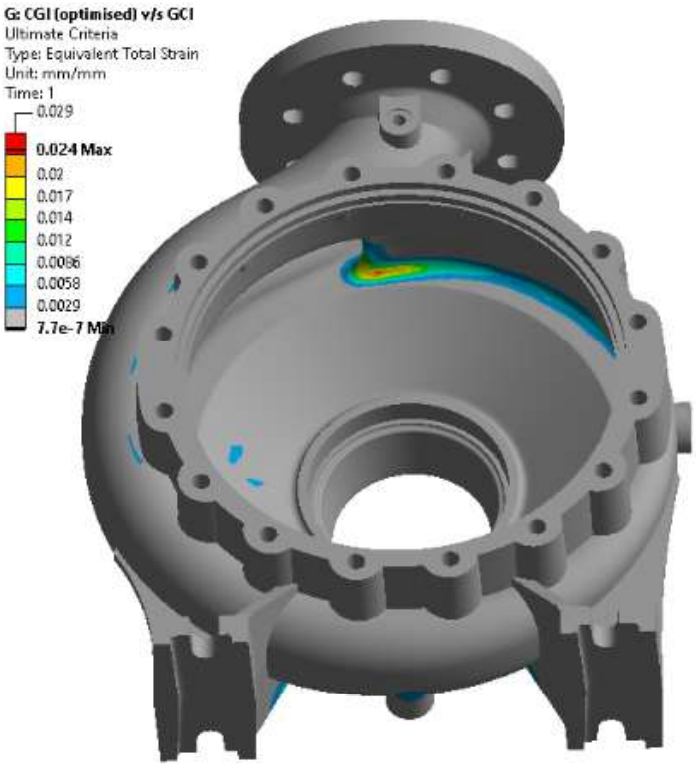

(b)

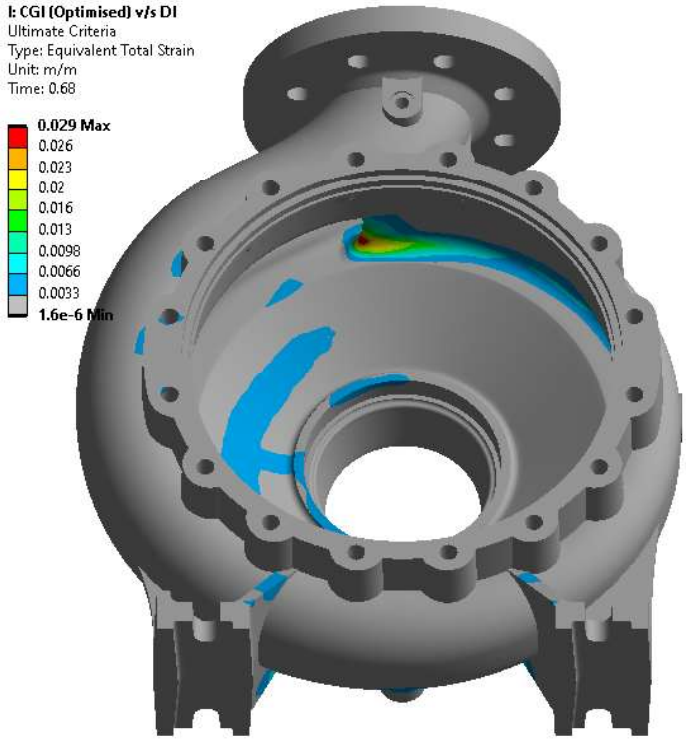

Figure 5.10 CGI volute results against rated baseline pressures while designing them over (a) GCI, and (b) DI

Table 5.7 Volute mass optimization using CGI over GCI for rated baseline pressure

Designing for Yield				Designing for Breakage			
Rated Baseline Pressure (Bar)	**GCI Volute Mass (kg)**	**CGI Optimised Volute Mass (kg)**	**Mass Optimisation (%)**	**Rated Baseline Pressure (Bar)**	**GCI Volute Mass (kg)**	**CGI Optimised Volute Mass (kg)**	**Mass Optimisation (%)**
1.2	72.6	34.9	51.9%	38.4	72.1	59.7	17.2%

Table 5.8 Volute mass optimization using CGI over DI for rated baseline pressure

Designing for Yield				Designing for Breakage			
Rated Baseline Pressure (Bar)	**DI Volute Mass (kg)**	**CGI Optimised Volute Mass (kg)**	**Mass Optimisation (%)**	**Rated Baseline Pressure (Bar)**	**DI Volute Mass (kg)**	**CGI Optimized Volute Mass (kg)**	**Mass Optimisation (%)**
28.5	72.6	76.1	-4.8%	135	72.1	77.3	-7.2%

5.4 Should cost analysis

In order to assess the potential cost saving opportunities for centrifugal pump manufacturing using CGI instead of DI and GCI, a thorough should cost analysis (SCA) has been performed. SCA is a comprehensive method used by organizations to evaluate and estimate the reasonable cost of a product or service. It involves breaking down the various components and processes involved in manufacturing or providing the service and determining the optimal cost for each. This analysis consists of every aspect of the production process, including materials, labor, overhead, and profit margins, and it is analyzed to determine the cost that a product or service "should" reasonably incur. It contrasts with the actual cost, which is what a company currently pays. By conducting this analysis, organizations can identify areas of inefficiency, waste, or inflated costs and develop strategies to reduce expenses while maintaining quality.

One of the primary advantages of SCA is its ability to drive cost reduction initiatives effectively. By meticulously scrutinizing every component of the production process, including materials, labor, overhead, and profit margins, companies can pinpoint

inefficiencies and areas of cost overrun. Armed with this detailed understanding, organizations can implement targeted strategies to trim expenses without compromising quality, with improving profitability. The SCA provides valuable insights for strategic decision-making. It involves outsourcing, vertical integration, or investment in automation technology, organizations can make more informed decisions about their future direction based on a comprehensive understanding of their cost structure and competitive landscape. Ultimately, this analytical approach is a critical methodology in the realm of manufacturing and business domain, providing a systematic approach to comprehending and appraising the genuine costs associated with product manufacturing.

The should cost analysis data are presented in Table 5.9 and Table 5.10, are prepared by utilizing aPriori (*Www.Apriori.Com*, 2022), a software tool that uses advanced algorithms and data analytics to automate the should-cost analysis process while providing real-time cost estimates and insights during the early stages of product development. It streamlines SCA by facilitating the input of relevant data, such as materials, labor rates, and manufacturing processes. The software then creates accurate cost models, considering factors like material usage and assembly complexity. Through detailed analysis, aPriori identifies inherent should cost of the product manufacturing and areas for cost savings and offers scenario analysis capabilities to explore different optimization strategies. It also supports collaboration with suppliers by providing cost breakdowns for negotiation. Continuous improvement is fostered through ongoing visibility into cost drivers and performance metrics. Finally, aPriori generates comprehensive reports and visualizations to communicate findings and support decision-making, ultimately enabling organizations to identify inherent product cost for its saving opportunities and enhance competitiveness.

Table 5.9 Should cost analysis between GCI and CGI

Material	Finished volute weight (kg)		Raw material price (INR/kg)	Casting process cost (INR/kg)	Machining lead-time (Hours)	Machine Burden Rate (INR/kg)	Machining cost (INR)	Finished product cost (INR)	
	Yield	Break						Yield	Break
	(A)	(B)	(C)	(D)	(E)	(F)	(G = ExF)	(H = Ax(C+D)+G)	(I = Bx(C+D)+G)
GCI	72.6	72.1	53.5	62.5	2.25	1780	4005	12427	12369
CGI	34.9	59.7	55.2	65.1	2.35	1780	4183	8381	11365
Cost reduction using CGI over GCI								**32.6%**	**8.1%**

Table 5.10 Should cost analysis between CGI and DI

Material	Finished volute weight (kg)		Raw material price (INR/kg)	Casting process cost (INR/kg)	Machining lead-time (Hours)	Machine Burden Rate (INR/kg)	Machining cost (INR)	Finished product cost (INR)	
	Yield	Break						Yield	Break
	(A)	(B)	(C)	(D)	(E)	(F)	(G = ExF)	(H = Ax(C+D)+G)	(I = Bx(C+D)+G)
CGI	76.1	77.3	55.2	65.1	2.35	1780	4183	13338	13482
DI	72.6	71.1	58.4	66.7	2.44	1780	4343.2	13425	13238
Cost reduction using CGI over DI								**0.7%**	**-1.8%**

5.5 Result discussion

The estimated maximum permissible load-carrying capacities of baseline pump volute geometries are summarized in Table 5.5, which confirms that while using CGI over GCI, load-carrying capacity significantly enhances to the extent of design margin improvement by 2150% and 111% when designing it for yield and breakage respectively. Such a superior CGI performance is led by its inherent elastic-plastic stiffnesses, especially under tensile loading. The improved design margin indicates an enormous opportunity of design optimization to reduce the material weight and prevailing cost without compromising its essential structural strength integrity. Conversely, CGI volute load carrying capacity is slightly lower as compared to DI volute by -5% and -40% while designing them for yield and breakage respectively.

It is crucial to recognize that opportunities for design optimization are influenced by the combined stiffness of both the material and the geometry. Table 5.5 demonstrates that the available design margin is determined solely by material stiffness, which might not achieve the desired reductions in product mass and cost when also optimizing the product geometry. Therefore, the CGI volute geometry is optimized with reference of rated permissible pressure limits of GCI and DI baseline geometries to assess the net design and cost optimization opportunities by capturing discussed cumulative stiffnesses.

The optimized CGI volutes mass is mentioned in Table 5.7 and Table 5.8. The CGI material may lead to mass optimization for 51% and 17% against GCI whereas it performs marginally poor by 5% to 7% against DI. Although CGI looks inferior strength against DI, its finished product cost may be cost competitive due to favourable machining cost against DI. The

should cost analysis data presented in Table 5.9, indicates that CGI offers 32.6% and 8.1% cost reduction opportunity while designing volute for yield and breakage, respectively over the usage of GCI material for identical pressure rating. Furthermore, despite the CGI volute exhibiting a higher weight volume by 4.8-7.2% as depicted in Table 5.10, its cost remains quite comparable (0.7-1.8%) to DI. Still, CGI remains the preferred choice due to its favorable attributes, including corrosion resistance, thermal strength, and ease of manufacturing.

CHAPTER 6

CONCLUSION, CONTRIBUTION, INDUSTRIAL APPLICATION AND FUTURE SCOPE

6.1 Conclusion

This investigative research gave a great opportunity to dwell on the inherent CGI behavior by performing a series of experiments under varying boundary conditions. Simultaneously, it highlighted the underlying challenges in ensuring quality and mass production. The achieved outcome of this investigation confirms the feasibility of CGI production through traditional foundry processes, which is a notable advancement in the field. However, it necessitates rigorous monitoring and strict control of the process to maintain consistency and quality. Detailed conclusions are drawn concerning CGI production and its commercial viability, paving the way for broader industry adoption and enabling cost-effective product designing with improved material performance.

6.1.1 CGI mass production feasibility using traditional foundry processes

- Compacted graphite iron production poses enough challenge due to the stable CGI plateau which is quite narrow through its range of approximately 0.008%-0.013% Mg, which is quite challenging to achieve because the active magnesium fades at a rate of approximately 0.001% every minute as a result usable magnesium range is even lessor in reality.

- Another challenge is caused by to nonstationary aspect of a stable CGI plateau. If the active oxygen and/or sulfur contents are high, it consumes the active magnesium and shifts the CGI plateau toward higher total magnesium values, making the control of process chemistry more complex.

- To achieve the desired CGI microstructure, the Mg and inoculant-aided multi-stage treatment method appears convincing for quality production. This method, when paired with continuous monitoring of instantaneous active Mg and other nodularising chemicals, enables real-time element adjustment to maintain stable Mg% in the range of 0.009%.

- The two-step molten metal treatment process effectively overcomes the challenge of abrupt transitions in graphite morphology caused by fluctuations in instantaneous Mg. Real-time monitoring of Mg levels and temperatures at various intervals supports essential chemical adjustments to preserve the required composition. This process reinforces the need for tight control over the metal treatment process, timing, and user discipline to consistently achieve quality production.

- The mechanical testing results show that developed CGI, offers that mechanical strength very much in line with ASTM 842-400 or ISO 16112 material grades.

6.1.2 CGI commercial viability for cost-effective product designing

- The available design opportunity realized endorses the potential benefits by leveraging the intermediate mechanical and physical properties exposed by CGI. While compared to GCI, ASTM A48 Class- 40 and DI, ASTM A536 60-40-18, for cost-effective product designing, especially for product applications where its strength exposures fall in between the void of GCI and DI materials inaccessible range.

- While pump volute designing, CGI viability becomes evident to compensate requisite structural strength integrity through its distinct material stiffness, yet intacting castability and machinability. Although CGI may not entirely replace DI strength exposure, it provides favorable manufacturing properties to control the finished product cost implication.

- Moreover, recent advancement in CGI production knowledge and technology enables mass-scale CGI production at a competitive cost. This advancement is poised to instill industry confidence and pave the way for widespread acceptance in the near future for numerous general-purpose product development initiatives.

6.2 Contribution

There are numerous advancements made through present work especially to evolve the knowledge concerning CGI, its production, and the establishment of the production process by means of the traditional foundry process.

Such advancement follows as:

- CGI microstructure transformation is comprehensively investigated by performing a series of experimental tests. It is learned that CGI vermicular graphite morphology is an intermediate state while graphite transformation takes place from flakes to nodules for CGI to SG iron formation or vice versa which can be achieved by playing with nodularising and anti-nodularising substances per raw material microstructure.

- The influencing chemical compositions and foundry processes are varied to check sensitivity over CGI microstructure formation. The Vermicular microstructure is highly sensitive to nodularising agents like Mg, Sulfur, etc while metal treatment along with inoculant gives better control over Mg fading rate. Moreover, molten metal temperature and solidification rate are crucial to bring success for CGI microstructure formation apart from chemical composition.

- Detailed investigative research has been made so far which is primarily posed through balancing the Mg and inoculant content, Mg fading volatility, measurement, and control mechanism to achieve quality and mass-scale production.

- While doing investigative experimental trials, it was learned that vermicular microstructure formation is highly sensitive to residual Mg which provides success while having a stable range of 0.008-0.013% of residual Mg in molten metal. It is also realized that Mg. is a highly volatile substance that fades rapidly after treatment so it's crucial to monitor real-time residual Mg in molten metal and control it by adjustment.

- The experimentally developed CGI mechanical strength quality parameters are at par with the available standard so that viability assessment for cost-effective product design has been done while designing the centrifugal pump designing using GCI, CGI & DI to make a comparative study of potential design optimization and cost saving.

6.3 Industrial application

The most prominent use of CGI is in the automotive sector. Due to its superior mechanical properties, it is often used in engine blocks and cylinder heads. The higher thermal conductivity and strength at high temperatures allow for more efficient and powerful engines. Engine manufacturers are increasingly using CGI for diesel engines, performance engines, and even some gasoline engines. Apart from this, there are many more technical opportunities to widen the application of CGI but due to higher production costs led by the distant reach of traditional foundries for CGI production, it is not commercially viable for many of the cost-competitive product applications.

The present research work brought distinct knowledge among a community of practice and established CGI production processes using traditional foundries that come with greater commercial viability. By leveraging conventional foundry infrastructure, this approach significantly reduces the cost barriers traditionally associated with CGI manufacturing. Consequently, this development opens a promising path to broaden the usage of CGI beyond automotive engines, making it suitable for a wider range of engineering applications that demand a combination of high structural strength and superior thermal loading capabilities.

As a result, its industrial application growth is anticipated for many of the untapped opportunities like heavy-duty industrial machinery, such as compressors, pumps, and hydraulic components, due to its strength, fatigue resistance, and wear resistance. Similarly, manufacturing of large wind turbine components such as gearboxes, where CGI's high strength and thermal conductivity make it an ideal material choice for high-load, high-stress applications, is expected to benefit from this advancement.

Moreover, the enhanced cost-viability established through this research supports the expansion of CGI usage in sectors previously constrained by economic limitations. The techno-commercial feasibility of CGI for centrifugal pump applications has already been studied during the present work, and the convincing outcome encourages the adoption of CGI by many potential industries. This breakthrough can be seen as a catalyst for accelerating CGI's integration into mainstream manufacturing by offering a sustainable and economically practical production model.

6.4 Future scope

Though the production of Compacted Graphite Iron (CGI) has been well-studied and developed, several areas could further benefit from research to refine its development process, improve its properties, and widen its applications. One potential research area could be the deployment of enhanced process control. Even though the present research brought greater insight into production process knowledge for CGI using traditional foundry practices, deployment of enhanced precise control protocol could enable mass-scale, consistent, and quality production of CGI, ensuring desired properties.

In tandem, the development of new alloys based on CGI could provide an additional research direction. This could involve creating alloys that enhance the already favorable properties of CGI or introduce new characteristics. The development of more accurate models of the CGI production process could be beneficial, aiding in optimizing the process and predicting the final product's properties. This could entail both experimental research and the formulation of computer simulation techniques.

The properties of CGI heavily depend on its microstructure, and an improved understanding of this could facilitate tailoring the material for specific applications. Research could focus on the relationship between the production process, the resulting microstructure, and the properties of CGI.

As sustainability becomes a crucial factor in development, exploring more environmentally friendly methods for producing CGI, such as using recycled materials or reducing energy consumption during production, could also be a significant research focus.

Lastly, future research could also delve into finding innovative applications for CGI. Potential areas could be in emerging industries such as electric vehicles, renewable energy, aerospace, and more. Thus, while CGI is a well-established material, there are numerous avenues for future research, offering exciting potential for improvements in production and expanded usage.

LIST OF REFERENCES

A.K., S. D., & S.S., M. N. (2009). New Method for the Development of Porous Gray Cast Iron Castings. *International Journal of Metalcasting*, 43–52.

Alonso, G., Larran, P., Stefanescu, D. M., & Suarez, R. (2020). Graphite Nucleation in Compacted Graphite Cast Iron. *International Journal of Metalcasting*. https://doi.org/10.1007/s40962-020-00441-2

Alonso, G., Stefanescu, D. M., Larrañaga, P., & Suarez, R. (2016). Understanding compacted graphite iron solidification through interrupted solidification experiments. *International Journal of Cast Metals Research*, *29*(1–2), 2–11.

Anjos, V., Baumgart, W., Kloetzen, O., Ribeiro, C. A. S., & Cunha, J. (2009). The Modern Thermal Analysis Route to the Compact Graphite Iron Production. *The Carl Loper Cast Iron Symposium (Madison, WI)*.

ANSYS Inc. (2022). *ANSYS Mechanical*. https://www.ansys.com/en-in/products/structures/ansys-mechanical

Belov, I., Fourlakidis, V., Domeij, B., Matsushita, T., & Diószegi, A. (2024). A Thermal Conductivity Model for Lamellar and Compacted Graphite Irons. *International Journal of Metalcasting*, *19*(2), 1129–1139. https://doi.org/10.1007/s40962-024-01373-x

Chisamera, M., Riposan, I., Stan, St., Sparkman, D., Kelley, D. and B. (2002). Experience Producing Compacted Graphite Cast Irons by Sulfur Addition After Magnesium Treatment. *AFS Transactions*, *Vol.110*, pp.851-859.

Chuang, C., Singh, D., Kenesei, P., Almer, J., Hyrn, J., & Huff, R. (2015). 3-D Quantitative Analysis of Graphite Morphology in High Strength Cast Iron by High-Energy X-Ray Tomography. *Scr. Mater.*, *106*, 5–8.

Cohen, P. H., Voigt, R. C., & Marwanga, R. O. (2000). Influence of graphite morphology and matrix structure on chip formation during machining of ductile irons. *AFS Casting Congress, Pittsburg*.

Compacted (Vermicular) Graphite Cast Iron—Classification. (2016). *ISO 16112, International Standards Organization*.

Composition, C., & Morphology, G. (1965). *Compacted Graphite Iron Castings*. *c*.

Cooper, K. P., & C.R. Loper Jr. (1978). A Critical Evaluation of the Production of Compacted Graphite Cast Iron. *Transactions of AFS*, *86*, 267.

Davis, J. R. (1996). ASM Specialty Handbook Cast Irons - 9.2 Melting Practice. *ASM International*, 147–149.

Dawson, S. (1999). Compacted graphite iron: Mechanical and physical properties for engine design. *VDI Berichte*, *1472*, 85–105.

Dawson, S., & S. Dawson. (2014). Compacted Graphite Iron - Mechanical and Physical Properties for Engine Design. *SinterCast Papers*, *1472*, 85–105.

Dawson, S. (1994). *Compacted Graphite Iron : Cast Iron Makes a Comeback*. *August*.

Dawson, Steve. (2002). *Process Control for the Production of Compacted Graphite Iron*. *May*.

Dawson, Steve, I. Hollinger, Robbins, M., Daeth, J., Reuter, U., & Schulz, H. (1999). The effect of metallurgical variables on the machinability of compacted graphite iron. *Design and Machining Workshop – CGI*.

Dawson, Steve, & Schroeder, T. (2000). *Compacted Graphite Iron : A Viable Alternative*.

E. Nechtelberger. (1980). *The properties of cast iron up to 500°C* (English). Technicopy Ltd, England.

Esposito, A. M., He, Q., DePaiva, J. M., & Veldhuis, S. C. (2025). Significance of Tool Coating Properties and Compacted Graphite Iron Microstructure for Tool Selection in Extreme Machining. *Nanomaterials*, *15*(2), 1–23. https://doi.org/10.3390/nano15020130

European Committee for Standardization. (2011). Founding - Compacted (vermicular) graphite cast irons. *EN 16079:2011*.

Evans, E. R., Dawson, J. V., & Lalich, M. J. (1976). Compacted Graphite Cast Irons and

Their Production by a Single Alloy Addition. *Transactions of AFS*, *84*, 215.

Fowler, J., Stefanescu, D. M., & Prucha, T. (1984). Production of Ferritic and Pearlitic Grades of Compacted Graphite Cast Iron by the In-Mold Process. *Transactions of AFS*, *92*, 361.

Gregorutti, R. W., & Grau, J. E. (2014). Mechanical properties of compacted graphite cast iron with different microstructures. *International Journal of Cast Metals Research*, *27*(5), 275–282.

Guesser, W., Fundições, T., Catarina, S., Schroeder, T., & Dawson, S. (2001). Production Experience With Compacted Graphite Iron Automotive Components. *Tupy & SinterCast Technical Paper*, *071*(Figure 2), 1–11.

H.H. Cornell, & C.R. Loper Jr. (1985). Variables Involved in the Production of Compacted Graphite Cast Iron Using Rare Earth-Containing Alloys. *Transactions of AFS*, *93*, 435.

Hahnel, M., & Wisniewski, H. (n.d.). *Method and Device for Fracture-Splitting a Workpiece*.

Heiber, A. F. (1979). . *AFS Transactions*, *87*, 569.

Hernando, J. C. (2017). *New Experimental Technique for Nodularity and Mg Fading Control in Compacted Graphite Iron Production on Laboratory Scale*. https://doi.org/10.1007/s11661-017-4315-3

Hughes, I. C. H., & Powell, J. (1984). Compacted Graphite Irons - High Quality Engineering Materials in the Cast Iron Family. *SAE Technical Paper*.

Kim, S., Cockcroft, S. L., & Omran, A. M. (2009). Optimization of the process parameters affecting the microstructures and properties of compacted graphite iron. *Journal of Alloys and Compounds*, *476*, 728–732.

Ko, M., & Konig, M. (2010). Literature review of microstructure formation in compacted graphite Iron. *International Journal of Cast Metals Research*, *23*(3), 185–193. https://doi.org/10.1179/136404609X12535244328378

Kurikuma, T., Makimura, Y., Tada, M., & Kobayashi, T. (1998). Effects of graphite

morphology and matrix microstructure on damping capacity, tensile strength and Young's modulus of casting irons. *Japan Engineering Society*, *68*, 876–882.

Lei, X., Calash, A., & Cagney, J. (2011). FEA-Based Fatigue Life Prediction of a Notched CGI Component. *SAE International Journal of Engines*, *4*(3), 2756–2766. http://www.jstor.org/stable/26278333

Loper, C. R., Lalich, M. J., Park, H. K., & Gyarmaty, A. M. (1980). The relationship of microstructure to mechanical properties in compacted graphite irons. *AFS Transactions*, *80–160*, 313–330.

Martinez, F., & Stefanescu, D. M. (1983). Properties of Compacted/Vermicular Graphite Cast Irons in the Fe-C-Al System Produced by Ladle and In-Mold Treatment. *Transactions of AFS*, *91*, 593.

Millis, K. D., Gagnebin, A. P., & Pilling, N. B. (1949). *Gray Cast Iron Having Improved Properties* (Patent No. US2485761A).

Mohammed, E. S. M. (2011). *The effect of CGI microstructure on fracture and machining*. http://hdl.handle.net/11375/11243

Murthy, V. S. ., & Seshan, S. (1984). Characteristics of Compacted Graphite Cast Iron. *AFS Transactions*, *84–76*, 373–380.

Nechtelberger, E., Hummer, R., & Thury, W. (1970). Aluminum-Alloyed Cast Iron with Vermicular Graphite. *Giesserei - Prax*, *24*, 387.

Nechtelberger, E., Puhr, H., J.B. von Nesselrode, & Nakayasu, A. (1982). Cast Iron with Vermicular/ Compacted Graphite—State of the Art Development, Production, Properties, Applications,. *49th International Foundry Congress, Chicago*.

Niu, J., Huang, C., Shi, Z., Liu, H., Tang, Z., Wang, Z., Li, B., Xu, L., Chen, Z., & Huang, S. (2025). Some new findings on formation mechanisms of the machined surface geometric quality of compacted graphite iron. *Journal of Alloys and Compounds*, *1010*(June 2024), 178120. https://doi.org/10.1016/j.jallcom.2024.178120

Patel, M., & Dave, K. (2023). Compacted graphite iron mass production challenges using traditional foundry practices. *Industrial Engineering Journal*, *52*(6).

Patel, M., & Dave, K. (2022). An Insight of Compacted Graphite Iron (CGI) Characteristics and Its Production: A Review. *Recent Advances in Manufacturing Processes and Systems*, 131–148. https://doi.org/10.1007/978-981-16-7787-8_10

Patel, P., & Patel, B. K. (2022). The Small Punch Test a Viable Alternate for In-service Components Preserved Strength Estimation. *Journal of The Institution of Engineers (India): Series C*, *103*(1), 121–133. https://doi.org/10.1007/s40032-021-00728-1

Patel, P., & Patel, B. K. (2023). Comprehensive correlations for small punch test response post-processing toward preserved mechanical strength estimation. *Journal of Nondestructive Evaluation, Diagnostics and Prognostics of Engineering Systems*, 1–13. https://doi.org/10.1115/1.4062093

QIU, H., & Chen, Z. (2007). The forty years of vermicular graphite cast iron development in China (Part 1, 2 & 3). *China Foundry*, *4*.

Ramberg, W., & Osgood, W. R. (1943). Description of stress-strain curves by three parameters. *National Advisory Committee For Aeronautics*, Technical Note No. 902. http://hdl.handle.net/2060/19930081614

Regordosa, A., Torre, U. De, Loizaga, A., Sertucha, J., & Lacaze, J. (2019). Microstructure Changes during Solidification of Cast Irons: Effect of Chemical Composition and Inoculation on Competitive Spheroidal and Compacted Graphite Growth. *International Journal of Metalcasting*, *1*. https://doi.org/10.1007/s40962-019-00389-y

Renfang, W., Yuanheng, P., & Manji, C. (1994). Research On and Experience In the Mass Production of Compacted Graphite Iron Exhaust Manifolds. *BCIRA Conference*.

Riposan, I, Chisamera, M., Kelley, R., Barstow, M., & Naro, R. L. (2003). Magnesium-Sulfur Relationships in Ductile and Compacted Graphite Cast Irons as Influenced by Late Sulfur Additions Copyright 2003 American Foundry Society. *AFS Transactions*, *093*(05), 1–15.

Riposan, Iulian. (2018). Modification and Inoculation of Cast Iron. *Cast Iron Science and Technology*, *1*, 160–176. https://doi.org/10.31399/asm.hb.v01a.a0006315

Ruff, G. F., & Vert, T. C. (1979). Investigation of Compacted Graphite Iron Using a High

Sulfur Gray Iron Base. *Transactions of AFS*, *87*, 459.

S. Dawson. (2002). *Microstructure and Porosity Control*.

Saito, R., Maruyama, T., Nakamura, T., Yanagitani, H., Sakai, T., & Nakamoto, K. (2018). Influence of Tellurium Addition to Spheroidal Graphite Cast Iron on the Number of Graphite Particles. *International Journal of Metalcasting*. https://doi.org/10.1007/s40962-018-00292-y

Schelling, R. D. (1969). *Cast Iron with At Least 50% of the Graphite in Vermicular Form and a Process for Making Same* (Patent No. U.S. Patent 3421886).

Sergeant, G. F., & Evans, E. R. (1978). The Production and Properties of Compacted Graphite Irons. *The British Foundryman*, *71*, 115.

Shao, S., Dawson, S., & Lampic, M. (1998). *The Mechanical and Physical Properties of Compacted Graphite Iron*. *Werkstofftech. 29*, 397–411.

Shikida, M., Kanayama, Y., & Nakayama, H. (1986). Strength and Crack Growth Behaviors of Compacted Graphite Vermicular Cast Iron in Rotating Bending. *29th Japan Congress on Materials Research*, 23–28.

Shy, Y., Hsu, C., Lee, S., & Hou, C. (2000). Effects of titanium addition and section size on microstructure and mechanical properties of compacted graphite cast iron. *Materials Science and Engineering*, *A278*, 54–60.

Simmons, W. (1976). A Sandwich Process Using Pure Magnesium. *The British Foundryman*.

SinterCast Nodularity Rating Charts. (1997).

Skaland, T. (n.d.). High Rare Earth Treatment of Compacted Graphite Iron. *AFS Congress, Panel 02-173*.

Standard Specification for Compacted Graphite Iron Castings. (2018). *ASTM 842*. https://doi.org/10.1520/A0842-11AR18E01

Standard Specification for Ductile Iron Castings. (2019). *ASTM A536*.

Standard Specification for Gray Iron Castings. (2022). *ASTM A48*.

Standard Test Method for Evaluating the Microstructure of Graphite in Iron Castings. (2019). *ASTM 247-19*. https://doi.org/10.1520/A0247-19

standard test methods for tension testing of metallic materials. (2010). *ASTM E8/E8M*, *C*, 1–27. https://doi.org/10.1520/E0008

Stefanescu, D. M. (2015). Thermal Analysis — Theory and Applications in Metalcasting. *International Journal of Metalcasting*, *9*(1), 7–22.

Stefanescu, D. M., Alonso, G., Larran, P., & Suarez, R. (2018). A Comparative Study of Graphite Growth in Cast Iron and in Analogous Systems. *International Journal of Metalcasting*. https://doi.org/10.1007/s40962-017-0204-1

Stefanescu, D. M., Dinescu, I., Craciun, S., & Popescu, M. (1979). Production of Vermicular Graphite Cast Irons by Operative Control and Correction of Graphite Shape. *46th International Foundry Congress (Madrid, Spain)*, *Paper 37*.

Stefanescu, D. M., Martinez, F., & I.G. Chen. (1983). Solidification Behavior of Hypoeutectic and Eutectic Compacted Graphite Cast Irons—Chilling Tendency and Eutectic Cells. *Transactions of AFS*, *91*, 205.

Sumimoto, H., Nakamura, K., & Umeda, Y. (n.d.). Relationship between graphite morphology and fatigue limit in compacted vermicular and ductile cast iron. *Kinki University Research Report*, *22*.

Svensson, I., & Sjogren, T. (2009). On Modeling and Simulation of Mechanical Properties of Cast Irons with Different Morphologies of Graphite. *International Journal of Metalcasting*, 67–77.

Ulrich, R. (2000). The wear process of CGI cutting and machining developments. *Compacted Graphite Iron – Machining Workshop, Darmstadt, Germany*.

Walton, C. F., & Opar, T. J. (1981). *Iron Castings Handbook*. Iron Castings Society.

Wu, Y., Li, J., Yang, Z., Ma, Z., Guo, Y., Tao, D., Yang, T., & Liang, M. (2019). Computational Assessment of Thermal Conductivity of Compacted Graphite Cast Iron.

Advances in Materials Science and Engineering, *2019*, 1–7. https://doi.org/10.1155/2019/8562102

www.apriori.com. (2022).

Xu, D. mei, Wang, G. quan, Chen, X., Li, Y. xiang, Liu, Y., & Zhang, H. wei. (2018). Effects of alloy elements on ductility and thermal conductivity of compacted graphite iron. *China Foundry*, *15*(3), 189–195. https://doi.org/10.1007/s41230-018-8055-9

Y.J. Park, Gundlach, R. B., & J.F. Janowak. (1987). Effects of Molybdenum on Thermal Fatigue Resistance of Ductile and Compacted Graphite Irons. *AFS Transactions*, *87–90*, 267–272.

Ziegler, K. R., & Wallace, J. F. (1984). The Effect of Matrix Structure and Alloying on the Properties of Compacted Graphite Iron. *Transactions of AFS*, *92*, 735.

LIST OF PUBLICATIONS

PUBLICATION 1

Title An Insight of Compacted Graphite Iron (CGI) Characteristics and Its Production: A Review

Publisher Springer, Singapore

Journal Recent Advances in Manufacturing Processes and Systems

Index Scopus

PUBLICATION 2

Title Assessment of compacted graphite iron viability for cost-effective product designing

Publisher Springer, India

Journal Journal of The Institution of Engineers (India): Series D

Index Scopus

PUBLICATION 3

Title Compacted Graphite Iron Mass Production Challenges Using Traditional Foundry Practices

Publisher Indian Institution of Industrial Engineering (IIIE)

Journal Industrial Engineering Journal

Index UGC CARE Group-1

PUBLICATION 4

Title	Pouring Time Influence on Residual Mg, Compacted Graphite Formation and Mechanical Properties of Compacted Graphite Iron
Publisher	IAEME Publication
Journal	International Journal of Production Technology and Management (IJPTM)
Index	UGC CARE Group-1

ANNEXURE 1

QUALITY ASSESSMENT REPORTS

MET-HEAT ENGINEERS PVT. LTD.

METALLURGICAL LABORATORY ON APPROVED LIST OF VARIOUS
GOVT. DEPARTMENTS & PUBLIC SECTOR UNDERTAKINGS (SINCE 1975)
857/2, G.I.D.C. Industrial Estate, ERDA Road, Makarpura, Vadodara - 390 010, Gujarat, India.
Telephone : +91-265-2632374, 2643655, 2648026, 93776 43655, 93776 48026
E-mail : info@metheat.com • Website : www.metheat.com • CIN : U28939GJ1996PTC029934

TEST REPORT

WO:11-1151 Sr. No. 1M / 4 -X-Cr-

Customer's Name : MAMTA PATEL
(MECHANICAL DEPARTMENT) BITS EDU.CAMPUS.VARNAMA, MUMBAI EXPRESS HIGHWAY, VADODARA

Particulars of Sample : TEST PIECE

Identification of Sample : SAMPLE NO:S1 WITH SULPHUR

Test Report No. : 583HX/ 2017
Date of Report : 13-11-2017
Date of Receipt : 09-11-2017

583HX MICROSTRUCTURE (Test Method : As per ASM HANDBOOK VOLUME-9:2004)

Etchant :	2% Nital
Magnification :	200X
Microstructure :	Microstructure consist of interdendretic pattern of austenite and interdendretic eutectic of austenite and carbide.

This microstructure is matching with general microstructure of white cast iron.

----------End of Report----------

MET HEAT ENGINEERS PVT. LTD. VADODARA

Tested By

Authorized Signatory
A.M. Dave (QM) / M.G. Dave (MD) / N.M. Dave (TM)

Witnessed By

Page 1 of 1

(1) Sample(s) not drawn by MHEPL. The results relate only to the sample(s) tested.
(2) This Certificate shall not be reproduced, except in full, without the written approval of MHEPL.
(3) If balance material is available after testing, it will be retained for 15 days maximum. If customer wants to retain it for one month from this date, he has to inform in written or he has to collect the same.
(4) While Met-Heat has made the best endeavors to provide accurate and reliable information, Met-Heat is not responsible for any financial liability due to act of omission or error made.
(5) "*" Indicates Out of NABL Approved Range.

MET-HEAT ENGINEERS PVT. LTD.

METALLURGICAL LABORATORY ON APPROVED LIST OF VARIOUS
GOVT. DEPARTMENTS & PUBLIC SECTOR UNDERTAKINGS (SINCE 1975)
857/2, G.I.D.C. Industrial Estate, ERDA Road, Makarpura, Vadodara - 390 010, Gujarat, India.
Telephone : +91-265-2632374, 2643655, 2648026, 93776 43655, 93776 48026
E-mail : info@metheat.com • Website : www.metheat.com • CIN : U28939GJ1996PTC029934

TEST REPORT

WO:11-1151 Sr. No. 2M / 4 -X-Cr-

Customer's Name	:	MAMTA PATEL (MECHANICAL DEPARTMENT) BITS EDU.CAMPUS.VARNAMA, MUMBAI EXPRESS HIGHWAY, VADODARA	Test Report No.	: 585HX/ 2017
			Date of Report	: 13-11-2017
Particulars of Sample	:	TEST PIECE	Date of Receipt	: 09-11-2017
Identification of Sample	:	SAMPLE NO:S2 WITHOUT SULPHUR		

585HX MICROSTRUCTURE (Test Method : As per ASM HANDBOOK VOLUME-9:2004)

Etchant :	2% Nital
Magnification :	200X
Microstructure :	Microstructure consist of interdendretic pattern of austenite and interdendretic eutectic of austenite and carbide.

This microstructure is matching with general microstructure of white cast iron.

----------End of Report----------

MET HEAT ENGINEERS PVT. LTD. VADODARA

Tested By

Authorized Signatory
A.M. Dave (QM) / M.G. Dave (MD) / N.M. Dave (TM)

Witnessed By

(1) Sample(s) not drawn by MHEPL. The results relate only to the sample(s) tested.
(2) This Certificate shall not be reproduced, except in full, without the written approval of MHEPL.
(3) If balance material is available after testing, it will be retained for 15 days maximum. If customer wants to retain it for one month from this date, he has to inform in written or he has to collect the same.
(4) While Met-Heat has made the best endeavors to provide accurate and reliable information, Met-Heat is not responsible for any financial liability due to act of omission or error made.
(5) "*" Indicates Out of NABL Approved Range.

MET-HEAT ENGINEERS PVT. LTD.

METALLURGICAL LABORATORY ON APPROVED LIST OF VARIOUS
GOVT. DEPARTMENTS & PUBLIC SECTOR UNDERTAKINGS (SINCE 1975)
857/2, G.I.D.C. Industrial Estate, ERDA Road, Makarpura, Vadodara - 390 010, Gujarat, India.
Telephone : +91-265-2632374, 2643655, 2648026, 93776 43655, 93776 48026
E-mail : info@metheat.com • Website : www.metheat.com • CIN : U28939GJ1996PTC029934

TEST REPORT

WO:11-1151 Sr. No. 3C / 4 -X-Cr-

Customer's Name : MAMTA PATEL
(MECHANICAL DEPARTMENT) BITS EDU.CAMPUS.VARNAMA,
MUMBAI EXPRESS HIGHWAY, VADODARA

Particulars of Sample : TEST PIECE

Material Specification : S.G.CAST IRON

Identification of Sample : ID.NO:S1 WITH SULPHUR

Test Report No. : 100HA/ 2017
Date of Report : 11-11-2017
Date of Receipt : 09-11-2017

100HA CHEMICAL ANALYSIS [WET FE BASE]

	Obtained Value
%Carbon (C)	3.200
%Silicon (Si)	1.750
%Manganese (Mn)	0.200
%Phosphorus (P)	0.106
%Sulphur (S)	0.350
%Nickel (Ni)	0.130
%Chromium (Cr)	Nil
%Molybdenum (Mo)	Nil

----------End of Report----------

MET HEAT ENGINEERS PVT. LTD. VADODARA

Tested By

Authorized Signatory
A.M. Dave (QM) / M.G. Dave (MD) / N.M. Dave (TM)

Witnessed By

Page 1 of 1

(1) Sample(s) not drawn by MHEPL. The results relate only to the sample(s) tested.
(2) This Certificate shall not be reproduced, except in full, without the written approval of MHEPL.
(3) If balance material is available after testing, it will be retained for 15 days maximum. If customer wants to retain it for one month from this date, he has to inform in written or he has to collect the same.
(4) While Met-Heat has made the best endeavors to provide accurate and reliable information, Met-Heat is not responsible for any financial liability due to act of omission or error made.
(5) "*" Indicates Out of NABL Approved Range.

MET-HEAT ENGINEERS PVT. LTD.

METALLURGICAL LABORATORY ON APPROVED LIST OF VARIOUS
GOVT. DEPARTMENTS & PUBLIC SECTOR UNDERTAKINGS (SINCE 1975)
857/2, G.I.D.C. Industrial Estate, ERDA Road, Makarpura, Vadodara - 390 010, Gujarat, India.
Telephone : +91-265-2632374, 2643655, 2648026, 93776 43655, 93776 48026
E-mail : info@metheat.com • Website : www.metheat.com • CIN : U28939GJ1996PTC029934

TEST REPORT

WO:11-1151 Sr. No. 4C / 4 -X-Cr-

Customer's Name : MAMTA PATEL
(MECHANICAL DEPARTMENT) BITS EDU.CAMPUS.VARNAMA, MUMBAI EXPRESS HIGHWAY, VADODARA

Particulars of Sample : TEST PIECE

Material Specification : S.G.CAST IRON

Identification of Sample : ID.NO:S2 WITHOUT SULPHUR

Test Report No. : 101HA/ 2017
Date of Report : 11-11-2017
Date of Receipt : 09-11-2017

101HA CHEMICAL ANALYSIS [WET FE BASE]

	Obtained Value
%Carbon (C)	3.360
%Silicon (Si)	1.760
%Manganese (Mn)	0.350
%Phosphorus (P)	0.101
%Sulphur (S)	0.012
%Nickel (Ni)	0.130
%Chromium (Cr)	Nil
%Molybdenum (Mo)	Nil

End of Report

MET HEAT ENGINEERS PVT. LTD. VADODARA

Tested By

Authorized Signatory
A.M. Dave (QM) / M.G. Dave (MD) / N.M. Dave (TM)

Witnessed By

(1) Sample(s) not drawn by MHEPL. The results relate only to the sample(s) tested.
(2) This Certificate shall not be reproduced, except in full, without the written approval of MHEPL.
(3) If balance material is available after testing, it will be retained for 15 days maximum. If customer wants to retain it for one month from this date, he has to inform in written or he has to collect the same.
(4) While Met-Heat has made the best endeavors to provide accurate and reliable information, Met-Heat is not responsible for any financial liability due to act of omission or error made.
(5) "*" Indicates Out of NABL Approved Range.

TCR Advanced Engineering P. Ltd.

TCR ADVANCED ENGINEERING PVT. LTD.

Research Center & Testing Division:
Regd. Off. : 250-252/9, GIDC Estate, Makarpura, Vadodara – 390010
PH: (0265) 2657233, 7574805594,7574805595,8511117993
Email : testing@tcradvanced.com Website : www.tcradvanced.com

Managing Director
Paresh U. Haribhakti
BE. (Met.), M.E. (Mat. Tech.) MIE, LMIIM,LMIIW, Chartered Engineer

ON APPROVED LIST OF VARIOUS GOVT. DEPARTMENTS AND PUBLIC SECTOR UNDERTAKINGS

TEST REPORT

Report No. Q-32019.1	Page 1 of 1	Date: 03/12/2018

To,
Mamta Patel
Ahmedabad

TEST: Microstructure Examination

TEST METHOD: ASTM E407-07 (2015)

Test Performed at: TCR Advanced Engineering Pvt. Ltd.

Instrument Utilized:	Optical Microscope, TCRADV/E-185		
*Customer's Reference:	Ref No - GTU/Phd/B_2015/Bonafide/2018/5944,Dated : 08.08.18		
Sample received on:	28/11/2018		
*Condition of sample:	Casting Sample		
*Specification:	-		
Date of completion of test:	03/12/2018	Sample Drawn by:	**Party**

***SAMPLE ID: Sample No - 10Mg**

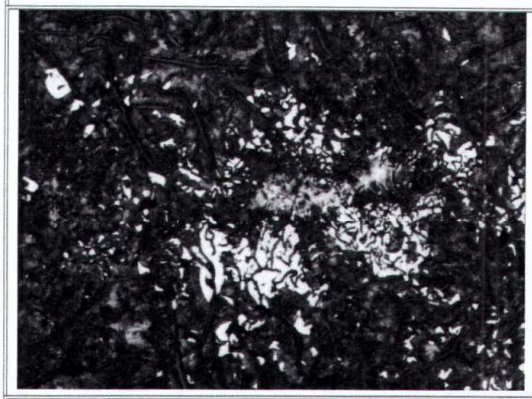

Plate 1: At Core 200X

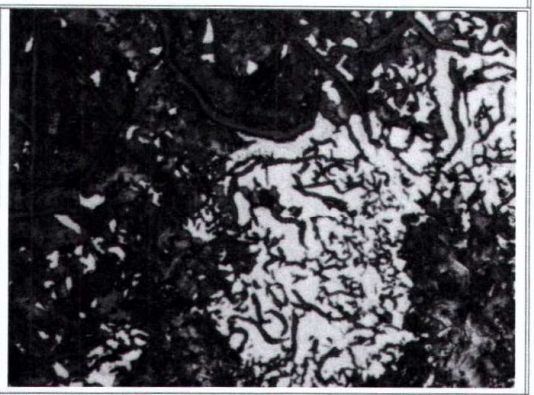

Plate 2: At Core 400X

Observation:	Microstructure shows graphite flakes in the matrix of pearlite with presence of ferrite.	
Observed at:	200-400X	**Etchant:** 2% Nital

End of report.

Checked By: Vaishnavi

TCR ADVANCED ENGINEERING PVT. LTD. VADODARA

Authorised Signatory
P. A. MEHTA

1. The results relate only to the sample tested. 2. Test certificate shall not be re-produced except in full without the written approval of laboratory. 3. TCR Advanced has made their best endeavours to provide accurate and reliable information, TCR Advanced is not responsible for any financial liability due to any act of omission or error made. 4. Samples are preserved for 15 days, Any ambiguity in test results should be brought forward to the lab management within this period. 5.* Information provided by customer.

TCR Advanced Engineering P. Ltd.

TCR ADVANCED ENGINEERING PVT. LTD.

Research Center & Testing Division:
Regd. Off. : 250-252/9, GIDC Estate, Makarpura, Vadodara – 390010
PH: (0265) 2657233, 7574805594,7574805595,8511117993
Email : testing@tcradvanced.com Website : www.tcradvanced.com

Managing Director
Paresh U. Haribhakti
BE. (Met.), M.E. (Mat. Tech.) MIE, LMIIM,LMIIW, Chartered Engineer

ON APPROVED LIST OF VARIOUS GOVT. DEPARTMENTS AND PUBLIC SECTOR UNDERTAKINGS

TEST REPORT

Report No: Q-32020.1	Page 1 of 1	Date: 03/12/2018

To,
Mamta Patel
Ahmedabad

TEST: Microstructure Examination

TEST METHOD: ASTM E407-07 (2015)

Test Performed at: TCR Advanced Engineering Pvt. Ltd.

Instrument Utilized:	Optical Microscope, TCRADV/E-185		
*Customer's Reference:	Ref No - GTU/Phd/B_2015/Bonafide/2018/5944,Dated : 08.08.18		
Sample received on:	28/11/2018		
*Condition of sample:	Casting Sample		
*Specification:	-		
Date of completion of test:	03/12/2018	Sample Drawn by:	**Party**

***SAMPLE ID: Sample No - 25Mg**

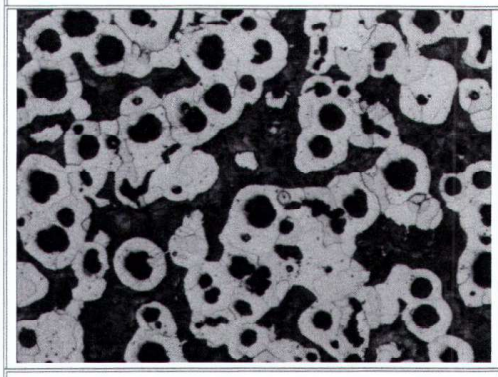

Plate 1: At Core 200X

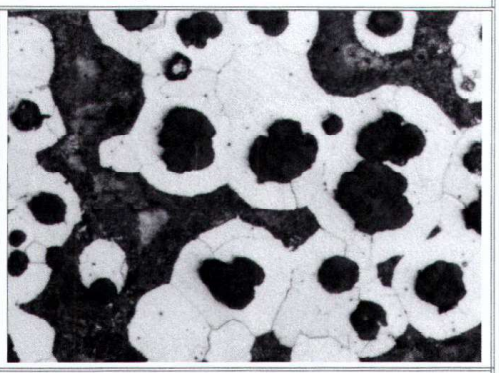

Plate 2: At Core 400X

Observation:	Microstructure shows graphite nodules surrounded by ferrite with presence of pearlite.	
Observed at:	200-400X	**Etchant:** 2% Nital

End of report.

TCR ADVANCED ENGINEERING PVT. LTD. VADODARA

Checked By: Vaishnavi

Authorised Signatory
P. A. MEHTA

1. The results relate only to the sample tested. 2. Test certificate shall not be re-produced except in full without the written approval of laboratory. 3. TCR Advanced has made their best endeavours to provide accurate and reliable information, TCR Advanced is not responsible for any financial liability due to any act of omission or error made. 4. Samples are preserved for 15 days, Any ambiguity in test results should be brought forward to the lab management within this period. 5.* Information provided by customer.

TCR Advanced Engineering P. Ltd.

TCR ADVANCED ENGINEERING PVT. LTD.

Research Center & Testing Division:
Regd. Off. : 250-252/9, GIDC Estate, Makarpura, Vadodara – 390010
PH: (0265) 2657233, 7574805594,7574805595,8511117993
Email : testing@tcradvanced.com Website : www.tcradvanced.com

Managing Director
Paresh U. Haribhakti
BE. (Met.), M.E. (Mat. Tech.) MIE, LMIIM,LMIIW, Chartered Engineer

ON APPROVED LIST OF VARIOUS GOVT. DEPARTMENTS AND PUBLIC SECTOR UNDERTAKINGS

TEST REPORT

Report No: Q-32021.1	Page 1 of 1	Date: 03/12/2018

To,
Mamta Patel
Ahmedabad

TEST: Microstructure Examination

TEST METHOD: ASTM E407-07 (2015)

Test Performed at: TCR Advanced Engineering Pvt. Ltd.

Instrument Utilized:	Optical Microscope, TCRADV/E-185		
*Customer's Reference:	Ref No - GTU/Phd/B_2015/Bonafide/2018/5944,Dated : 08.08.18		
Sample received on:	28/11/2018		
*Condition of sample:	Casting Sample		
*Specification:	-		
Date of completion of test:	03/12/2018	Sample Drawn by:	**Party**

***SAMPLE ID: Sample No - 40Mg**

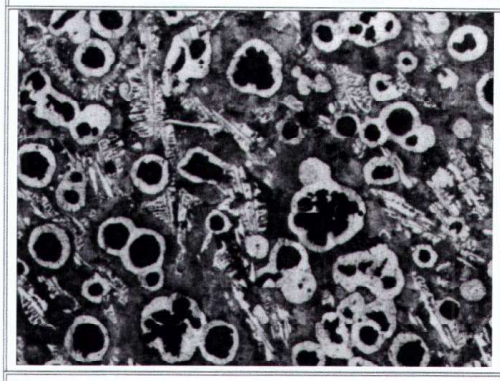

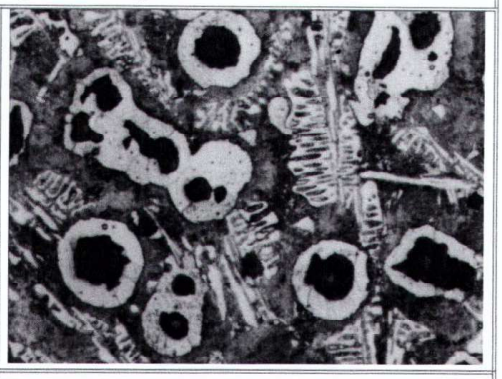

Plate 1: At Core	200X	Plate 2: At Core	400X

Observation:	Microstructure shows graphite nodules/few compacted graphite surrounded by ferrite with presence of pearlite and carbides.	
Observed at:	200-400X	**Etchant:** 2% Nital

End of report.

Checked By: Vaishnavi

TCR ADVANCED ENGINEERING PVT. LTD. VADODARA

Authorised Signatory
P. A. MEHTA

1. The results relate only to the sample tested. 2. Test certificate shall not be re-produced except in full without the written approval of laboratory. 3. TCR Advanced has made their best endeavours to provide accurate and reliable information, TCR Advanced is not responsible for any financial liability due to any act of omission or error made. 4. Samples are preserved for 15 days. Any ambiguity in test results should be brought forward to the lab management within this period. 5.* Information provided by customer.

TCR Advanced Engineering P. Ltd.

TCR ADVANCED ENGINEERING PVT. LTD.

Research Center & Testing Division:
Regd. Off. : 250-252/9, GIDC Estate, Makarpura, Vadodara – 390010
PH: (0265) 2657233, 7574805594,7574805595,8511117993
Email : testing@tcradvanced.com Website : www.tcradvanced.com

Managing Director
Paresh U. Haribhakti
BE. (Met.), M.E. (Mat. Tech.) MIE, LMIIM,LMIIW, Chartered Engineer

ON APPROVED LIST OF VARIOUS GOVT. DEPARTMENTS AND PUBLIC SECTOR UNDERTAKINGS

TEST REPORT

Report No: Q-32022.1	Page 1 of 1	Date: 03/12/2018

To,
Mamta Patel
Ahmedabad

TEST: Microstructure Examination

TEST METHOD: ASTM E407-07 (2015)

Test Performed at: TCR Advanced Engineering Pvt. Ltd.

Instrument Utilized:	Optical Microscope, TCRADV/E-185		
*Customer's Reference:	Ref No - GTU/Phd/B_2015/Bonafide/2018/5944,Dated : 08.08.18		
Sample received on:	28/11/2018		
*Condition of sample:	Casting Sample		
*Specification:	-		
Date of completion of test:	03/12/2018	Sample Drawn by:	**Party**

***SAMPLE ID: Sample No - 70Mg**

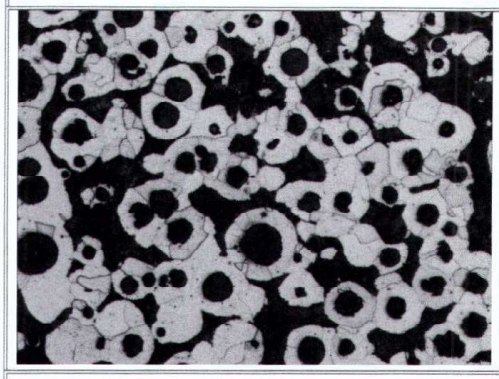

Plate 1: At Core 200X

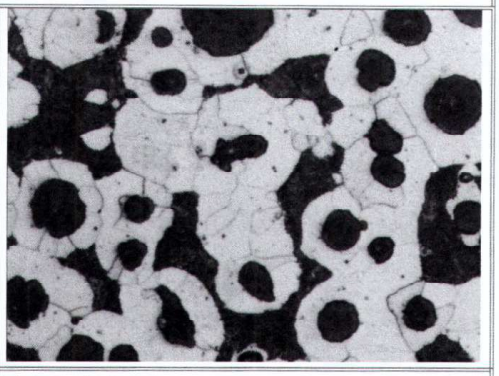

Plate 2: At Core 400X

Observation:	Microstructure shows graphite nodules surrounded by ferrite with presence of pearlite.	
Observed at:	200-400X	**Etchant:** 2% Nital

End of report.

TCR ADVANCED ENGINEERING PVT. LTD. VADODARA

Checked By: Vaishnavi

Authorised Signatory
P. A. MEHTA

1. The results relate only to the sample tested. 2. Test certificate shall not be re-produced except in full without the written approval of laboratory. 3. TCR Advanced has made their best endeavours to provide accurate and reliable information, TCR Advanced is not responsible for any financial liability due to any act of omission or error made. 4. Samples are preserved for 15 days, Any ambiguity in test results should be brought forward to the lab management within this period. 5.* Information provided by customer.

TCR Advanced Engineering P. Ltd.

TCR ADVANCED ENGINEERING PVT. LTD.

Research Center & Testing Division:
Regd. Off. : 250-252/9, GIDC Estate, Makarpura, Vadodara – 390010
PH: (0265) 2657233, 7574805594,7574805595,8511117993
Email : testing@tcradvanced.com Website : www.tcradvanced.com

Managing Director
Paresh U. Haribhakti
BE. (Met.), M.E. (Mat. Tech.) MIE, LMIIM,LMIIW, Chartered Engineer

ON APPROVED LIST OF VARIOUS GOVT. DEPARTMENTS AND PUBLIC SECTOR UNDERTAKINGS

TEST REPORT

Report No: Q-32015.1	Page 1 of 1	Date: 03/12/2018

To,
Mamta Patel
Ahmedabad

TEST: Microstructure Examination

TEST METHOD: ASTM E407-07 (2015)

Test Performed at: TCR Advanced Engineering Pvt. Ltd.

Instrument Utilized:	Optical Microscope, TCRADV/E-185		
*Customer's Reference:	Ref No - GTU/Phd/B_2015/Bonafide/2018/5944,Dated : 08.08.18		
Sample received on:	28/11/2018		
*Condition of sample:	Casting Sample		
*Specification:	-		
Date of completion of test:	03/12/2018	Sample Drawn by:	**Party**

***SAMPLE ID: Sample No - 5S1**

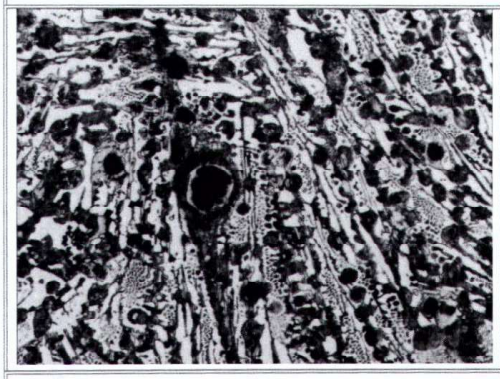

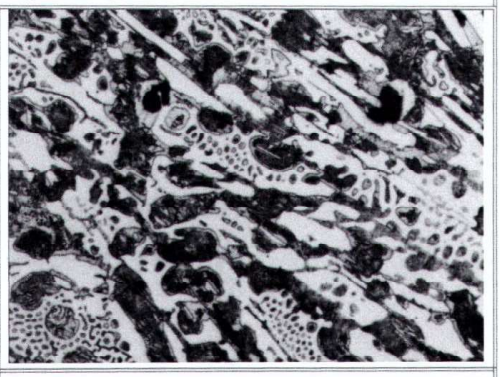

Plate 1: At Core	200X	Plate 2: At Core	400X

Observation:	Microstructure shows graphite nodules surrounded by ferrite with presence of pearlite and carbides.	
Observed at:	200-400X	**Etchant:** 2% Nital

End of report.

Checked By: Vaishnavi

TCR ADVANCED ENGINEERING PVT. LTD. VADODARA

Authorised Signatory
P. A. MEHTA

1. The results relate only to the sample tested. 2. Test certificate shall not be re-produced except in full without the written approval of laboratory. 3. TCR Advanced has made their best endeavours to provide accurate and reliable information, TCR Advanced is not responsible for any financial liability due to any act of omission or error made. 4. Samples are preserved for 15 days, Any ambiguity in test results should be brought forward to the lab management within this period. 5.* Information provided by customer.

TCR Advanced Engineering P. Ltd.

Managing Director
Paresh U. Haribhakti
BE. (Met.), M.E. (Mat. Tech.) MIE, LMIIM,LMIIW, Chartered Engineer

TCR ADVANCED ENGINEERING PVT. LTD.

Research Center & Testing Division:
Regd. Off. : 250-252/9, GIDC Estate, Makarpura, Vadodara – 390010
PH: (0265) 2657233, 7574805594,7574805595,8511117993
Email : testing@tcradvanced.com Website : www.tcradvanced.com

ON APPROVED LIST OF VARIOUS GOVT. DEPARTMENTS AND PUBLIC SECTOR UNDERTAKINGS

TEST REPORT

Report No: Q-32016.1	Page 1 of 1	Date: 03/12/2018

To,
Mamta Patel
Ahmedabad

TEST: Microstructure Examination

TEST METHOD: ASTM E407-07 (2015)

Test Performed at: TCR Advanced Engineering Pvt. Ltd.

Instrument Utilized:	Optical Microscope, TCRADV/E-185		
*Customer's Reference:	Ref No - GTU/Phd/B_2015/Bonafide/2018/5944,Dated : 08.08.18		
Sample received on:	28/11/2018		
*Condition of sample:	Casting Sample		
*Specification:	-		
Date of completion of test:	03/12/2018	Sample Drawn by:	**Party**

***SAMPLE ID: Sample No - 5S2**

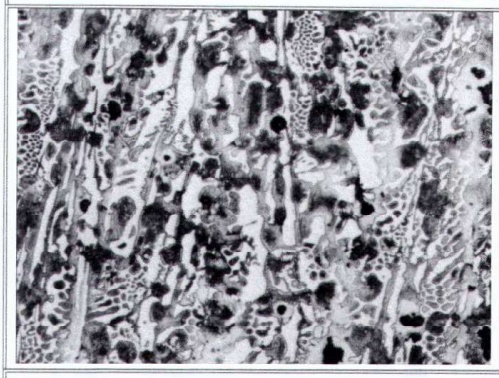

Plate 1: At Core 200X

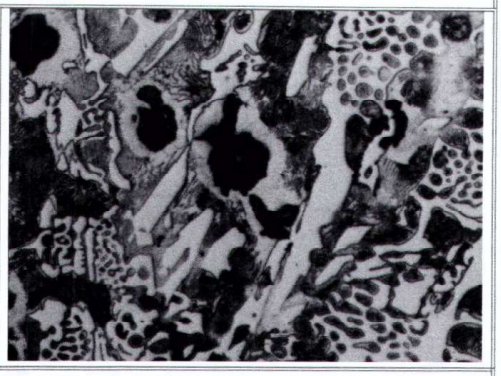

Plate 2: At Core 400X

Observation:	Microstructure shows graphite nodules surrounded by ferrite with presence of pearlite and carbides.	
Observed at:	200-400X	**Etchant:** 2% Nital

End of report.

Checked By: Vaishnavi

TCR ADVANCED ENGINEERING PVT. LTD. VADODARA

Pooja
Authorised Signatory
P. A. MEHTA

1. The results relate only to the sample tested. 2. Test certificate shall not be re-produced except in full without the written approval of laboratory. 3. TCR Advanced has made their best endeavours to provide accurate and reliable information, TCR Advanced is not responsible for any financial liability due to any act of omission or error made. 4. Samples are preserved for 15 days, Any ambiguity in test results should be brought forward to the lab management within this period. 5.* Information provided by customer.

TCR Advanced Engineering P. Ltd.

TCR ADVANCED ENGINEERING PVT. LTD.

Research Center & Testing Division:
Regd. Off. : 250-252/9, GIDC Estate, Makarpura, Vadodara – 390010
PH: (0265) 2657233, 7574805594,7574805595,8511117993
Email : testing@tcradvanced.com Website : www.tcradvanced.com

Managing Director
Paresh U. Haribhakti
BE. (Met.), M.E. (Mat. Tech.) MIE, LMIIM,LMIIW, Chartered Engineer

ON APPROVED LIST OF VARIOUS GOVT. DEPARTMENTS AND PUBLIC SECTOR UNDERTAKINGS

TEST REPORT

Report No: Q-32018.1	Page 1 of 1	Date: 03/12/2018

To,
Mamta Patel
Ahmedabad

TEST: Microstructure Examination

TEST METHOD: ASTM E407-07 (2015)

Test Performed at: TCR Advanced Engineering Pvt. Ltd.

Instrument Utilized:	Optical Microscope, TCRADV/E-185		
*Customer's Reference:	Ref No - GTU/Phd/B_2015/Bonafide/2018/5944,Dated : 08.08.18		
Sample received on:	28/11/2018		
*Condition of sample:	Casting Sample		
*Specification:	-		
Date of completion of test:	03/12/2018	Sample Drawn by:	**Party**

***SAMPLE ID: Sample No - 1.25S2**

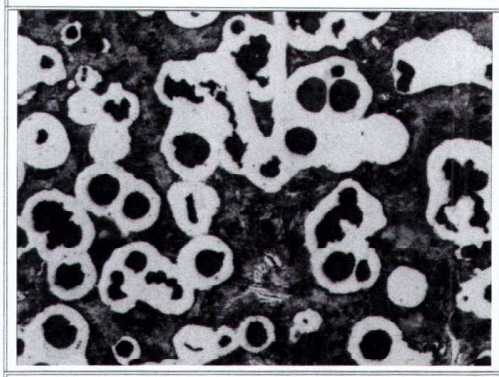

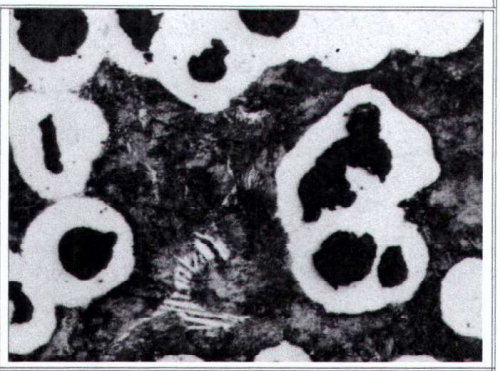

Plate 1: At Core	200X	Plate 2: At Core	400X

Observation:	Microstructure shows graphite nodules surrounded by ferrite with presence of pearlite.	
Observed at:	200-400X	**Etchant:** 2% Nital

End of report.

TCR ADVANCED ENGINEERING PVT. LTD. VADODARA

Checked By: Vaishnavi

Authorised Signatory
P. A. MEHTA

1. The results relate only to the sample tested. 2. Test certificate shall not be re-produced except in full without the written approval of laboratory. 3. TCR Advanced has made their best endeavours to provide accurate and reliable information, TCR Advanced is not responsible for any financial liability due to any act of omission or error made. 4. Samples are preserved for 15 days, Any ambiguity in test results should be brought forward to the lab management within this period. 5.* Information provided by customer.

TCR Advanced Engineering P. Ltd.

Managing Director
Paresh U. Haribhakti
BE. (Met.), M.E. (Mat. Tech.) MIE, LMIIM,LMIIW, Chartered Engineer

TCR ADVANCED ENGINEERING PVT. LTD.

Research Center & Testing Division:
Regd. Off. : 250-252/9, GIDC Estate, Makarpura, Vadodara – 390010

PH: (0265) 2657233, 7574805594,7574805595,8511117993
Email : testing@tcradvanced.com Website : www.tcradvanced.com

ON APPROVED LIST OF VARIOUS GOVT. DEPARTMENTS AND PUBLIC SECTOR UNDERTAKINGS

TEST REPORT

Report No: Q-32017.1	Page 1 of 1	Date: 03/12/2018

To,
Mamta Patel
Ahmedabad

TEST: Microstructure Examination

TEST METHOD: ASTM E407-07 (2015)

Test Performed at: TCR Advanced Engineering Pvt. Ltd.

Instrument Utilized:	Optical Microscope, TCRADV/E-185		
*Customer's Reference:	Ref No - GTU/Phd/B_2015/Bonafide/2018/5944,Dated : 08.08.18		
Sample received on:	28/11/2018		
*Condition of sample:	Casting Sample		
*Specification:	-		
Date of completion of test:	03/12/2018	Sample Drawn by:	**Party**

***SAMPLE ID: Sample No - 1.25S1**

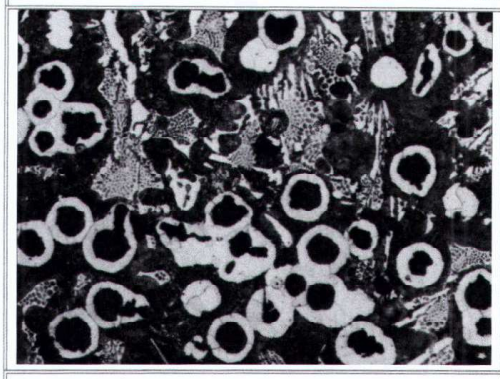

Plate 1: At Core 200X

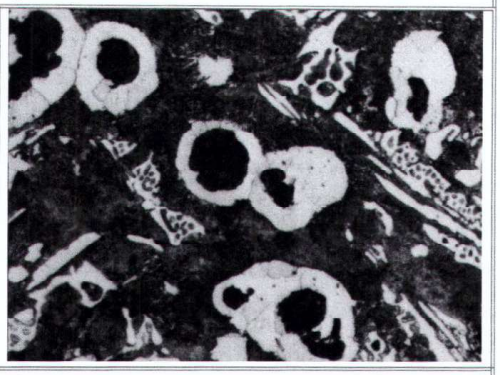

Plate 2: At Core 400X

Observation:	Microstructure shows graphite nodules surrounded by ferrite with presence of pearlite and carbides.	
Observed at:	200-400X	**Etchant:** 2% Nital

End of report

Checked By: Vaishnavi

TCR ADVANCED ENGINEERING PVT. LTD. VADODARA

Authorised Signatory
P. A. MEHTA

1. The results relate only to the sample tested. 2. Test certificate shall not be re-produced except in full without the written approval of laboratory. 3. TCR Advanced has made their best endeavours to provide accurate and reliable information, TCR Advanced is not responsible for any financial liability due to any act of omission or error made. 4. Samples are preserved for 15 days, Any ambiguity in test results should be brought forward to the lab management within this period. 5.* Information provided by customer.

		Date	4
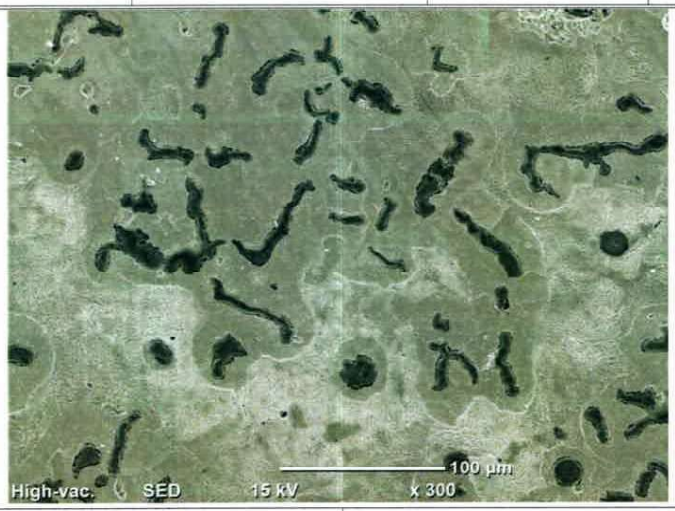			
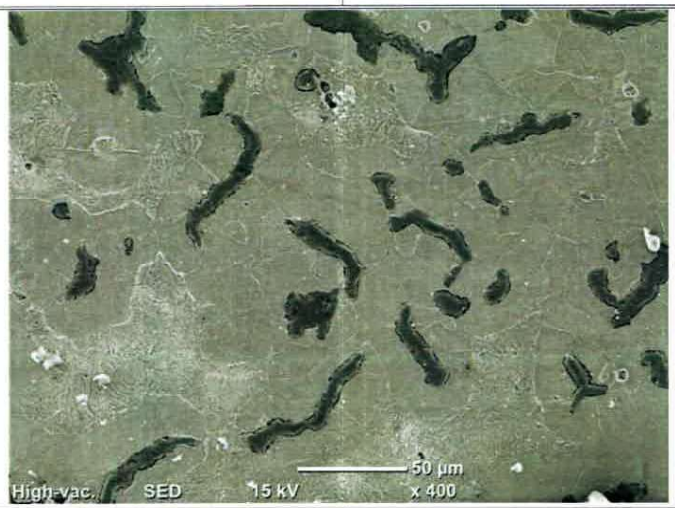			

	ULR - TC673922000015379F	4
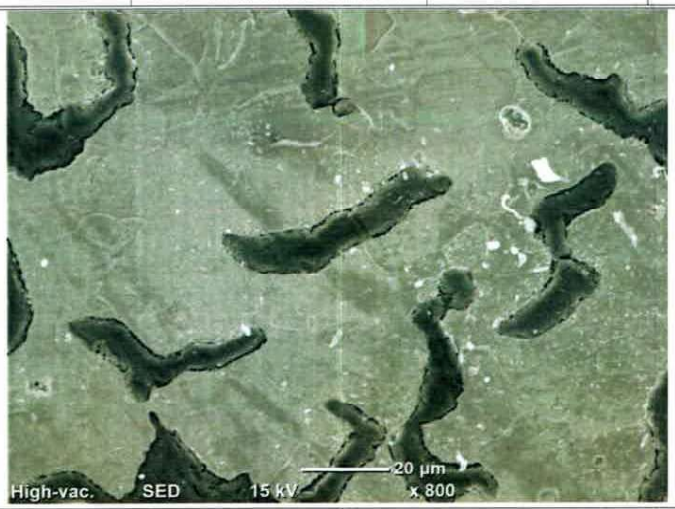		

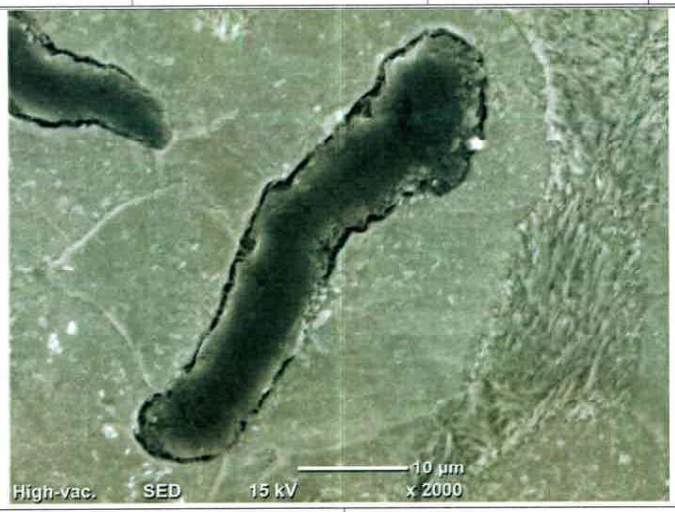

rise Signato

RIDH

AADHYA ENGINEERING SERVICES
Works: 346/B/2, Beside Lalji Mulji Transport, GIDC, Makarpura, Vadodara-390010
Email: testing.aes2019@gmail.com / aadhya.engineers@gmail.com
Contact : 9537530900 / 7567158821 / 8000296579

TEST REPORT

	Test Report No: M/22F/0007	Report Date: 16.06.2022	Page No. : 1 Of 1
Decipline : Mechanical		Group : Metallography Test	
Customer Name & Address	Mamta Patel Ahmedabad		
Location	Aadhya Engineering Services	# Customer Ref No.	By hand Dt 10.06.2022
Sample Condition	Test Piece	Received Date	10.06.2022
Sample Description & Identification	Casting Sample - 7.1	Test Date	16.06.2022
		Instrument No & Name	AES/E/09 Metallurgical Microscope
Material Specification	-		
Test performed	Microstructure Examination	Test Method	ASM Hand Book Vol 9:2004

TEST RESULTS

Sample ID : 22F/0007

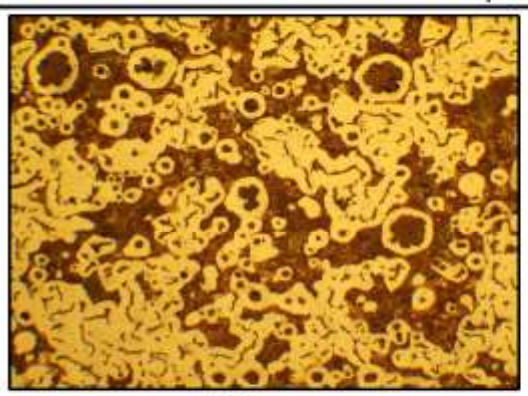

100 X

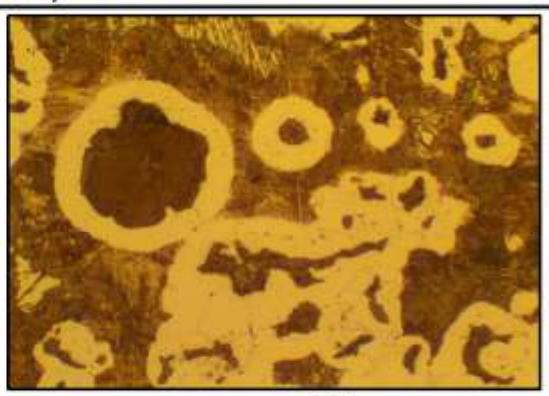

400X

Magnification : 100 - 400 X	Etchant - 2 % Nital

Observation : Microstructure shows graphite nodules/compacted graphite surrounded by ferrite with presence of pearlite and few carbides.

Remarks : -

Tested by	Authorised Signatory (T.B Patel/R.H Vasava/R.P Joshi) TM / QM / CEO	Witnessed By

Note: (a) The results relate only to the sample(s) tested. (b) The Test Report shall not be reproduced, except in full, without the written approval of AES can provide assurance that parts of a report are not taken out of context. (c) The results applied to the sample as received. Sample(s) not drawn by AES. (d) #The information is supplied by the customer and can affect the validity of result.(e) If balance material is available after testing, it will be retained for 15 days maximum. (f) While ' AES' has made their best endeavors to provide accurate and reliable information, AES' is not responsible for any financial liability due to any act of omission or error made.

AADHYA ENGINEERING

AADHYA ENGINEERING SERVICES

Works: 346/B/2, Beside Lalji Mulji Transport, GIDC, Makarpura, Vadodara-390010
Email: testing.aes2019@gmail.com / aadhya.engineers@gmail.com
Contact : 9537530900 / 7567158821 / 8000296579

TEST REPORT

	Test Report No: M/22F/0008	Report Date: 16.06.2022	Page No. : 1 Of 1
Decipline : Mechanical		Group : Metallography Test	
Customer Name & Address	Mamta Patel Ahmedabad		
Location	Aadhya Engineering Services	# Customer Ref No.	By hand Dt 10.06.2022
Sample Condition	Test Piece	Received Date	10.06.2022
Sample Description & Identification	Casting Sample - 7.2	Test Date	16.06.2022
		Instrument No & Name	AES/E/09 Metallurgical Microscope
Material Specification	-		
Test performed	Microstructure Examination	Test Method	ASM Hand Book Vol 9:2004

TEST RESULTS

Sample ID : 222F/0008

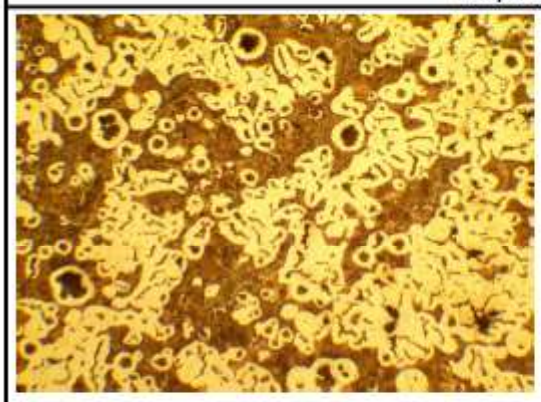

100 X

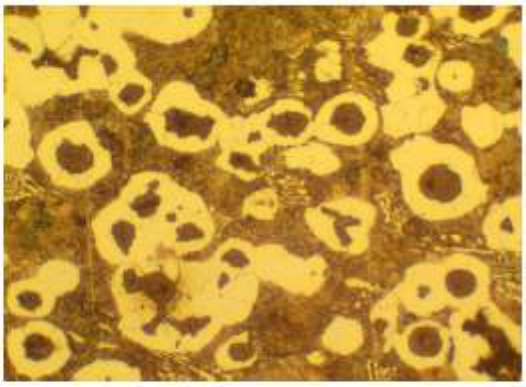

400X

Magnification : 100 - 400 X	Etchant - 2 % Nital

Observation : Microstructure shows graphite nodules/compacted graphite surrounded by ferrite with presence of pearlite and few carbides.

Remarks : -

Tested by	Authorised Signatory (T.B Patel/R.H Vasava/R.P Joshi) TM / QM / CEO	Witnessed By

Note: (a) The results relate only to the sample(s) tested. (b) The Test Report shall not be reproduced, except in full, without the written approval of AES can provide assurance that parts of a report are not taken out of context. (c) The results applied to the sample as received. Sample(s) not drawn by AES. (d) #The information is supplied by the customer and can affect the validity of result.(e) If balance material is available after testing, it will be retained for 15 days maximum. (f) While ' AES' has made their best endeavors to provide accurate and reliable information, AES' is not responsible for any financial liability due to any act of omission or error made.

AADHYA ENGINEERING

AADHYA ENGINEERING SERVICES

Works: 346/B/2, Beside Laiji Mulji Transport, GIDC, Makarpura, Vadodara-390010
Email: testing.aes2019@gmail.com / aadhya.engineers@gmail.com
Contact : 9537530900 / 7567158821 / 8000296579

TEST REPORT

	Test Report No: M/22F/0009	Report Date: 16.06.2022	Page No. : 1 Of 1
Decipline : Mechanical		Group : Metallography Test	
Customer Name & Address	Mamta Patel Ahmedabad		
Location	Aadhya Engineering Services	# Customer Ref No.	By hand Dt 10.06.2022
Sample Condition	Test Piece	Received Date	10.06.2022
		Test Date	16.06.2022
Sample Description & Identification	Casting Sample - 7.3	Instrument No & Name	AES/E/09 Metallurgical Microscope
Material Specification	-		
Test performed	Microstructure Examination	Test Method	ASM Hand Book Vol 9:2004

TEST RESULTS

Sample ID : 22F/0009

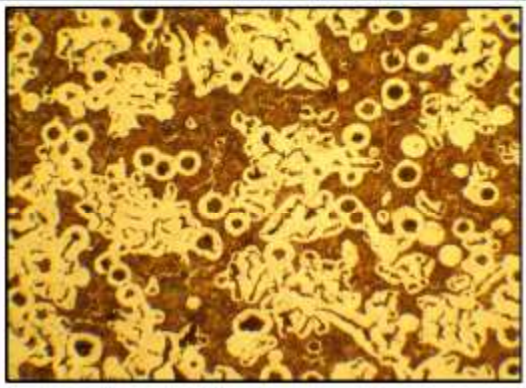

100 X

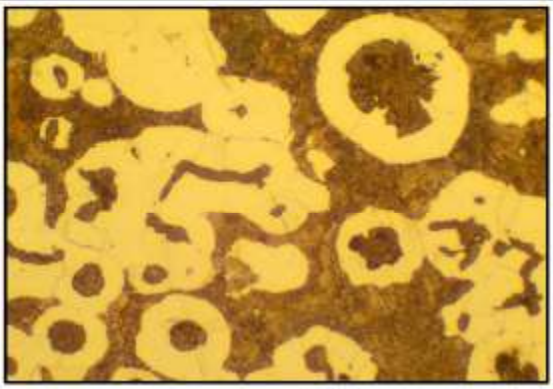

400X

Magnification : 100 - 400 X	Etchant - 2 % Nital

Observation : Microstructure shows graphite nodules/compacted graphite surrounded by ferrite with presence of pearlite and few carbides.

Remarks : -

Tested by	Authorised Signatory (T.B Patel/R.H Vasava/R.P Joshi) TM / QM / CEO	Witnessed By

Note: (a) The results relate only to the sample(s) tested. (b) The Test Report shall not be reproduced, except in full, without the written approval of AES can provide assurance that parts of a report are not taken out of context. (c) The results applied to the sample as received. Sample(s) not drawn by AES. (d) #The information is supplied by the customer and can affect the validity of result.(e) If balance material is available after testing, it will be retained for 15 days maximum. (f) While ' AES' has made their best endeavors to provide accurate and reliable information, AES' is not responsible for any financial liability due to any act of omission or error made.

Doc. No.: F/7.8/06/Issue No.01/Issue Date: 01-10-2019/ Amend No.:00 / Amend Date:--

Office : D/34, Madhav Nagar Society, Rahajanand Marg, Mujmahuda, Vadodara-20

AADHYA ENGINEERING

AADHYA ENGINEERING SERVICES

Works: 346/B/2, Beside Lalji Mulji Transport, GIDC, Makarpura, Vadodara-390010
Email: testing.aes2019@gmail.com / aadhya.engineers@gmail.com
Contact : 9537530900 / 7567158821 / 8000296579

TEST REPORT

	Test Report No: M/22F/0010	Report Date: 16.06.2022	Page No. : 1 Of 1
Decipline : Mechanical		Group : Metallography Test	
Customer Name & Address	Mamta Patel Ahmedabad		
Location	Aadhya Engineering Services	# Customer Ref No.	By hand Dt 10.06.2022
Sample Condition	Test Piece	Received Date	10.06.2022
Sample Description & Identification	Casting Sample - 7.4	Test Date	16.06.2022
		Instrument No & Name	AES/E/09 Metallurgical Microscope
Material Specification	-		
Test performed	Microstructure Examination	Test Method	ASM Hand Book Vol 9:2004

TEST RESULTS

Sample ID : 22F/0010

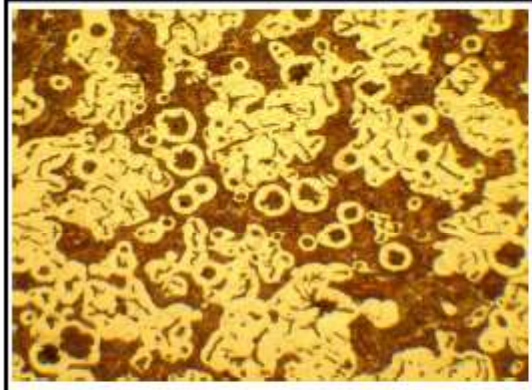

100 X

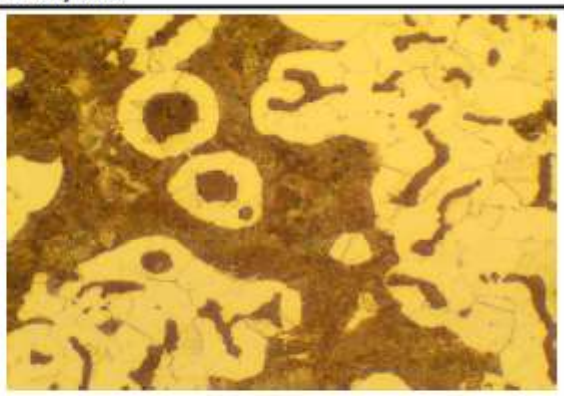

400X

Magnification : 100 - 400 X	Etchant - 2 % Nital

Observation : Microstructure shows graphite nodules/compacted graphite surrounded by ferrite with presence of pearlite and few carbides.

Remarks : -

Tested by	Authorised Signatory (T.B Patel/R.H Vasava/R.P Joshi) TM / QM / CEO	Witnessed By

Note: (a) The results relate only to the sample(s) tested. (b) The Test Report shall not be reproduced, except in full, without the written approval of AES can provide assurance that parts of a report are not taken out of context. (c) The results applied to the sample as received. Sample(s) not drawn by AES. (d) #The information is supplied by the customer and can affect the validity of result.(e) If balance material is available after testing, it will be retained for 15 days maximum. (f) While ' AES' has made their best endeavors to provide accurate and reliable information, AES' is not responsible for any financial liability due to any act of omission or error made.

AADHYA ENGINEERING SERVICES

Works: 346/B/2, Beside Lalji Mulji Transport, GIDC, Makarpura, Vadodara-390010
Email: testing.aes2019@gmail.com / aadhya.engineers@gmail.com
Contact : 9537530900 / 7567158821 / 8000296579

TEST REPORT

	Test Report No: M/22F/0011	Report Date: 16.06.2022	Page No. : 1 Of 1
Customer Name & Address	Mamta Patel Ahmedabad		
Location	Aadhya Engineering Services	# Customer Ref No.	By Hand Dt 10.06.2022
Sample Condition	Test Piece	Received Date	10.06.2022
Sample Description & Identification	Casting Sample-7.1	Test Date	16.06.2022
		Instrument No & Name	AES/E/09 Metallurgical Microscope
Material Specification	-		
Test performed	Volume Fraction	Test Method	ASTM E 562:2019a

TEST RESULTS

Sample ID : 22F/0011

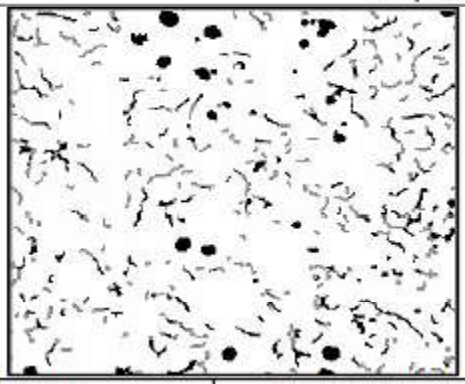

FRAMES	Compacted Graphite Iron (%)	Matrix
1	42.45	57.55
2	40.56	59.44
3	41.89	58.11
4	42.16	57.84
5	39.52	60.48
Avg. of 5 Frames	41.316	58.684

Etchant:As Polish | Magnification: 100 X

Remarks:

Tested by	Authorised Signatory (T.B Patel/R.H Vasava/R.P Joshi) TM / QM / CEO	Witnessed By

Note: (a) The results relate only to the sample(s) tested. (b) The Test Report shall not be reproduced, except in full, without the written approval of AES can provide assurance that parts of a report are not taken out of context. (c) The results applied to the sample as received. Sample(s) not drawn by AES. (d) #The information is supplied by the customer and can affect the validity of result.(e) If balance material is available after testing, it will be retained for 15 days maximum. (f) While ' AES' has made their best endeavors to provide accurate and reliable information, AES' is not responsible for any financial liability due to any act of omission or error made.

End of Report

AADHYA ENGINEERING SERVICES

Works: 346/B/2, Beside Lalji Mulji Transport, GIDC, Makarpura, Vadodara-390010
Email: testing.aes2019@gmail.com / aadhya.engineers@gmail.com
Contact : 9537530900 / 7567158821 / 8000296579

TEST REPORT

	Test Report No: M/22F/0012	Report Date: 16.06.2022	Page No. : 1 Of 1
Customer Name & Address	Mamta Patel Ahmedabad		
Location	Aadhya Engineering Services	# Customer Ref No.	By Hand Dt 10.06.2022
Sample Condition	Test Piece	Received Date	10.06.2022
Sample Description & Identification	Casting Sample-7.2	Test Date	16.06.2022
		Instrument No & Name	AES/E/09 Metallurgical Microscope
Material Specification	-		
Test performed	Volume Fraction	Test Method	ASTM E 562:2019a

TEST RESULTS

Sample ID : 22F/0012

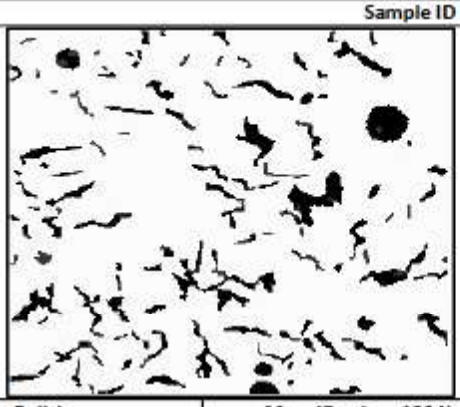

FRAMES	Compacted Graphite Iron (%)	Matrix
1	52.67	47.33
2	51.36	48.64
3	50.48	49.52
4	53.26	46.74
5	53.74	46.26
Avg. of 5 Frames	52.302	47.698

Etchant:As Polish | Magnification: 100 X

Remarks:

Tested by	Authorised Signatory (T.B Patel/R.H Vasava/R.P Joshi) TM / QM / CEO	Witnessed By

Note: (a) The results relate only to the sample(s) tested. (b) The Test Report shall not be reproduced, except in full, without the written approval of AES can provide assurance that parts of a report are not taken out of context. (c) The results applied to the sample as received. Sample(s) not drawn by AES. (d) #The information is supplied by the customer and can affect the validity of result.(e) If balance material is available after testing, it will be retained for 15 days maximum. (f) While ' AES' has made their best endeavors to provide accurate and reliable information, AES' is not responsible for any financial liability due to any act of omission or error made.

End of Report

AADHYA ENGINEERING SERVICES
Works: 346/B/2, Beside Lalji Mulji Transport, GIDC, Makarpura, Vadodara-390010
Email: testing.aes2019@gmail.com / aadhya.engineers@gmail.com
Contact : 9537530900 / 7567158821 / 8000296579

TEST REPORT

	Test Report No: M/22F/0013	Report Date: 16.06.2022	Page No. : 1 Of 1
Customer Name & Address	Mamta Patel Ahmedabad		
Location	Aadhya Engineering Services	# Customer Ref No.	By Hand Dt 10.06.2022
Sample Condition	Test Piece	Received Date	10.06.2022
Sample Description & Identification	Casting Sample-7.3	Test Date	16.06.2022
		Instrument No & Name	AES/E/09 Metallurgical Microscope
Material Specification	-		
Test performed	Volume Fraction	Test Method	ASTM E 562:2019a

TEST RESULTS

Sample ID : 22F/0013

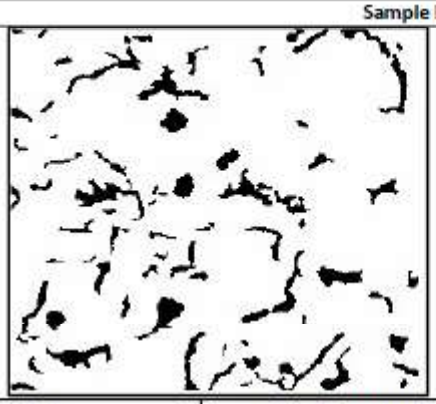

FRAMES	Compacted Graphite Iron (%)	Matrix
1	65.81	34.19
2	64.58	35.42
3	64.89	35.11
4	66.42	33.58
5	63.78	36.22
Avg. of 5 Frames	65.096	34.904

Etchant:As Polish | Magnification: 100 X

Remarks:

Tested by

Authorised Signatory
(T.B Patel/R.H Vasava/R.P Joshi)
TM / QM / CEO

Witnessed By

Note: (a) The results relate only to the sample(s) tested. (b) The Test Report shall not be reproduced, except in full, without the written approval of AES can provide assurance that parts of a report are not taken out of context. (c) The results applied to the sample as received. Sample(s) not drawn by AES. (d) #The information is supplied by the customer and can affect the validity of result.(e) If balance material is available after testing, it will be retained for 15 days maximum. (f) While ' AES' has made their best endeavors to provide accurate and reliable information, AES' is not responsible for any financial liability due to any act of omission or error made.

End of Report

AADHYA ENGINEERING

AADHYA ENGINEERING SERVICES

Works: 346/B/2, Beside Laiji Mulji Transport, GIDC, Makarpura, Vadodara-390010
Email: testing.aes2019@gmail.com / aadhya.engineers@gmail.com
Contact : 9537530900 / 7567158821 / 8000296579

TEST REPORT

	Test Report No: M/22F/0014	Report Date: 16.06.2022	Page No. : 1 Of 1
Customer Name & Address	Mamta Patel Ahmedabad		
Location	Aadhya Engineering Services	# Customer Ref No.	By Hand Dt 10.06.2022
Sample Condition	Test Piece	Received Date	10.06.2022
Sample Description & Identification	Casting Sample-7.4	Test Date	16.06.2022
		Instrument No & Name	AES/E/09 Metallurgical Microscope
Material Specification	-		
Test performed	Volume Fraction	Test Method	ASTM E 562:2019a

TEST RESULTS

Sample ID : 22F/0014

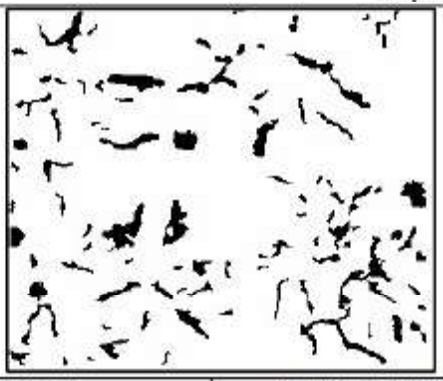

FRAMES	Compacted Graphite Iron (%)	Matrix
1	59.52	40.48
2	57.30	42.70
3	58.67	41.33
4	58.10	41.90
5	59.48	40.52
Avg. of 5 Frames	58.614	41.386

Etchant:As Polish | Magnification: 100 X

Remarks:

Tested by

Authorised Signatory
(T.B Patel/R.H Vasava/R.P Joshi)
TM / QM / CEO

Witnessed By

Note: (a) The results relate only to the sample(s) tested. (b) The Test Report shall not be reproduced, except in full, without the written approval of AES can provide assurance that parts of a report are not taken out of context. (c) The results applied to the sample as received. Sample(s) not drawn by AES. (d) #The information is supplied by the customer and can affect the validity of result.(e) If balance material is available after testing, it will be retained for 15 days maximum. (f) While ' AES' has made their best endeavors to provide accurate and reliable information, AES' is not responsible for any financial liability due to any act of omission or error made.

End of Report

AADHYA ENGINEERING

AADHYA ENGINEERING SERVICES

Works: 346/B/2, Beside Lalji Mulji Transport, GIDC, Makarpura, Vadodara-390010
Email: testing.aes2019@gmail.com / aadhya.engineers@gmail.com
Contact : 9537530900 / 7567158821 / 8000296579

TEST REPORT

	Test Report No : T/23B/0015	Report Date: 25.01.2023	Page No. : 1 Of 1

Customer Name & Address	Mamta Patel Vadodara		
Location	Aadhya Engineering Services	# Customer Ref No.	By Hand Dt-20.01.2023
Sample Condition	Test Piece (Round Bar)	Received Date	20.01.2023
Sample Description & Identification	Casting Sample-8.1	Test Date	25.01.2023
		Instrument No & Name	AES/E/02 Universal Testing Machine
Material Specification	GJV 400		
Test performed	Tensile Testing	Test Method	BS EN ISO 6892-1 2019

TEST RESULTS

Sample ID	Parameters	Required Value	Observed Value
23B/0015	Dia/Width (mm)	-	19.90
	Thk (mm)	-	-
	Area (mm2)	-	310.87
	Gauge Length(mm)	-	100.00
	Final Length(mm)	-	102.94
	Proof Load(0.2% Offset)(kN)	-	90.85
	Ultimate Load(kN)	-	146.50
	Proof Strength(0.2% Offset)(Mpa)	280.0 Min	292.25
	Tensile Strength (MPa)	400.0 - 475.0	471.26
	Elongation (%)	1.0 Min	2.94
	R.A (%)	-	-

Remarks: Above results are meeting with Tensile requirments of ISO 16112 Grade GJV 400(Customer Requirement) with respect of test carried out.

Tested by	Authorised Signatory (T.B Patel/R.H Vasava/R.P Joshi) TM / QM / CEO	Witnessed By

Note: (a) The results relate only to the sample(s) tested. (b) The Test Report shall not be reproduced, except in full, without the written approval of AES can provide assurance that parts of a report are not taken out of context. (c) The results applied to the sample as received. Sample(s) not drawn by AES. (d) #The information is supplied by the customer and can affect the validity of result.(e) If balance material is available after testing, it will be retained for 15 days maximum. (f) While ' AES' has made their best endeavors to provide accurate and reliable information, AES' is not responsible for any financial liability due to any act of omission or error made.

End of Report

Office : D/34, Madhav Nagar Society, Sahajanand Marg, Mujmahuda, Vadodara-20

AADHYA ENGINEERING SERVICES

Works: 346/B/2, Beside Laiji Mulji Transport, GIDC, Makarpura, Vadodara-390010
Email: testing.aes2019@gmail.com / aadhya.engineers@gmail.com
Contact : 9537530900 / 7567158821 / 8000296579

TEST REPORT

	Test Report No : T/23B/0016	Report Date: 25.01.2023	Page No. : 1 Of 1
Customer Name & Address	Mamta Patel Vadodara		
Location	Aadhya Engineering Services	# Customer Ref No.	By Hand Dt-20.01.2023
Sample Condition	Test Piece (Round Bar)	Received Date	20.01.2023
Sample Description & Identification	Casting Sample-8.2	Test Date	25.01.2023
		Instrument No & Name	AES/E/02 Universal Testing Machine
Material Specification	GJV 400		
Test performed	Tensile Testing	Test Method	BS EN ISO 6892-1 2019

TEST RESULTS

Sample ID	Parameters	Required Value	Observed Value
23B/0016	Dia/Width (mm)	-	20.04
	Thk (mm)	-	-
	Area (mm2)	-	315.26
	Gauge Length(mm)	-	100.00
	Final Length(mm)	-	103.26
	Proof Load(0.2% Offset)(kN)	-	101.50
	Ultimate Load(kN)	-	153.29
	Proof Strength(0.2% Offset)(Mpa)	280.0 Min	321.96
	Tensile Strength (MPa)	400.0 - 475.0	486.24
	Elongation (%)	1.0 Min	3.26
	R.A (%)	-	-

Remarks: Above results are meeting with Tensile requirments of ISO 16112 Grade GJV 400(Customer Requirement) with respect of test carried out.

Tested by	Authorised Signatory (T.B Patel/R.H Vasava/R.P Joshi) TM / QM / CEO	Witnessed By

Note: (a) The results relate only to the sample(s) tested. (b) The Test Report shall not be reproduced, except in full, without the written approval of AES can provide assurance that parts of a report are not taken out of context. (c) The results applied to the sample as received. Sample(s) not drawn by AES. (d) #The information is supplied by the customer and can affect the validity of result.(e) If balance material is available after testing, it will be retained for 15 days maximum. (f) While ' AES' has made their best endeavors to provide accurate and reliable information, AES' is not responsible for any financial liability due to any act of omission or error made.

Doc. No.: F/7.8/02/Issue No.01/Issue Date: 01-10-2019/ Amend No.:00 / Amend Date:--

End of Report

AADHYA ENGINEERING SERVICES

Works: 346/B/2, Beside Lalji Mulji Transport, GIDC, Makarpura, Vadodara-390010
Email: testing.aes2019@gmail.com / aadhya.engineers@gmail.com
Contact : 9537530900 / 7567158821 / 8000296579

TEST REPORT

	Test Report No : T/23B/0017	Report Date: 25.01.2023	Page No. : 1 Of 1

Customer Name & Address	Mamta Patel Vadodara		
Location	Aadhya Engineering Services	# Customer Ref No.	By Hand Dt-20.01.2023
Sample Condition	Test Piece (Round Bar)	Received Date	20.01.2023
Sample Description & Identification	Casting Sample-8.3	Test Date	25.01.2023
		Instrument No & Name	AES/E/02 Universal Testing Machine
Material Specification	GJV 400		
Test performed	Tensile Testing	Test Method	BS EN ISO 6892-1 2019

TEST RESULTS

Sample ID	Parameters	Required Value	Observed Value
23B/0017	Dia/Width (mm)	-	19.91
	Thk (mm)	-	-
	Area (mm2)	-	311.18
	Gauge Length(mm)	-	100.00
	Final Length(mm)	-	102.73
	Proof Load(0.2% Offset)(kN)	-	92.75
	Ultimate Load(kN)	-	144.75
	Proof Strength(0.2% Offset)(Mpa)	280.0 Min	298.06
	Tensile Strength (MPa)	400.0 - 475.0	465.16
	Elongation (%)	1.0 Min	2.73
	R.A (%)	-	-

Remarks: Above results are meeting with Tensile requirments of ISO 16112 Grade GJV 400(Customer Requirement) with respect of test carried out.

Tested by	Authorised Signatory (T.B Patel/R.H Vasava/R.P Joshi) TM / QM / CEO	Witnessed By

Note: (a) The results relate only to the sample(s) tested. (b) The Test Report shall not be reproduced, except in full, without the written approval of AES can provide assurance that parts of a report are not taken out of context. (c) The results applied to the sample as received. Sample(s) not drawn by AES. (d) #The information is supplied by the customer and can affect the validity of result.(e) If balance material is available after testing, it will be retained for 15 days maximum. (f) While ' AES' has made their best endeavors to provide accurate and reliable information. AES' is not responsible for any financial liability due to any act of omission or error made.

End of Report

Office : D/34, Madhav Nagar Society, Sahajanand Marg, Mujmahuda, Vadodara-20

AADHYA ENGINEERING SERVICES
Works: 346/B/2, Beside Laji Mulji Transport, GIDC, Makarpura, Vadodara-390010
Email: testing.aes2019@gmail.com / aadhya.engineers@gmail.com
Contact : 9537530900 / 7567158821 / 8000296579

TEST REPORT

	Test Report No : H/23B/0015	Report Date: 25.01.2023	Page No. : 1 Of 1
Customer Name & Address	Mamta Patel Vadodara		
Location	Aadhya Engineering Services	# Customer Ref No.	By Hand Dt-20.01.2023
Sample Condition	Test Piece (Round Bar)	Received Date	20.01.2023
		Test Date	25.01.2023
Sample Description & Identification	Casting Sample-8.1	Instrument No & Name	AES/E/06 Vicker Cum Brinell Hardness Tester
Material Specification	GJV 400		
Test performed	Hardness (Brinell)	Test Method	ISO 6506-1:2014

TEST RESULTS

Sample ID	Load / Type	Location	Observed Value				AVG. Value	Min.	Max.
			1	2	3	-			
			Required Value					--	--
23B/0015	2.5/62.5 (HBW)	On Surface	139.0	138.0	138.0	-	138.3	138.0	139.0

Remarks: -

Tested by	Authorised Signatory (T.B Patel/R.H Vasava/R.P Joshi) TM / QM / CEO	Witnessed By

Note: (a) The results relate only to the sample(s) tested. (b) The Test Report shall not be reproduced, except in full, without the written approval of AES can provide assurance that parts of a report are not taken out of context. (c) The results applied to the sample as received. Sample(s) not drawn by AES. (d) #The information is supplied by the customer and can affect the validity of result.(e) If balance material is available after testing, it will be retained for 15 days maximum. (f) While ' AES' has made their best endeavors to provide accurate and reliable information, AES' is not responsible for any financial liability due to any act of omission or error made.

Doc. No.: F/7.8/05/Issue No.01/Issue Date: 01-10-2019/ Amend No.:00 / Amend Date:--

End of Report

AADHYA ENGINEERING

AADHYA ENGINEERING SERVICES

Works: 346/B/2, Beside Laji Mulji Transport, GIDC, Makarpura, Vadodara-390010
Email: testing.aes2019@gmail.com / aadhya.engineers@gmail.com
Contact : 9537530900 / 7567158821 / 8000296579

TEST REPORT

	Test Report No : H/23B/0016	Report Date: 25.01.2023	Page No. : 1 Of 1
Customer Name & Address	Mamta Patel Vadodara		
Location	Aadhya Engineering Services	# Customer Ref No.	By Hand Dt-20.01.2023
Sample Condition	Test Piece (Round Bar)	Received Date	20.01.2023
		Test Date	25.01.2023
Sample Description & Identification	Casting Sample-8.2	Instrument No & Name	AES/E/06 Vicker Cum Brinell Hardness Tester
Material Specification	GJV 400		
Test performed	Hardness (Brinell)	Test Method	ISO 6506-1:2014

TEST RESULTS

Sample ID	Load / Type	Location	Observed Value 1	2	3	-	AVG. Value	Min.	Max.
			Required Value					--	--
23B/0016	2.5/62.5 (HBW)	On Surface	147.0	146.0	147.0	-	146.7	146.0	147.0

Remarks: -

Tested by

Authorised Signatory
(T.B Patel/R.H Vasava/R.P Joshi)
TM / QM / CEO

Witnessed By

Note: (a) The results relate only to the sample(s) tested. (b) The Test Report shall not be reproduced, except in full, without the written approval of AES can provide assurance that parts of a report are not taken out of context. (c) The results applied to the sample as received. Sample(s) not drawn by AES. (d) #The information is supplied by the customer and can affect the validity of result.(e) If balance material is available after testing, it will be retained for 15 days maximum. (f) While ' AES' has made their best endeavors to provide accurate and reliable information, AES' is not responsible for any financial liability due to any act of omission or error made.

Doc. No.: F/7.8/05/Issue No.01/Issue Date: 01-10-2019/ Amend No.:00 / Amend Date:--

End of Report

AADHYA ENGINEERING SERVICES

Works: 346/B/2, Beside Laji Mulji Transport, GIDC, Makarpura, Vadodara-390010
Email: testing.aes2019@gmail.com / aadhya.engineers@gmail.com
Contact : 9537530900 / 7567158821 / 8000296579

TEST REPORT

	Test Report No : H/23B/0017	Report Date: 25.01.2023	Page No. : 1 Of 1
Customer Name & Address	Mamta Patel Vadodara		
Location	Aadhya Engineering Services	# Customer Ref No.	By Hand Dt-20.01.2023
Sample Condition	Test Piece (Round Bar)	Received Date	20.01.2023
		Test Date	25.01.2023
Sample Description & Identification	Casting Sample-8.3	Instrument No & Name	AES/E/06 Vicker Cum Brinell Hardness Tester
Material Specification	GJV 400		
Test performed	Hardness (Brinell)	Test Method	ISO 6506-1:2014

TEST RESULTS

Sample ID	Load / Type	Location	Observed Value				AVG. Value	Min.	Max.
			1	2	3	-			
			Required Value					--	--
23B/0017	2.5/62.5 (HBW)	On Surface	137.0	136.0	137.0	-	136.7	136.0	137.0

Remarks: -

Tested by	Authorised Signatory (T.B Patel/R.H Vasava/R.P Joshi) TM / QM / CEO	Witnessed By

Note: (a) The results relate only to the sample(s) tested. (b) The Test Report shall not be reproduced, except in full, without the written approval of AES can provide assurance that parts of a report are not taken out of context. (c) The results applied to the sample as received. Sample(s) not drawn by AES. (d) #The information is supplied by the customer and can affect the validity of result.(e) If balance material is available after testing, it will be retained for 15 days maximum. (f) While ' AES' has made their best endeavors to provide accurate and reliable information, AES' is not responsible for any financial liability due to any act of omission or error made.

End of Report

Office : D/34, Madhav Nagar Society, Sahajanand Marg, Mujmahuda, Vadodara-20

AADHYA ENGINEERING

AADHYA ENGINEERING SERVICES

Works: 346/B/2, Beside Lalji Mulji Transport, GIDC, Makarpura, Vadodara-390010
E-mail: testing.aes2019@gmail.com / aadhya.engineers@gmail.com
Contact : 9537530900 / 7567158821 / 8000295579

TEST REPORT

	Test Report No: CH/23B/0015	Report Date: 25.01.2023	Page No : 1 of 1
Customer Name & Address	Mamta Patel Vadodara		
Location	Aadhya Engineering Services	# Customer Ref No.	By Hand Dt-20.01.2023
Sample Condition	Test Piece (Round Bar)	Received Date	20.01.2023
Sample Description & Identification	Casting Sample-8.1	Test Date	25.01.2023
		Instrument No & Name	AES/E/01 Optical Emission Spectrometer
Material Specification	GJV 400		
Test performed	Chemical Analysis By OES	Test Method	ASTM E 1999-18

TEST RESULTS

Sample ID	Elements	Required Value(%)	Observed Value(%)
23B/0015	Carbon	-	3.571
	Silicon	-	2.502
	Manganese	-	0.402
	Phosphorus	-	0.011
	Sulphur	-	0.011
	Chromium	-	0.030
	Magnesium	-	0.023
	Copper	-	0.410
	Tin	-	0.039

Remarks : -

Tested by	Authorised Signatory (T.B Patel/R.H.Vasava/T.D.Bhatt) TM / QM / TE	Witnessed By

Note: (a) The results relate only to the sample(s) tested. (b) The Test Report shall not be reproduced, except in full, without the written approval of AES can provide assurance that parts of a report are not taken out of context. (c) The results applied to the sample as received. Sample(s) not drawn by AES. (d) #The information is supplied by the customer and can affect the validity of result.(e) If balance material is available after testing, it will be retained for 15 days maximum. (f) While ' AES' has made their best endeavors to provide accurate and reliable information, AES' is not responsible for any financial liability due to any act of omission or error made.

Doc. No.: F/7.8/01/Issue No.01/Issue Date: 01-10-2019/ Amend No.:00 / Amend Date:--

End of Report

AADHYA ENGINEERING

AADHYA ENGINEERING SERVICES

Works: 346/B/2, Beside Lalji Mulji Transport, GIDC, Makarpura, Vadodara-390010
Email: testing.aes2019@gmail.com / aadhya.engineers@gmail.com
Contact : 9537530900 / 7567158821 / 8000296579

TEST REPORT

	Test Report No: CH/23B/0016	Report Date: 25.01.2023	Page No : 1 of 1
Customer Name & Address	Mamta Patel Vadodara		
Location	Aadhya Engineering Services	# Customer Ref No.	By Hand Dt-20.01.2023
Sample Condition	Test Piece (Round Bar)	Received Date	20.01.2023
Sample Description & Identification	Casting Sample-8.2	Test Date	25.01.2023
		Instrument No & Name	AES/E/01 Optical Emission Spectrometer
Material Specification	GJV 400		
Test performed	Chemical Analysis By OES	Test Method	ASTM E 1999-18

TEST RESULTS

Sample ID	Elements	Required Value(%)	Observed Value(%)
23B/0016	Carbon	-	3.860
	Silicon	-	2.671
	Manganese	-	0.370
	Phosphorus	-	0.031
	Sulphur	-	0.010
	Chromium	-	0.030
	Magnesium	-	0.065
	Copper	-	0.361
	Tin	-	0.098

Remarks : -

Tested by	Authorised Signatory (T.B Patel/R.H.Vasava/T.D.Bhatt) TM / QM / TE	Witnessed By

Note: (a) The results relate only to the sample(s) tested. (b) The Test Report shall not be reproduced, except in full, without the written approval of AES can provide assurance that parts of a report are not taken out of context. (c) The results applied to the sample as received. Sample(s) not drawn by AES. (d) #The information is supplied by the customer and can affect the validity of result.(e) If balance material is available after testing, it will be retained for 15 days maximum. (f) While ' AES' has made their best endeavors to provide accurate and reliable information, AES' is not responsible for any financial liability due to any act of omission or error made.

Doc. No.: F/7.8/01/Issue No.01/Issue Date: 01-10-2019/ Amend No.:00 / Amend Date:–

End of Report

AADHYA ENGINEERING

AADHYA ENGINEERING SERVICES

Works: 346/B/2, Beside Lalji Mulji Transport, GIDC, Makarpura, Vadodara-390010
E-mail: testing.aes2019@gmail.com / aadhya.engineers@gmail.com
Contact : 9537530900 / 7567158821 / 8000296579

TEST REPORT

Test Report No: CH/23B/0017			Report Date: 25.01.2023	Page No : 1 of 1
Customer Name & Address	Mamta Patel Vadodara			
Location	Aadhya Engineering Services	# Customer Ref No.	By Hand Dt-20.01.2023	
Sample Condition	Test Piece (Round Bar)	Received Date	20.01.2023	
Sample Description & Identification	Casting Sample-8.3	Test Date	25.01.2023	
		Instrument No & Name	AES/E/01 Optical Emission Spectrometer	
Material Specification	GJV 400			
Test performed	Chemical Analysis By OES	Test Method	ASTM E 1999-18	

TEST RESULTS

Sample ID	Elements	Required Value(%)	Observed Value(%)
23B/0017	Carbon	-	3.671
	Silicon	-	2.672
	Manganese	-	0.371
	Phosphorus	-	0.028
	Sulphur	-	0.019
	Chromium	-	0.021
	Magnesium	-	0.009
	Copper	-	0.371
	Tin	-	0.035

Remarks : -

Tested by	Authorised Signatory (T.B Patel/R.H.Vasava/T.D.Bhatt) TM / QM / TE	Witnessed By

Note: (a) The results relate only to the sample(s) tested. (b) The Test Report shall not be reproduced, except in full, without the written approval of AES can provide assurance that parts of a report are not taken out of context. (c) The results applied to the sample as received. Sample(s) not drawn by AES. (d) #The information is supplied by the customer and can affect the validity of result.(e) If balance material is available after testing, it will be retained for 15 days maximum. (f) While ' AES' has made their best endeavors to provide accurate and reliable information, AES' is not responsible for any financial liability due to any act of omission or error made.

Doc. No.: F/7.8/01/Issue No.01/Issue Date: 01-10-2019/ Amend No.:00 / Amend Date:--

End of Report

AADHYA ENGINEERING SERVICES
Works: 346/B/2, Beside Laji Mulji Transport, GIDC, Makarpura, Vadodara-390010
Email: testing.aes2019@gmail.com / aadhya.engineers@gmail.com
Contact : 9537530900 / 7567158821 / 8000296579

TEST REPORT

	Test Report No: M/23B/0015	Report Date: 25.01.2023	Page No. : 1 Of 1
Customer Name & Address	Mamta Patel Vadodara		
Location	Aadhya Engineering Services	# Customer Ref No.	By hand Dt 20.01.2023
Sample Condition	Test Piece (Round Bar)	Received Date	20.01.2023
Sample Description & Identification	Casting Sample - 8.1	Test Date	25.01.2023
		Instrument No & Name	AES/E/09 Metallurgical Microscope
Material Specification	GJV 400		
Test performed	Microstructure Examination	Test Method	ASM Hand Book Vol 9:2004

TEST RESULTS

Sample ID : 23B/0015

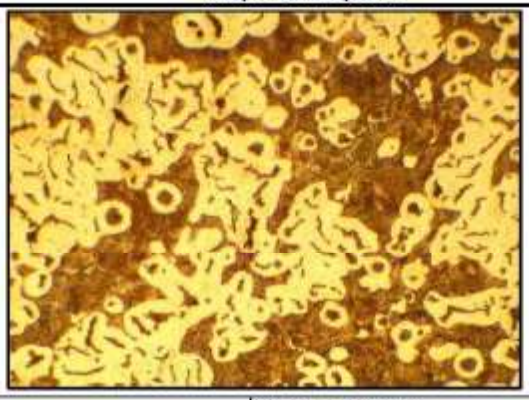

Magnification : 100 X	Etchant - 2 % Nital

Observation : Microstructure shows graphite nodules/compacted graphite surrounded by ferrite with presence of pearlite and few carbides.

Remarks : -

Tested by	Authorised Signatory (T.B Patel/R.H Vasava/R.P Joshi) TM / QM / CEO	Witnessed By

Note: (a) The results relate only to the sample(s) tested. (b) The Test Report shall not be reproduced, except in full, without the written approval of AES can provide assurance that parts of a report are not taken out of context. (c) The results applied to the sample as received. Sample(s) not drawn by AES. (d) #The information is supplied by the customer and can affect the validity of result.(e) If balance material is available after testing, it will be retained for 15 days maximum. (f) While ' AES' has made their best endeavors to provide accurate and reliable information, AES' is not responsible for any financial liability due to any act of omission or error made.

AADHYA ENGINEERING SERVICES

Works: 346/B/2, Beside Laji Mulji Transport, GIDC, Makarpura, Vadodara-390010
Email: testing.aes2019@gmail.com / aadhya.engineers@gmail.com
Contact : 9537530900 / 7567158821 / 8000296579

TEST REPORT

	Test Report No: M/23B/0016	Report Date: 25.01.2023	Page No. : 1 Of 1
Customer Name & Address	Mamta Patel Vadodara		
Location	Aadhya Engineering Services	# Customer Ref No.	By hand Dt 20.01.2023
Sample Condition	Test Piece (Round Bar)	Received Date	20.01.2023
Sample Description & Identification	Casting Sample - 8.2	Test Date	25.01.2023
		Instrument No & Name	AES/E/09 Metallurgical Microscope
Material Specification	GJV 400		
Test performed	Microstructure Examination	Test Method	ASM Hand Book Vol 9:2004

TEST RESULTS

Sample ID : 23B/0016

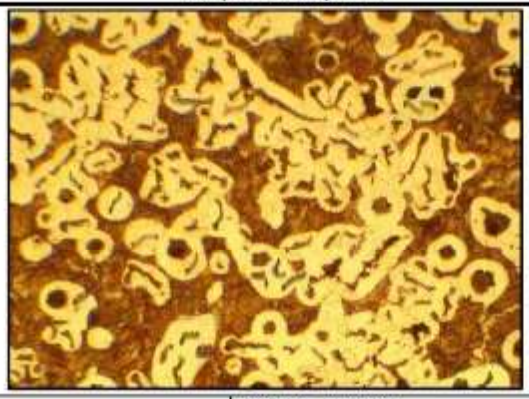

Magnification : 100 X	**Etchant - 2 % Nital**

Observation : Microstructure shows graphite nodules/compacted graphite surrounded by ferrite with presence of pearlite and few carbides.

Remarks : -

Tested by	Authorised Signatory (T.B Patel/R.H Vasava/R.P Joshi) TM / QM / CEO	Witnessed By

Note: (a) The results relate only to the sample(s) tested. (b) The Test Report shall not be reproduced, except in full, without the written approval of AES can provide assurance that parts of a report are not taken out of context. (c) The results applied to the sample as received. Sample(s) not drawn by AES. (d) #The information is supplied by the customer and can affect the validity of result.(e) If balance material is available after testing, it will be retained for 15 days maximum. (f) While ' AES' has made their best endeavors to provide accurate and reliable information, AES' is not responsible for any financial liability due to any act of omission or error made.

AADHYA ENGINEERING SERVICES

Works: 346/B/2, Beside Laji Mulji Transport, GIDC, Makarpura, Vadodara-390010
Email: testing.aes2019@gmail.com / aadhya.engineers@gmail.com
Contact : 9537530900 / 7567158821 / 8000296579

TEST REPORT

	Test Report No: M/23B/0017	Report Date: 25.01.2023	Page No. : 1 Of 1
Customer Name & Address	Mamta Patel Vadodara		
Location	Aadhya Engineering Services	# Customer Ref No.	By hand Dt 20.01.2023
Sample Condition	Test Piece (Round Bar)	Received Date	20.01.2023
Sample Description & Identification	Casting Sample - 8.3	Test Date	25.01.2023
		Instrument No & Name	AES/E/09 Metallurgical Microscope
Material Specification	GJV 400		
Test performed	Microstructure Examination	Test Method	ASM Hand Book Vol 9:2004

TEST RESULTS

Sample ID : 23B/0017

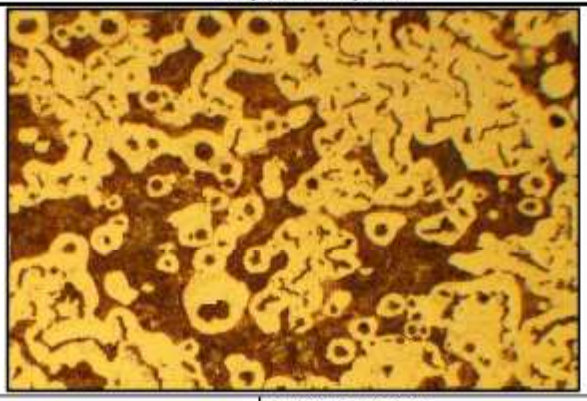

Magnification : 100 X	**Etchant - 2 % Nital**

Observation : Microstructure shows graphite nodules/compacted graphite surrounded by ferrite with presence of pearlite and few carbides.

Remarks : -

Tested by	Authorised Signatory (T.B Patel/R.H Vasava/R.P Joshi) TM / QM / CEO	Witnessed By

Note: (a) The results relate only to the sample(s) tested. (b) The Test Report shall not be reproduced, except in full, without the written approval of AES can provide assurance that parts of a report are not taken out of context. (c) The results applied to the sample as received. Sample(s) not drawn by AES. (d) #The information is supplied by the customer and can affect the validity of result.(e) If balance material is available after testing, it will be retained for 15 days maximum. (f) While ' AES' has made their best endeavors to provide accurate and reliable information, AES' is not responsible for any financial liability due to any act of omission or error made.

AADHYA ENGINEERING SERVICES

Works: 346/B/2, Beside Lalji Mulji Transport, GIDC, Makarpura, Vadodara-390010
Email: testing.aes2019@gmail.com / aadhya.engineers@gmail.com
Contact : 9537530900 / 7567158821 / 8000296579

TEST REPORT

	Test Report No: M/23B/0015	Report Date: 25.01.2023	Page No. : 1 Of 1
Customer Name & Address	Mamta Patel Vadodara		
Location	Aadhya Engineering Services	# Customer Ref No.	By Hand Dt-20.01.2023
Sample Condition	Test Piece (Round Bar)	Received Date	20.01.2023
Sample Description & Identification	Casting Sample-8.1	Test Date	25.01.2023
		Instrument No & Name	AES/E/09 Metallurgical Microscope
Material Specification	GJV 400		
Test performed	Volume Fraction	Test Method	ASTM E 562:2019a

TEST RESULTS

Sample ID : 23B/0015

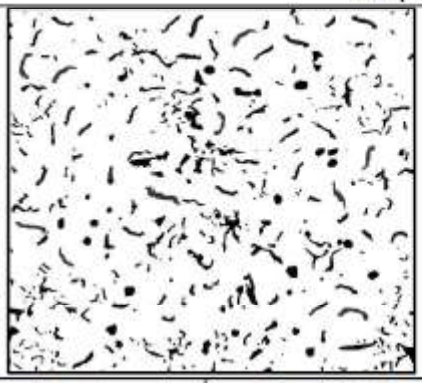

FRAMES	Compacted Graphite Iron (%)	Nodularity (%)
1	65.34	34.66
2	64.55	35.45
3	65.10	34.90
4	66.02	33.98
5	65.09	34.91
Avg. of 5 Frames	65.22	34.78

Etchant:As Polish | Magnification: 100 X

Remarks:

Tested by	Authorised Signatory (T.B Patel/R.H Vasava/R.P Joshi) TM / QM / CEO	Witnessed By

Note: (a) The results relate only to the sample(s) tested. (b) The Test Report shall not be reproduced, except in full, without the written approval of AES can provide assurance that parts of a report are not taken out of context. (c) The results applied to the sample as received. Sample(s) not drawn by AES. (d) #The information is supplied by the customer and can affect the validity of result.(e) If balance material is available after testing, it will be retained for 15 days maximum. (f) While ' AES' has made their best endeavors to provide accurate and reliable information, AES' is not responsible for any financial liability due to any act of omission or error made.

End of Report

AADHYA ENGINEERING SERVICES
Works: 346/B/2, Beside Laiji Mulji Transport, GIDC, Makarpura, Vadodara-390010
Email: testing.aes2019@gmail.com / aadhya.engineers@gmail.com
Contact : 9537530900 / 7567158821 / 8000296579

TEST REPORT

	Test Report No: M/23B/0016	Report Date: 25.01.2023	Page No. : 1 Of 1
Customer Name & Address	Mamta Patel Vadodara		
Location	Aadhya Engineering Services	# Customer Ref No.	By Hand Dt-20.01.2023
Sample Condition	Test Piece (Round Bar)	Received Date	20.01.2023
Sample Description & Identification	Casting Sample-8.2	Test Date	25.01.2023
		Instrument No & Name	AES/E/09 Metallurgical Microscope
Material Specification	GJV 400		
Test performed	Volume Fraction	Test Method	ASTM E 562:2019a

TEST RESULTS

Sample ID : 23B/0016

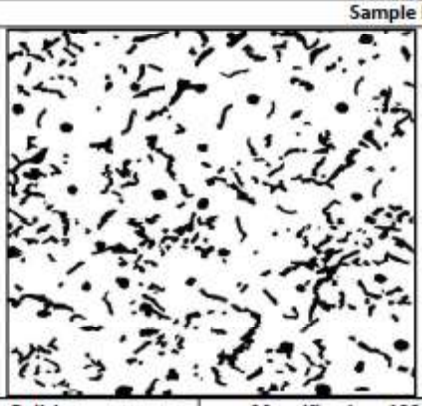

FRAMES	Compacted Graphite Iron (%)	Nodularity (%)
1	70.59	29.41
2	71.12	28.88
3	70.85	29.15
4	70.98	29.02
5	71.32	28.68
Avg. of 5 Frames	70.97	29.03

Etchant:As Polish | Magnification: 100 X

Remarks:

Tested by	Authorised Signatory (T.B Patel/R.H Vasava/R.P Joshi) TM / QM / CEO	Witnessed By

Note: (a) The results relate only to the sample(s) tested. (b) The Test Report shall not be reproduced, except in full, without the written approval of AES can provide assurance that parts of a report are not taken out of context. (c) The results applied to the sample as received. Sample(s) not drawn by AES. (d) #The information is supplied by the customer and can affect the validity of result.(e) If balance material is available after testing, it will be retained for 15 days maximum. (f) While ' AES' has made their best endeavors to provide accurate and reliable information, AES' is not responsible for any financial liability due to any act of omission or error made.

End of Report

AADHYA ENGINEERING

AADHYA ENGINEERING SERVICES

Works: 346/B/2, Beside Laji Mulji Transport, GIDC, Makarpura, Vadodara-390010
Email: testing.aes2019@gmail.com / aadhya.engineers@gmail.com
Contact : 9537530900 / 7567158821 / 8000296579

TEST REPORT

	Test Report No: M/23B/0017	Report Date: 25.01.2023	Page No. : 1 Of 1
Customer Name & Address	Mamta Patel Vadodara		
Location	Aadhya Engineering Services	# Customer Ref No.	By Hand Dt-20.01.2023
Sample Condition	Test Piece (Round Bar)	Received Date	20.01.2023
Sample Description & Identification	Casting Sample-8.3	Test Date	25.01.2023
		Instrument No & Name	AES/E/09 Metallurgical Microscope
Material Specification	GJV 400		
Test performed	Volume Fraction	Test Method	ASTM E 562:2019a

TEST RESULTS

Sample ID : 23B/0017

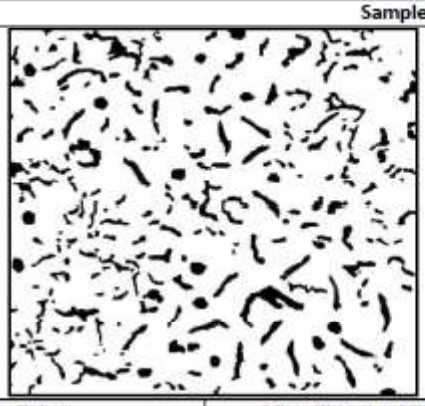

FRAMES	Compacted Graphite Iron (%)	Nodularity (%)
1	68.35	31.65
2	67.92	32.08
3	68.12	31.88
4	67.39	32.61
5	68.55	31.45
Avg. of 5 Frames	68.07	31.93

Etchant:As Polish | Magnification: 100 X

Remarks:

Tested by	Authorised Signatory (T.B Patel/R.H Vasava/R.P Joshi) TM / QM / CEO	Witnessed By

Note: (a) The results relate only to the sample(s) tested. (b) The Test Report shall not be reproduced, except in full, without the written approval of AES can provide assurance that parts of a report are not taken out of context. (c) The results applied to the sample as received. Sample(s) not drawn by AES. (d) #The information is supplied by the customer and can affect the validity of result.(e) If balance material is available after testing, it will be retained for 15 days maximum. (f) While ' AES' has made their best endeavors to provide accurate and reliable information, AES' is not responsible for any financial liability due to any act of omission or error made.

End of Report